COMBINATION IMMUNOTHERAPY TARGETING IMMUNOSUPPRESSIVE SIGNALS IN THE TUMOR MICROENVIRONMENT PREVENTS CANCER PROGRESSION IN BREAST AND PANCREATIC CANCER

by

Bridget P. Keenan

A dissertation submitted to Johns Hopkins University in conformity with the requirements for the degree of Doctor of Philosophy

Baltimore, Maryland
March, 2015

ABSTRACT:

Mechanisms of immune tolerance and suppression occur early at the site of developing tumors and inhibit protective responses induced by cancer vaccines, limiting their efficacy in the treatment of cancer. Combinatorial approaches to cancer immunotherapy were used to investigate the simultaneous inhibition of suppressive signals in the tumor microenvironment and induction of protective T cell responses. The inhibition of an immune checkpoint, LAG-3, in a mouse model of HER-2/neu-overexpressing mammary adenocarcinoma was found to improve CD8$^+$ T cell function in an intrinsic manner when used in combination with a GM-CSF-secreting whole cell vaccine and Treg depletion. LAG-3 signaling also altered the phenotype of antigen-presenting cells in the tumor-draining nodes of mice. Early mechanisms of immune tolerance in a mouse model of pancreatic cancer development were characterized and targeted with Treg depletion and an attenuated *Listeria* vaccine targeting mutated Kras. Local, but not systemic, T cell responses were found to correlate with survival and the alteration of the tumor microenvironment towards an anti-cancer response. In both models of cancer, combination immunotherapy incorporating a vaccine and immunomodulation of the tumor microenvironment was necessary for successful immune responses that inhibited the progression of cancer.

Readers:
Dr. Elizabeth M. Jaffee (PhD Advisor)
Dr. Charles Drake

PREFACE:

I would like to thank my PhD mentor, Dr. Elizabeth Jaffee, for her inspiration, support, and faith in me. She has provided an excellent role model as a physician scientist and mentor, that I hope to live up to in my future career. I would also like to thank my parents, Frank and Ceil Keenan, as well as my brother, Patrick, and sister, Maura, for all the ways they have helped support me over the years. I am grateful for and to my life partner and best friend, Ryan Weidmann, who has been my greatest supporter.

The work presented herein was made possible by the scientific contributions of the following members of Johns Hopkins University School of Medicine and Sidney Kimmel Cancer Center, Aduro Biotech, and Oregon Health & Science University. Data that can be partially or fully attributed to my colleagues is noted here.

I would also like to thank the following past and present Jaffee lab members for helpful discussions, assistance with mice and supplies, and camaraderie:

Darshil Jhaveri
Kelly Foley
Tony Wamwea
Guanglan Mo
Lanqing Huang
Allison Yager
Sara Solt-Linville
Eric Lutz
Kevin Soares
Lei Zheng
Ted Kouo
Chelsea Black
Vivian Weiss
Nina Chu
Heather Kinkead
Emily Flynn
Cindy Freisner

I would also like to thank the following members of my thesis committee, in particular Dr. Todd Armstrong for his support and mentorship:

Dr. Cynthia Sears
Dr. Christine Iacobuzio-Donahue
Dr. Charles Drake
Dr. Todd Armstrong

TABLE OF CONTENTS:

LIST OF FIGURES:

CHAPTER 1: INTRODUCTION

The Status of the "War on Cancer"

Cancer, the second leading cause of death in the United States, is a disease that will directly affect approximately one in two people at some point during their life [1]. Survival rates have improved for some cancers due to early detection and more effective treatments; however, it is predicted that 1 in 4 people in the United States will succumb to cancer [1]. In the lab of Dr. Elizabeth Jaffee, we are focused on two particularly common and lethal cancers. Pancreatic ductal adenocarcinoma (PDA) is the fourth leading cause of cancer deaths in men and women in the United States, with five year survival rates ranging from 1-14% depending on the stage at which it is diagnosed [2,3]. The standard of treatment for pancreatic cancer, depending on stage, includes surgery, chemotherapy and radiation; gemcitabine, the most commonly used chemotherapeutic agent used in both early and late stage PDA gives patients a survival benefit of just a few additional months [3]. Despite improvements in the detection, prevention, and treatment of breast cancer over the past few decades, breast cancer remains the most commonly diagnosed cancer and the second most common cancer-related cause of death in women [1]. Five year survival rates for all stages of breast cancer approach 75%; however, for more advanced breast cancers that have metastasized to other organs, that rate falls to 24% [1]. Even given recent treatment advances and scientific breakthroughs in the underlying biology of cancer, there is an obvious and dire need for new therapies.

1

The promise of immunotherapy for cancer

Inflammation has been linked to cancer and has been shown to include both protective immune responses to tumor antigens and pro-oncogenic inflammatory cells which suppress the anti-cancer response [4]. The effectiveness of immunotherapy may rely on intervention in the timeframe in which this inflammatory response can still be re-directed to a protective, anti-cancer response [5]. Cancer vaccines attempt to harness the power of the body's protective immune response to eliminate cancer and bypass tolerance mechanisms. Cancer vaccines and immunotherapy have several advantages over conventional therapies for cancer. T and B cell responses to tumor antigens are specific, unlike chemotherapy and radiation, and therefore, have the potential for efficacy with few adverse effects. Due to the ability to generate novel immune responses through the recombination of the T and B cell receptor subunits, immunotherapy also has the advantage of adapting and evolving with tumors that acquire frequent mutations, as well as long-lasting memory responses, so there is potential for long-term benefits. Two novel cancer therapies utilizing the immune system to fight cancer, a dendritic cell vaccine and an immune checkpoint inhibitor, have recently been FDA-approved, bringing immunotherapy into the mainstream [6,7]. However, benefits seen with these immunotherapies in comparison to conventional treatments are still small (though significant) and many other immune-modulating agents have had little success in clinical trials for cancer patients. The challenges posed by pre-existing T cell tolerance and tumor immune evasion in patients have been the source of much investigation as the overcoming these is the key to fulfilling the promise of immunotherapy.

The challenge of tolerance and immunosuppression

The potential of immunotherapy combined with its failures in the treatment of cancer demands a deeper understanding of how to induce and direct the best immune response. Cancer patients have been shown to harbor tumor antigen-specific T cells and antibodies, even in the setting of advanced disease, demonstrating that the generation of an immune response is not sufficient for protection against disease [8,9]. There are many mechanisms that tumors possess for downregulating the anti-tumor response, including recruiting and inducing myeloid derived suppressor cells (MDSC) and regulatory T cell populations (Treg), enhancing secretion directly and indirectly of anti-inflammatory cytokines such Transforming Growth Factor beta (TGFβ) and IL-10, and upregulating inhibitory ligands [10]. These mechanisms of immune evasion act to inhibit effector CD4^{+} and CD8^{+} T cells, as well as APCs which are responsible for activating the T cell response to cancer. As a result, APCs (such as dendritic cells), no longer support the anti-tumor immune response, but rather are tolerogenic [10]. There are many more mechanisms of immunosuppression used by tumors to evade the immune system, including those that have been described and those yet to be uncovered.

T regulatory cells

One subset of inhibitory CD4^{+} lymphocytes, T regulatory cells (Tregs), has been shown to correlate with poor prognosis and metastasis in cancer patients [11-15]. Depleting Tregs has been shown to be beneficial to survival and now is a therapeutic goal of many immune-based approaches to cancer treatment [16,17]. There are many mechanisms that are

utilized by Tregs to dampen the anti-cancer immune response that explain the benefit of depleting Tregs in cancer patients.

Different Treg subsets have been shown to be capable of producing immunosuppressive cytokines, such as TGFβ and IL-10, which can inhibit the anti-tumor function of CD4^{+} and CD8^{+} T lymphocytes, skew differentiation of CD4^{+} T cells away from a Th1/Th2 effector subset and towards Treg, and tolerize APCs [18-20]. TGFβ also controls B cell class switching from IgG to IgA, suppresses the proliferation of B cells, induces suppressive N2 type neutrophils, and results in the production of angiogenic factors such as VEGF and extracellular matrix remodeling factors such as matrix metalloproteases that aid in tumor metastasis [21-25]. Immature dendritic cells induced by IL-10 and TGFβ result in less antigen presentation and downregulation of CD40, CD80, and CD86 co-stimulatory molecule expression [26,27]. Furthermore, direct suppression of effector T cells by Tregs has also been suggested, through both competition for IL-2 in the tumor microenviroment and killing of T cells by granzyme [18].

Immune checkpoints

"Immune checkpoint" signals that turn off T cell function exist as a natural mechanism to dampen signaling that occurs downstream of the TCR when cognate antigen is encountered, in order to prevent excessive activation of the immune system and resulting tissue damage. The most notable example of an immune checkpoint is CTLA-4, a molecule on the surface of T lymphocytes, which binds to CD80 and CD86 (B7.1 and B7.2) as does the costimulatory ligand CD28, but with the opposite effect on TCR

signaling. Immune checkpoint molecules have been found to be expressed by tumor-infiltrating lymphocytes (TIL) with impaired ability to secrete multiple cytokines in response to tumor antigen and therefore, serve as markers of T cell "exhaustion." When CTLA-4 signaling is blocked by a monoclonal antibody (now approved for the treatment of metastatic melanoma), its inhibition of effector T cells is released, allowing for powerful anti-tumor effects [28]. The anti-tumor effects of CTLA-4 blockade are accompanied, however, with severe autoimmune adverse effects, which may be related to its expression on Tregs as well as effector cells [28,29]. Additional immune checkpoint molecules found to be upregulated on dysfunctional T cells include LAG-3, PD-1, Tim-3 and Adenosine 2a Receptor (A2aR) [30-32]. Blockade of PD-1 and its ligand, B7-H1 (PD-L1), have also been found to be effective in mouse models and clinical trials, with some, but not as severe, autoimmunity as CTLA-4 blockade [6,33].

Similarly to CTLA-4 and PD-1, blockade of LAG-3 signaling with antibody treatment or knockout of LAG-3 in effector CD8$^+$ T cells can result in increased activation and tumor infiltration by T cells [30]. However, LAG-3 seems responsible for fine-tuning of the T cell response rather than a master on/off switch, as there is no autoimmunity observed in LAG-3 knockout mice, except in combination with PD-1 deletion [34]. Additionally, in patient TIL, suppression of LAG-3 signaling alone was not sufficient for complete reversal of dysfunction [35]. However, LAG-3 has also been found to be expressed by other cell types, such as Tregs and plasmacytoid dendritic cells (DC), and there may be a role for LAG-3 in signaling to the APC through MHC II [36,37]. As cancer patients harbor tolerized APCs and Tregs within the tumor microenvironment, determining the effect of LAG-3 in these populations, as well as in CD8$^+$ T cells, is an

important goal and makes LAG-3 an attractive candidate for blockade in the treatment of cancer.

Innate suppressive cells

The paradigm of pro- or anti-tumorigenic populations as with suppressive $CD4^+$ T regulatory cells (Tregs) and anti-tumor effector $CD4^+$ and $CD8^+$ T cells also pertains to innate cells of the immune system. Tumor-associated macrophages have been identified as an important pro-oncogenic cell type in the tumor microenvironment, enhancing metastasis through interaction with $CD4^+$ T cells, promoting angiogenesis, and inhibiting anti-tumor immune responses [13,38,39]. However, compared with tumor-associated "M2" macrophages, mature macrophages of the "M1" phenotype are known to promote the anti-tumor immune response and are associated with a favorable prognosis [40,41]. Similarly, the duality of anti- or pro-tumor phenotype exists for neutrophils. Tumor-associated "N2" neutrophils have been shown to promote metastasis and angiogenesis by secreting matrix mellatoproteinase-9 and neutrophil elastase and to suppress T cell responses by production of arginase [42]. N2 neutrophils have been found in untreated mouse tumors, contributing to tumor progression; however, they can be converted to "N1" neutrophils with enhanced cytotoxicity to tumor cells when mice are treated with anti-TGFβ [23].

In addition to tolerized DCs, N2 neutrophils, and M2 macrophages in the tumor microenvironment, MDSC, a mixed population of immature monocytic and granulocytic cells, can contribute to the pro-oncogenic inflammatory milieu in the microenvironment

and suppress effector T cells. MDSC express high levels of arginase which results in a depletion of the arginine in their extracellular environment that is required for production of new CD3 zeta chain molecules, leading to TCR downregulation [43,44]. MDSC can also sequester other essential metabolites such as cysteine and tryptophan required for T cell proliferation and cytokine secretion [44,45]. Another mechanism that leads to tumor antigen-specific tolerance by MDSC is via the nitrosylation of tyrosine residues in the TCR by production of reactive oxygen species and peroxynitrates, preventing downstream signaling in the TCR pathway [46,47].

Tolerance in the *neu*-N and KPC mouse models

As discussed generally throughout this section, many immune tolerance mechanisms are in place by tumors to escape the protective immune response. These have also been observed in the two mouse models utilized in my thesis. In the *neu*-N mouse model in which the proto-oncogene HER2/neu (neu) is over-expressed in mammary tissue, there is tolerance to the neu antigen as evidenced by a deficient T cell and antibody response to neu-targeted vaccination that fails to protect from neu-expressing tumors [48]. However, treatment with the neu–targeted vaccine (3T3neuGM) in combination with low dose cyclophosphamide (Cy) to deplete Tregs, can uncover a high avidity population of T cells, such as exists in vaccinated wild type parental strain mice, with the result that a small percentage of these mice can reject established tumors [49]. In the *neu*-N mice, an adoptive transfer of high avidity CD8^{+} T cells specific for neu can result in tumor rejection when given in combination with Cy and 3T3neuGM; however,

these cells fail to reach full potency as seen in wild type tumor-bearing mice in terms of the dose of T cells needed to control tumors and the amount of cytokines produced [50].

In the $Kras^{G12D/+};Trp53^{R172H/+};Pdx-1-Cre$ mouse model, mice express mutated Kras and p53 proteins in the pancreas and develop pancreatic intraepithelial neoplasms (PanIN), precursors that progress to invasive pancreatic ductal adenocarcinoma (PDA). There is early evidence of immunosuppression in KPC mice, starting in the earliest stage PanINs, including infiltration of Tregs and MDSC as well as lack of effector CD8^{+} T cells [51]. Additionally, pancreatic cancer has a unique biology in its characteristic stromal response, often termed "desmoplasia," which contributes to its extreme treatment resistance. Oncogenic signals derived from the tumor cells can induce pancreatic stellate cells to secrete extraceullar matrix proteins such as collagen and hyaluronan leading to elevated interstitial pressure [3,52]. Pancreatic cancer is also characterized by a relative hypovascularity, in comparison to most tumors which become hypervascular through angiogenic processes [53]. The impenetrable stroma and hypovascularity impair the delivery of chemotherapy, and it has been shown that the inhibition of stromal signaling pathways such as the Sonic Hedgehog pathway is required for improved delivery of gemcitabine [54]. Thus, both immune and non-immune populations in the stroma contribute to a microenvironmental milieu that is suppressive to conventional and immune-based therapy. The observations of multiple tolerance mechanisms active in the mouse models of pancreatic and breast cancer correlate with the profound T cell dysfunction and exhaustion of TIL observed in cancer patients, as well as evidence of Tregs and suppressive innate cell populations in human tumors. These mice provide

clinically relevant models of early and late stage cancer to investigate the use of cancer vaccines along with additional therapies to overcome immune suppression.

Overview of this Thesis Work:

The overall goal of this dissertation is to explore the effects of inhibiting immunosuppressive signals in the tumor microenvironment to improve upon the progress made thus far with immunotherapy to treat cancer. In two separate but related projects, I have:

1. Studied the inhibition of an immune checkpoint molecule, LAG-3, as a signal that controls the potency of tumor antigen-specific $CD8^+$ T cells

2. Investigated the role of LAG-3 on other immune cell populations present in the tumor microenvironment and the subsequent effects on tumor immunity

3. Evaluated a novel combination of a *Listeria* vaccine targeting a mutant allele of Kras and Treg depletion in altering the course of pancreatic cancer progression in a mouse model of PDA development

4. Characterized the immunosuppressive signals present in the early stages of pancreatic cancer and the ability of immunotherapy to alter these signals

In chapter 2, the role of LAG-3 in tumor immunity is explored in the HER2/neu mouse model. However, the mouse model of pancreatic cancer utilized in chapter 3 provided a more relevant model in terms of understanding how cancer develops and progresses in its natural site of development with all of the interactions between tumor, immune, and stromal cell populations intact. Due to this reasoning as well as technical

difficulties in this first project, I switched my focus and energy to the second project. In chapter 3, the second project, characterizing the effect of immunotherapy on earlier stages of cancer is fully detailed.

CHAPTER 2: THE ABSENCE OF LYMPHOCYTE ACTIVATION GENE 3 (LAG-3) ENHANCES ANTIGEN-SPECIFIC T CELL FUNCTION INTRINSICALLY IN THE HER-2/NEU BREAST CANCER MODEL

Introduction

Transgenic mice expressing the rat proto-oncogene neu under the control of the MMTV mammary-specific promoter (*neu*-N mice) that develop spontaneous mammary adenocarcinoma tumors are a clinically relevant model of breast cancer that closely mimics the immune tolerance seen in cancer patients [55]. *neu*-N mice exhibit a poor anti-tumor immune response following vaccination with a HER-2/neu and GM-CSF-expressing irradiated whole cell vaccine compared to wild type mice of the same genetic background (FVB/N) [48]. The majority of the T cell receptors (TCR) of CD8^{+} T cells in vaccine-alone treated *neu*-N mice are of low avidity for the immunodominant epitope of HER-2/neu, RNEU$_{420-429}$ [56]. However, with the addition of low dose cyclophosphamide (Cy), a Treg depleting agent, to the vaccine regimen, 20% of *neu*-N mice develop a high avidity anti-*neu* CD8^{+} T cell response, similar to what is seen in FVB/N mice after vaccination, and are protected from tumor challenge [49]. High avidity (from vaccinated FVB/N mice) and low avidity (from vaccinated *neu*-N mice) TCR sequences specific for HER-2/neu were cloned and TCR transgenic mice were created to use as a source of CD8^{+} T cells for further study. In *neu*-N mice, both high avidity (HA) and low avidity (LA) adoptively transferred T cells are unable to produce the same level or number of effector cytokines as when the respective HA or LA CD8^{+} T cells are transferred into FVB/N mice [50]. The majority of HA cells transferred into *neu*-N tumor bearing mice

produce low levels of IFNγ and very little to no TNFα or IL-2 whereas HA cells transferred into FVB-N mice have the capability to secrete multiple cytokines (known as polyfunctionality) in response to neu-expressing tumors. Administration of Cy with vaccine enhances cytokine production in HA cells in comparison to vaccine alone-treated *neu*-N mice. LA cells are severely impaired in cytokine production in *neu*-N mice, even in the presence of Cy and vaccine, and fail to protect against tumor challenge [50].

Exhausted T cells in tumor-bearing mice or cancer patients show upregulation of immune checkpoints, such as PD-1, CTLA-4, and LAG-3, and blockade of these checkpoints has been found to be efficacious in both the clinical setting and in mouse models of cancer [6]. LAG-3, an immune checkpoint molecule, structurally related to CD4 and expressed after T cell activation, has found to be upregulated on anergic CD8^{+} cells and regulatory CD4^{+} T cells [30,36,57]. Blockade of LAG-3 with a monoclonal antibody or by genetic deletion results in increased T cell proliferation and IFNγ production by model tumor antigen-specific CD8^{+} T cells in combination with a vaccine; however, it has also been shown that blockade of more than one checkpoint is required in human TIL for function to be completely restored [30,35]. I hypothesized that deletion of LAG-3 expression in HA and LA T cells would reverse the CD8^{+} T cell dysfunction seen in tumor-bearing *neu*-N mice and result in greater survival when mice are treated in combination with Treg-depleting Cy and a whole cell vaccine targeting neu and expressing GM-CSF. I hypothesized that with modulation of immune checkpoints, the function of HA T cells in *neu*-N mice could be recovered to the level of that seen in non-tolerant FVB/N mice and that LA T cells would also recover some, if still limited, effector function. As LAG-3 can

be expressed by CD4^{+} T cells, B cells, NK cells, and plasmacytoid dendritic cells (DCs), I also predicted that deletion of LAG-3 in tumor antigen-tolerant mice would have CD8^{+} T cell-extrinsic effects, resulting in enhanced tumor immunity and impaired tumor growth [58,59]. In initial experiments, HA cells with genetic deletion of LAG-3 (HA LAG-3^{-/-}) CD8^{+} T cells more effectively infiltrated mammary tumors, had increased polyfunctionality, and had enhanced ability to clear tumors in *neu*-N mice compared to HA cells. However, I was unable to repeat these results consistently in this model, perhaps due to technical issues with the mouse colony. Abrogation of endogenous LAG-3 signaling in *neu*-N mice did not enhance the function of adoptively transferred HA or HA LAG-3^{-/-} CD8^{+} T cells compared to their function in *neu*-N mice with intact LAG-3 expression, suggesting contradictory roles for LAG-3 in T cells and non-T cells. Additionally, LA cells did not show the same ability in regards to enhanced tumor clearance when LAG-3 signaling was abrogated in these mice.

Materials and Methods

Mice

Female 6-12 week old mice were used for all experiments. FVB/N mice (Harlan Laboratories) and *neu*-N mice (Jackson Laboratory) were purchased and then further propagated at Johns Hopkins. FVB/N Thy1.2$^+$ mice were created by backcrossing the Thy1.2 allele onto the FVB/N background for 10 generations. TCR transgenic mice were generated using TCR sequences from high-avidity (HA) and low-avidity (LA) RNEU$^{420-429}$-specific T-cell clones, crossed to the FVB/N Thy1.2$^+$, and phenotyped with Vβ, Thy1.2, and tetramer staining as previously described [50]. The high avidity TCR pairs the Vβ4 and Vα1.1 chains while the low avidity TCR contains the Vβ4 and Vα5 chains [49]. LAG-3$^{-/-}$ mice were kindly provided by Charles Drake (Johns Hopkins University) and have germline deletion of LAG-3 as originally described [60]. Both HA and LA TCR transgenic mice were crossed with LAG-3$^{-/-}$ mice after backcrossing the LAG-3$^{-/-}$ mouse from C57BL/6 genetic background onto the FVB/N genetic background. These HA and LA TCR transgenic LAG-3$^{-/-}$ mice were also crossed to FVB/N mice that express the Thy1.2 marker for some experiments to identify adoptively transferred T cells versus endogenous T cells in *neu*-N mice (expressing Thy1.1). *neu*-N mice were crossed to LAG-3$^{-/-}$ mice to generate *neu*-N LAG-3$^{-/-}$ mice, on a FVB/N Thy1.1 genetic background. Once stable colonies were established, genotyping was performed at regular intervals to ensure integrity of the transgenes. Animals were kept in pathogen-free conditions and treated in accordance with institutional and American Association of Laboratory Animal

Committee approved policies. All animal studies were approved by the Institutional Animal Care and Use Committee of the Johns Hopkins University.

Cell lines

The neu-expressing mammary adenocarcinoma cell line, NT2.5, originally derived from a *neu*-N spontaneous tumor, was maintained in RPMI with 20% fetal bovine serum, 1.2% HEPES, 1% L-glutamine, 1% non-essential amino acids, 1% sodium pyruvate, 0.5% penicillin-streptomycin, 0.2% insulin, and 0.02% gentamycin [48]. The 3T3neuGM cell line, expressing neu and GM-CSF and used as a whole cell vaccine, was generated as previously described and grown in DMEM with 10% bovine calf serum, 1% sodium pyruvate, 0.5% penicillin-streptomycin, and 0.3 μM methotrexate selection [48]. The T2-D^q cells were derived as previously described and grown in RPMI with 10% FBS, 1% L-glutamine, 1% sodium pyruvate, 1% non-essential amino acids, 0.5% penicillin-streptomycin, and 0.68% hygromycin B [56].

Cy and vaccine administration

Cyclophosphamide (Cytoxan, Cy, Bristol Myers Squibb) was reconstituted in sterile water at 20 mg/ml and then diluted in sterile PBS. Cy (100 mg/kg) was given as an intra-peritoneal injection (IP) of 0.5 ml one day prior to vaccine according to treatment group. neu and GM-CSF-expressing 3T3neuGM vaccine cells were irradiated at 50 Gy and injected subcutaneously (SC) at a dose of 3 x 10^6 cells per mouse, divided into three

0.1ml injections in PBS in the left axillary lymph node regions and right and left inguinal lymph node regions.

Tumor clearance studies

Mice were given SC injections into the right upper mammary fat pad of 2×10^6 (FVB/N) and 5×10^4 (*neu*-N and *neu*-N LAG-3$^{-/-}$) NT2.5 cells in 0.1ml PBS 3 days prior to vaccine [48]. Tumors were measured every 3 days and mice were euthanized when tumors grew to over 1 cm^2 in accordance with Animal Care and Use Committee guidelines.

Adoptive transfer

CD8$^+$ T cells were isolated from harvested spleens and lymph nodes of TCR transgenic mice using Dynabeads untouched mouse CD8$^+$ cells (Invitrogen) negative isolation kit and washed twice in sterile PBS. For LA and LA LAG-3$^{-/-}$ CD8$^+$ T cells, 10 μg Vβ4 and Vβ6 depleting antibodies (BD Pharmingen) were added to the negative selection antibody cocktail to enhance purity of the adoptively transferring T cell population. 6×10^6 cells were injected intraveneously (IV) in 0.5 ml for flow cytometry analysis or in the decreasing doses indicated for tumor clearance studies one day after vaccination.

T cell Trafficking and Cytokine Production Assays

For evaluation of cytokine production and T cell trafficking, NT2.5 cells were given to mice at a dose of 5 x 10^6 (FVB/N) and 1 x 10^6 (*neu*-N and *neu*-N LAG-3$^{-/-}$), 8 days prior to vaccination, unless otherwise specified. T cells isolated from spleens, vaccine or tumor-draining nodes, and tumors were harvested 3 or 5 days after adoptive transfer and stimulated with peptide and T2-D^q cells for 5 hours in the presence of a protein transport inhibitor (GolgiStop, BD Biosciences) for intracellular cytokine assays [50,61]. Tumors were digested in hyaluronidase and collagenase-containing media for 1 hour prior to cell isolation. The RNEU[420-429] (PDSLRDLSVF) and NP[118-126] (RPQASGVYM) peptides were produced in the Johns Hopkins Biosynthesis and Sequence Facility at a purity >95% [50]. Adoptively transferred cells were identified by surface staining with fluorescently conjugated antibodies for CD8 and either the Vβ4 chain or Thy1.2 marker in FACS buffer. The following stains and antibodies were used: Live/Dead Fixable Dead Cell Stain Kit (Invitrogen Molecular Probes), Thy1.2-Alexa Fluor 700 (BioLegend), CD8-Pacific Blue, Vβ4- Fluorescein isothiocyanate (FITC), CD49f- Phycoerythrin (PE) (BioLegend), CD49d-FITC (BD Pharmingen), CD29-Alexa Fluor 647 (BioLegend), CXCR3- Peridinin chlorophyll (PerCP)-Cyanine (Cy)5.5 (eBioscience), IFNγ-PerCP-Cy5.5 (BD Pharmingen), IL-2- Allophycocyanin (APC) (BD Pharmingen), TNF-Alexa Fluor 700 (BD Pharmingen), Granzyme B-PE (eBioscience), CD107a and b-PE-Cy7 (BD Pharmingen), Tbet-PE (eBioscience), CD11c-PerCP (BioLegend), CD86-Pacific Blue (BioLegend), CD80-Alexa Fluor 647 (BioLegend), CD40-FITC (BD Pharmingen), IL-12-PE (BD Pharmingen), and MHC II (I-A/I-E)-Alexa Fluor 700 (Biolegend). For intracellular protein staining, cells were permeabilized with CytoFix Fixation Buffer and

washed with Perm/Wash Buffer (BD Biosciences). To stain for intranuclear transcription factors, the PE anti-mouse/rat Foxp3 staining set (eBioscience) was used to fix and permeabilize, and stain cells. FcBlock was routinely used prior to staining (anti-CD16/CD32 antibody, BD Biosciences). Flow cytometry was performed using FACSCalibur and LSR II instruments (BD Biosciences) and analyzed using FlowJo (Tree Star, Inc.) and FACSDiva (BD Biosciences), depending on the number of fluorochromes utilized.

In vitro stimulation

4 days post vaccination of *neu*-N and *neu*-N LAG-3$^{-/-}$ mice, vaccine-draining lymph nodes (axillary, inguinal) were harvested and CD11c MicroBeads (Miltenyi Biotec Inc.) were used to isolate with CD11c$^+$ cells. Naïve CD8$^+$ T cells were isolated by negative isolation from the spleens of TCR transgenic mice and CFSE labeled with 1.5 µM CFSE using the CellTrace CFSE Proliferation kit (Invitrogen). 2.5 x 10^5 CD11c$^+$ cells were plated 7.5 x 10^5 CD8$^+$ T cells per well in a 96 well U-bottom plate for 3, 5, or 7 days at 37°C and 5% CO_2 in RPMI supplemented with 10% fetal bovine serum, 1% penicillin-streptomycin, 0.5% L-glutamine, and 50 µM 2-mercaptoethanol. Golgistop was incubated with cells for 5 hours prior to staining and flow cytometry analysis.

Data analysis

For analyzing polyfunctional cytokine data, Pestle and SPICE software were used, as provided by Mario Roederer (NIAID Vaccine Research Center) [62]. Data for cytokine

response to RNEU$^{420\text{-}429}$ peptide was normalized for response to the negative control NP$^{118\text{-}126}$ peptide. Statistical significance was analyzed using GraphPad Prism (GraphPad Software, Inc.) and assessed using a two-tailed student T test unless otherwise noted. Significance was defined as $p<0.05$.

Results

HA LAG-3$^{-/-}$ cells clear tumors at lower doses than HA cells in combination with Cy and vaccine

HA CD8^{+} T cells, given in combination with Cy and the 3T3neuGM vaccine have been shown to mediate tumor rejection (100% tumor-free with 6 x 10^6 cells, 75% with 4 x 10^6 cells) in *neu*-N mice [50]. A dose titration experiment of decreasing numbers of cells starting with 6 x 10^6 HA and HA LAG-3$^{-/-}$ cells was used to compare differences in the ability to control neu-expressing NT2.5 tumors in *neu*-N mice. It was demonstrated that HA LAG-3$^{-/-}$ T cells are superior to HA T cells in their ability to clear tumors in *neu*-N mice at lower doses of cells, an effect that was dependent on Cy treatment (**Figure 1**). Mice receiving HA LAG-3$^{-/-}$ cells cleared tumor regardless of dose, with the exception of 1 out of 2 mice in the 4 x 10^6 dose, whereas wild type HA cells required a dose of 6 x 10^6 cells or higher to remain tumor-free as 1 out of 2 mice developed tumors in this dose and 2 out of 2 mice developed tumors in the medium and low dose of HA cells. With the vaccine alone, there was no difference between the HA LAG-3$^{-/-}$ and HA CD8^{+} T cells at any dose and all mice receiving the vaccine and T cells alone developed tumors (**Figure 1**).

HA LAG-3$^{-/-}$ cells have enhanced tumor trafficking and upregulation of adhesion molecules

6 x 10^6 T cells were adoptively transferred into *neu*-N mice 10 days after tumor implantation, one day following vaccination and 2 days after Cy. T cells were isolated from the harvested tumor-draining lymph nodes and tumors of *neu*-N mice 5 days post-

transfer and identified by staining for the Thy1.2 marker. As previously published, Cy enhanced the ability of T cells to traffic into tumors and both HA and HA LAG-3^{-/-} cells were found in significantly increased numbers in the presence of Cy compared to vaccine alone in tumors (**Figure 2A**). Cy enhanced the trafficking of HA T cells into the tumor-draining nodes as well (**Figure 2B**). Although it was not significant, there was a trend towards increased cell number per mg of tumor or per lymph node in the HA LAG-3^{-/-} groups compared to the HA groups. The enhanced infiltration of HA LAG-3^{-/-} T cells into tumors depended on the co-administration of Cy, but in the lymph node, HA LAG-3^{-/-} T cells given without Cy were found to infiltrate in numbers equivalent to that of the HA cells with Cy and vaccine (**Figure 2A-B**). The adhesion molecules VLA-4, VLA-6, and CXCR3 have been found to be upregulated on HA TCR transgenic CD8^{+} T cells trafficking to the tumor, when given with Cy and 3T3neuGM vaccination [50]. I hypothesized that these molecules would be upregulated to a greater degree on HA LAG-3^{-/-} T cells compared to HA cells, accounting for their enhanced trafficking to the tumor microenvironment, and would occur as early as 3 days following adoptive transfer in the tumor-draining lymph nodes, preceding their arrival in the tumor. For this study, I isolated lymphocytes from tumor-draining nodes in *neu*-N mice after treatment with vaccine plus or minus Cy and adoptive transfer of HA or HA LAG-3^{-/-} cells at days 3 and 5 post-adoptive transfer and performed surface staining for CD8, Thy1.2 and β1 (VLA-4 or VLA-6 beta chain), α4 (VLA-4 alpha chain) and α6 (VLA-6 alpha chain) integrins and CXCR3. There was a small but significant increase in the mean fluorescence intensity of α6 and β1 on day 5 after T cell transfer on HA LAG-3^{-/-} T cells given with

Cy and vaccine compared to HA cells (**Figure 2C-D**). There was also a trend towards increased level of α4 and β1 integrins on HA LAG-3$^{-/-}$ cells on day 3 post-adoptive transfer (**Figure 2D-E**). However, the percent of Thy1.2$^+$CD8$^+$ T cells expressing CXCR3 on day 3 was increased among the HA cells with or without Cy compared to the same treatment group for HA LAG-3$^{-/-}$ cells, while there was no significant difference in CXCR3 on day 5 (**Figure 2F**).

HA LAG-3$^{-/-}$ cells are polyfunctional in the setting of Cy and vaccine

Previous studies reported that FVB/N mice vaccinated against HER-2/neu develop polyfunctional T cells with the ability to produce multiple cytokines such as IL-2, TNFα, IFNγ, and Granzyme B, characteristic of a productive immune response, whereas the T cells induced in *neu*-N mice lack this ability [50]. Therefore, I characterized the cytokine profile of the HA T cell populations, with and without LAG-3 expression, transferred into tumor-bearing *neu*-N mice. T cells were compared by intracellular cytokine staining (ICS) for production of the 4 cytokines and surface upregulation of CD107a and CD107b (LAMP-1 and LAMP-2), a marker of T cell lytic capability. *neu*-N mice were treated with vaccine alone and with the combination of vaccine and Cy to assess the dependence of cytokine production on Treg depletion as well as LAG-3 signaling and the interaction of the two treatments. It is evident from Figure 2A that without Cy, few HA LAG-3$^{-/-}$ nor HA cells infiltrate into tumors in *neu*-N mice and as is seen Figure 3, both types of T cells fail to make abundant cytokines without the addition of Cy. However, comparisons made between HA T cells and HA LAG-3$^{-/-}$ T cells

demonstrate that HA LAG-3$^{-/-}$ cells produce significantly more IFNγ, TNFα, IL-2, and have higher surface levels of CD107 (**Figure 3A-C and E**). There was also a trend towards increased Granzyme B production in HA LAG-3$^{-/-}$ cells when given with Cy and vaccine (**Figure 3D**). In addition, vaccine alone-treated *neu*-N mice given HA LAG-3$^{-/-}$ cells have higher expression of CD107 than HA cells in mice given vaccine alone (**Figure 3E**). In addition to showing that HA LAG-3$^{-/-}$ CD8$^+$ T cells have enhanced production of each cytokine, I also analyzed each possible combination of cytokines to assess polyfunctionality. In **Figure 3F**, it is evident that many HA LAG-3$^{-/-}$ cells in *neu*-N mice given Cy and vaccine are capable of producing 4 to 5 cytokines, whereas most of HA cells in mice treated with Cy and vaccine produce 3-4 cytokines and the majority of either T cell type in mice treated with vaccine alone produce 0, 1, or 2 cytokines. The increase in effector cytokine secretion also correlated with upregulation of the transcription factor, Tbet, which is associated with cytotoxic CD8$^+$ T cell function, in HA LAG-3$^{-/-}$ T cells compared to HA T cells in mice treated with Cy and vaccine or vaccine alone (**Figure 3G**). Thus, LAG-3 deletion can enhance the effects of Cy given with 3T3neuGM on adoptively transferred CD8$^+$ T cells in a tolerant mouse model.

Deletion of endogenous LAG-3$^{-/-}$ enhances tumor clearance, but not T cell activation

After confirming the CD8$^+$ T cell intrinsic effects of LAG-3 in high avidity neu-specific T cells in *neu*-N mice, I hypothesized there may be additional effects of LAG-3 signaling in a tumor antigen tolerance model as LAG-3 is known to be expressed by many immune cell types. Additionally, there may be an interaction between LAG-3

signaling in adoptively transferred CD8^{+} T cells and in endogenous immune cells. *neu*-N mice were crossed to LAG-3^{-/-} mice backcrossed onto the FVB/N genetic background to generate *neu*-N mice with complete knockout of LAG-3. The ability of these mice to clear tumor was assessed with a tumor challenge experiment and compared with what has previously been published in *neu*-N mice. Without treatment, *neu*-N LAG-3^{-/-} mice developed tumors with slower kinetics than *neu*-N mice, although the majority of mice did develop tumors by 3 weeks after injection with NT2.5 cells (**Figure 4A**) [55]. Only 1 out of 5 mice that received the neu-directed vaccine alone developed a tumor, compared to all *neu*-N mice that develop tumors with vaccine alone (**Figure 4A**) [55]. Given this, it was hard to make comparisons between mice treated with Cy, vaccine, and an adoptive transfer of HA or HA LAG-3^{-/-} T cells, as no mice developed tumors in these groups, regardless of the presence of Cy or the dose of T cells given, unlike the *neu*-N mice (compare Figure 1 with 4A). I was able to compare trafficking and cytokine responses of HA or HA LAG-3^{-/-} cells transferred into *neu*-N and *neu*-N LAG-3^{-/-} mice using ICS to assess differences in T cell activation in each mouse model. As seen before in the *neu*-N mice, HA LAG-3^{-/-} T cells had enhanced trafficking to the tumor compared to HA cells when given with Cy and vaccine (**Figure 4B**). HA LAG-3^{-/-} T cells in the *neu*-N mouse model had enhanced infiltration into NT2.5 tumors compared to HA LAG-3^{-/-} T cells in *neu*-N LAG-3^{-/-} mice. Surprisingly, adoptively transferred T cells were found in the highest numbers in the tumors of *neu*-N LAG-3^{-/-} mice treated with vaccine alone, increased in comparison to vaccine and HA–treated mice and close to the level of HA LAG-3^{-/-} T cells in Cy and vaccine-treated *neu*-N mice (**Figure 4B**). HA LAG-3^{-/-} T cells in Cy and vaccine-treated *neu*-N mice had the highest number of cytokine producing

cells, with significantly more TNF and CD107 expression than HA LAG-3$^{-/-}$ T cells in Cy and vaccine-treated *neu*-N LAG-3$^{-/-}$ mice, indicating that endogenous deletion of LAG-3 did not synergize with CD8^{+} intrinsic deletion of LAG-3 to enhance cytokine production (**Figure 4C-G**). The only advantage in activation that T cells in Cy and vaccine-treated *neu*-N LAG-3$^{-/-}$ mice appeared to have compared to T cells in similarly treated *neu*-N mice was in increased production of Granzyme B and this was not significant (**Figure 4G**). For vaccine alone-treated mice, the only benefit of host LAG-3 deletion on adoptively transferred T cell activation was increased IFNγ production in HA LAG-3$^{-/-}$ T cell-treated mice compared to the same T cell type and treatment group in *neu*-N mice (**Figure 4C**). Polyfunctionality analysis revealed that HA LAG-3$^{-/-}$ T cells in Cy and vaccine-treated *neu*-N mice produced the most cytokines per cell, with many cells expressing 3-5 cytokines, compared to other treatment groups in both *neu*-N mice and *neu*-N LAG-3$^{-/-}$ mice (**Figure 4H**). HA LAG-3$^{-/-}$ T cells in Cy and vaccine-treated *neu*-N LAG-3$^{-/-}$ mice had an intermediate phenotype, similar to that of HA T cells in Cy and vaccine-treated *neu*-N mice and *neu*-N LAG-3$^{-/-}$ mice or HA LAG-3$^{-/-}$ T cells in vaccine alone-treated in *neu*-N mice and *neu*-N LAG-3$^{-/-}$ mice. Overall, the data suggests there is not an additional benefit to LAG-3 deletion endogenously in terms of adoptively transferred high avidity CD8^{+} T cell cytokine production and tumor infiltration, and therefore, the enhanced tumor clearance seen in *neu*-N LAG-3$^{-/-}$ mice cannot be accounted for by change in the function of adoptively transferred CD8^{+} T cells.

Endogenous CD8⁺ T cell and APC activation are not enhanced in neu-N LAG-3⁻/⁻ mice

One hypothesis for the lack of enhanced anti-neu CD8$^+$ T cell activation yet increased protection against tumor challenge is that *neu*-N LAG-3$^{-/-}$ mice harbor endogenous CD8$^+$ T cells that are less tolerant to neu than what has been observed in endogenous CD8$^+$ T cells following vaccination in *neu*-N mice [48]. To test this hypothesis, *neu*-N and *neu*-N LAG-3$^{-/-}$ mice were given a dose of 5 x 10^4 NT2.5 cells on day 0, followed by Cy on day 2 and vaccine on day 3, and harvested 12 days after vaccination to allow for activation of the endogenous T cell response. As has been shown in other models, LAG-3$^{-/-}$ mice have increased numbers of total CD8$^+$ T cells in the spleen (**Figure 5A**). However, inconsistent with data from previously published models regarding the effect of LAG-3 on CD8$^+$ activation, there was not an enhanced number of antigen-specific IFNγ$^+$CD8$^+$ T cells per spleen in *neu*-N LAG-3$^{-/-}$ mice compared to *neu*-N mice (**Figure 5B**). Few mice overexpressing neu would be expected to respond to neu compared to wild type FVB/N mice which consistently develop an endogenous CD8$^+$ response, a population that makes up 1-2% of their total CD8$^+$ T cells. Indeed this was the case, with only 1 *neu*-N mouse and 1 *neu*-N LAG-3$^{-/-}$ mouse having a response equivalent to the vaccinated FVB/N controls, when IFNγ responses were shown on an individual basis (**Figure 5C**).

While this experiment demonstrates that the difference in tumor control between *neu*-N and *neu*-N LAG-3$^{-/-}$ mice is unlikely to result from CD8$^+$ intrinsic effects of LAG-3 on the endogenous CD8$^+$ T cell population, it does not rule out another effector population responsible for control of neu-expressing tumors. LAG-3 is known to have

effects in dendritic cells, an important antigen presenting cell (APC) type, among other immune cell populations [37]. I hypothesized that abrogation of LAG-3 signaling may increase the activation status of these cells, resulting in more activated CD4$^+$ and CD8$^+$ T cells. Alternatively, deletion of LAG-3 could result in less activated APCs which could explain the failure of CD8$^+$ T cells to produce more effector cytokines in *neu*-N LAG-3$^{-/-}$ mice. To test these hypotheses, I evaluated the ability of CD11c$^+$ cells from *neu*-N and *neu*-N LAG-3$^{-/-}$ mice to induce proliferation and cytokine secretion in naïve HA and HA LAG-3$^{-/-}$ T cells. Four days following vaccination, vaccine-draining lymph nodes were removed from *neu*-N and *neu*-N LAG-3$^{-/-}$ mice and subsequently isolated CD11c$^+$ cells were cultured with CFSE-labeled CD8$^+$ T cells for 5 or 7 days. The differences in dilution of CFSE dye were not dramatic but showed, most notably, that HA LAG-3$^{-/-}$ T cells divided the most in culture, regardless of APC type, consistent with what has previously published about the effect of LAG-3 on T cell proliferation (**Figure 5D**). There were also slight differences between the two APC types, with the *neu*-N LAG-3$^{-/-}$-derived APCs causing more T cell stimulation for both HA and HA LAG-3$^{-/-}$ cells (**Figure 5D**). In contrast to proliferation, these trends between *neu*-N LAG-3$^{-/-}$ and wild type *neu*-N dendritic cells did not correlate completely with respect to cytokine secretion from the same culture conditions. There was more IFNγ secretion from HA LAG-3$^{-/-}$ cells but only in the T cells cultured with *neu*-N LAG-3$^{-/-}$ APCs; IFNγ secretion was equivalent between HA LAG-3$^{-/-}$ and HA cells cultured with *neu*-N APCs (**Figure 5E**). The reverse effect of APC type was seen with cytokine expression as *neu*-N LAG-3$^{-/-}$ APCs induced

27

less IFNγ in T cells than *neu*-N APCs (**Figure 5E**). Overall, deletion of LAG-3 signaling had complex effects on both APC and T cell populations.

The enhanced proliferation but decreased T cell cytokine production driven by LAG-3$^{-/-}$ APCs was further investigated through staining for the costimulatory molecules CD80, CD86 and CD40, and IL-12 expressed by CD11c$^+$ cells in *neu*-N mice and *neu*-N LAG-3$^{-/-}$ mice. Adoptive transfer of HA LAG-3$^{-/-}$ T cells or HA T cells was also included in the comparisons to assess the effect of the absence or presence of LAG-3 on the transferred T cell on APCs, as cleaved LAG-3 from the surface of activated T cells can also be a source of soluble LAG-3. Vaccine-draining and tumor-draining lymph nodes harvested 7 days after vaccination were isolated and examined for upregulation of the co-stimulatory molecules and IL-12 to assess the effect of the absence of LAG-3 on the APC population. There were not many consistent differences between APCs from *neu*-N LAG-3$^{-/-}$ and *neu*-N mice receiving the same treatment. In the tumor-draining nodes, there were higher levels of CD80 expression in vaccinated *neu*-N versus *neu*-N LAG-3$^{-/-}$ mice in the group that received HA LAG-3$^{-/-}$ cells (**Figure 5F**). However, *neu*-N LAG-3$^{-/-}$ mice had an increased number of IL-12-expressing CD11c$^+$MHCII$^+$ cells than *neu*-N mice that received vaccine, with or without Cy, and HA LAG-3$^{-/-}$ T cells. CD40 appeared to have increased expression in *neu*-N LAG-3$^{-/-}$ CD11c$^+$ cells for some of the treatment groups and CD86 appeared to have decreased expression in the same mice, although neither of these trends was found to be significant. In the vaccine-draining nodes, although there were some differences between the APCs of mice receiving the two different T cell types, there were no significant differences observed between *neu*-N LAG-3$^{-/-}$ and *neu*-N host

28

APCs in the level of CD80, CD86, or CD40 or in IL-12, by percentage or number of cells. However, it is possible that vaccine-draining nodes examined at an earlier time point would have shown differences evident in the tumor-draining node at 7 days following vaccination.

LAG-3 deletion in low avidity T cells does not enhance function in non-tolerant mice

I examined the effect of LAG-3 on low avidity cells (LA) in the model available at the time of experimentation, the FVB/N wild type mice, which do not express neu under the MMTV promoter, to confirm if deletion of LAG-3 can improve LA function in this model. It has been previously shown that LA cells secrete lower levels of cytokines than HA cells in both *neu*-N and FVB/N mice and fail to control tumors in *neu*-N mice, even when given with Cy and the 3T3neuGM vaccine [50]. HA cells can clear tumors in FVB/N mice without Cy or 3T3neuGM but LA cells fail to completely control tumor growth without co-administration of vaccine [50]. I compared the ability of LA and LA LAG-3$^{-/-}$ cells to control NT2.5 tumors in a tumor clearance assay in which FVB/N mice were given an adoptive transfer of 6 x 10^6 LA or LA LAG-3$^{-/-}$ cells without Cy or vaccine. 6 x 10^6 HA cells, given as a control, demonstrated complete control of tumors within the duration of the study (45 days) (**Figure 6A-B**). All 3 FVB/N mice that received LA cells initially had tumors that grew with faster kinetics than mice given HA cells but eventually all tumors regressed; however, only 2 out of 4 mice receiving LA LAG-3$^{-/-}$ cells had NT2.5 tumors that regressed (**Figure 6A-B**). All tumors in FVB/N mice with tumors that were left untreated grew to greater than 100 mm^2 (the experimental endpoint).

The ability of LA and LA LAG-3^{-/-} cells to infiltrate tumors and produce cytokines was also investigated in the FVB/N mice. Larger doses of tumors were given to ensure tumor growth for analysis of infiltrating cells and tumors were harvested 5 days after adoptive transfer. FVB/N mice were also given Cy and vaccine as this has been shown to result in optimal cytokine expression in LA cells [50]. There was no significant difference in the number of cells that trafficked into NT2.5 tumors in FVB/N mice between the LA and LA LAG-3^{-/-}-treated mice (**Figure 6C**). Additionally, there were no significant differences in the number of IFNγ, TNF and Granzyme B-producing CD8^{+} T cells and there was a trend towards less cytokine-producing T cells in the mice receiving LA LAG-3^{-/-} cells compared to the LA-treated group (**Figure 6C**). Overall, LAG-3 deletion in LA cells did not augment their function and may have actually decreased the function of LA cells in non-tolerant mice. It remains to be seen if LA LAG-3^{-/-} would have enhanced function in the *neu*-N tolerant model.

Discussion

In this study of LAG-3 in a tolerant mouse model of breast cancer, LAG-3 was shown to have diverse and complex effects, perhaps resulting from the interaction of LAG-3 signaling in different cell types. First and most evident, LAG-3 had cell intrinsic effects on neu-specific CD8$^+$ T cells. The ability to produce multiple cytokines simultaneously, known as polyfunctionality, is a hallmark of potent CD8$^+$ T cells able to clear viral infections, and is often defective in TIL [63]. HA cells in FVB/N mice can produce multiple cytokines, but HA cells in tumor tolerant *neu*-N mice fail to fully function even in the presence of Treg depletion and vaccination [50]. The augmentation of function in tumor antigen-specific CD8$^+$ T cells in terms of proliferation and cytokine production with blockade of LAG-3 signaling has been shown in other models and patient-derived T cells [30,35]. I hypothesized that the addition of a checkpoint inhibitor would enhance neu-specific CD8$^+$ T cell function. Indeed, I observed increased HA cell expansion and tumor trafficking with LAG-3 deletion as well as greater control of tumors.

In our system, there was a requirement for Treg depletion with Cy as seen in Figures 1-3 for tumor control and polyfunctionality of HA T cells even in the setting of modulation of immune checkpoints and vaccination. Although increased CD8$^+$ T cell proliferation and IFNγ production has been shown before in other mouse models when LAG-3 is blocked in CD8$^+$ T cells, the increased TNF and IL-2 seen in our system with Cy and vaccine has not been shown before. Antibody blockade of LAG-3 alone (without co-blockade of PD-1) failed to upregulate cytokine production in patient TIL [35]. There is

synergy observed with LAG-3 blockade in CD8$^+$ T cells and vaccination against a tumor antigen with a Vaccinia viral vector and with dual antibody blockade of LAG-3 and PD-1 in mouse tumor models [30,34]. LAG-3 and PD-1 single knockout mice do not experience the autoimmunity that causes mortality in LAG-3$^{-/-}$PD-1$^{-/-}$ (double knockout) mice; however, PD-1 antibody therapy has been shown to cause some autoimmune adverse effects in clinical trials [34]. There was no autoimmunity observed grossly in the mice receiving HA or LA LAG-3$^{-/-}$ cells in my studies. The more subtle regulation of CD8$^+$ T cell activation and function by LAG-3 may make it an ideal candidate for cancer treatment in terms of side effect profile, but only when paired with other forms of immunotherapy that serve to enhance the efficacy of LAG-3 blockade without inducing autoimmunity.

The role of LAG3 in restoring function of LA T cells was also explored with surprising results. Although it remains unclear how the function of LA cells would be altered in tolerant *neu*-N mice with deletion of LAG-3, there was no advantage to genetic deletion of LAG-3 in LA cells when transferred into wild type FVB/N mice in terms of tumor clearance or cytokine production. It is possible that no increased activation in terms of cytokine production was seen in the FVB/N mice as T cells transferred into wild type mice, without being subject to tolerizing mechanisms, may peak in their ability to produce cytokines. However, I did observe a decreased ability to control neu-expressing tumors; only 2 out of 4 LA LAG-3$^{-/-}$ mice cleared tumors after 45 days versus all 3 LA-treated mice in Figure 6B, demonstrating that deletion of LAG-3 in the LA cells does not seem to be beneficial. Unfortunately, I could not make direct comparisons with the HA cells as those experiments were done in *neu*-N mice only. It is interesting that the anti-

tumor ability of LA cells did not increase with deletion of LAG-3 as it has been shown that low affinity CD8$^+$ T cells have higher expression of checkpoint molecules including LAG-3, PD-1, and NKG2A than high affinity CD8$^+$ T cells, correlating with their decreased function [64]. Despite my findings' inconsistency with the generally observed CD8-intrinsic effects of LAG-3, it is possible that LA T cells require blockade of more than one inhibitory signaling pathway, due to their pre-existing dysfunction and lower avidity for tumor antigen. This is relevant to cancer treatment as these cells with lower avidity and functional capability are similar to what is observed in patient TIL. However, for complete understanding of the different effects of LAG-3 in HA and LA cells, a comparison of the LA and LA LAG-3$^{-/-}$ cells would need to be completed in *neu*-N mice.

The effect of LAG-3 deletion on CD8 function in a non-intrinsic manner was investigated by using *neu*-N LAG-3$^{-/-}$ mice. This system of adoptively transferring HA and HA LAG-3 CD8$^+$ T cells into *neu*-N and *neu*-N LAG-3$^{-/-}$ mice revealed surprisingly complex effects of deleting LAG-3 globally. *neu*-N LAG-3$^{-/-}$ mice were able to clear tumors with or without Cy in addition to vaccine and an adoptive transfer, suggesting that endogenous blockade of LAG-3 signaling resulted in enhanced T cell function. However, dual deletion of intrinsic and extrinsic LAG-3 signaling did not result in increased T cell tumor infiltration or polyfunctionality as had been expected. Thus, the effects of LAG-3 deletion in CD8$^+$ T cells may be countered by opposing CD8$^+$ T cell-extrinsic effects as seen in the *neu*-N LAG-3$^{-/-}$ mice, resulting in another anti-tumor cell population which becomes more activated, but also less activated adoptively-transferred cells. Based on cytokine assays of endogenous CD8$^+$ T cells in vaccinated *neu*-N and *neu*-N LAG-3$^{-/-}$ mice, this was not explained by enhanced endogenous CD8$^+$ T cell function.

Dendritic cells, potent activators of the T cell response, can become tolerogenic in the setting of tumors in mice and humans, downregulating the costimulatory molecules required for activation of T cells [10]. In the *neu*-N mouse, it was demonstrated that low dose Paclitaxel could enhance the activation status of APCs and together with 3T3neuGM vaccination, increased survival and tumor rejection through this mechanism [65]. LAG-3 is known to have different effects on the APC population; in one study, LAG-3 present on the surface of Tregs was shown to deliver an inhibitory signal through MHC II to APCs [66]. Alternatively, a soluble LAG-3-Ig fusion protein has been given as an adjuvant and appears to increase the humoral and cell-mediated response through increased APC activation [67,68]. Based on these controversial findings, the absence of LAG-3 endogenously may have either inhibitory or stimulatory effects on the APC population. The source of LAG-3 may not be of consequence as long as LAG-3 is present in the proximity of APCs, so I designed experiments to test different combinations of LAG-3 wild type and LAG-3$^{-/-}$ APCs and T cells. In Figure 5, I demonstrated that while the combination of HA LAG-3$^{-/-}$ cells with *neu*-N LAG-3$^{-/-}$ APCs resulted in the highest T cell proliferative capacity, *neu*-N APCs activated more T cell cytokine production than the *neu*-N LAG-3$^{-/-}$ APCs regardless of the T cell type, providing a partial explanation for the decreased cytokine expression seen in adoptively transferred T cells in the *neu*-N LAG-3$^{-/-}$ mice. The expression of co-stimulatory molecules and IL-12 was equally divergent in that *neu*-N LAG-3$^{-/-}$ APCs produced more IL-12, but had lower levels of CD80. The lack of a consistent phenotype failed to fully explain the differences in T cell function seen in these models.

There could also be potential contributions from other cell types which I did not explore, including plasmacytoid DCs (pDCs) and Tregs, among others. pDCs are an abundant source of soluble LAG-3 which regulates their own homeostasis and can also effect T cell homeostasis independently of CD8-intrinsic LAG-3 control of homeostatic proliferation [37]. Tregs are known to express LAG-3 and *neu*-N mice contain Tregs shown to inhibit adoptively transferred CD8^{+} T cells [50]. Blockade of LAG-3 on Tregs can inhibit their suppressive function and ectopic expression of LAG-3 can augment suppressive function of CD4^{+}CD25^{+} cells, demonstrating that LAG-3 contributes to suppression function of Tregs [36]. While I did not directly study this population, decreased Tregs or Treg function could be one explanation why the vaccine alone-treated *neu*-N LAG-3^{-/-} mice have enhanced function of adoptively transferred HA LAG-3^{-/-} cells in terms of polyfunctionality and tumor infiltration as seen in Figure 4.

While using pre-isolated CD8^{+} T cells for adoptive transfer into *neu*-N mice limits the knockout of LAG-3 to the CD8^{+} T cell, the caveat of the *neu*-N LAG-3^{-/-} mice is that the deletion of LAG-3 is not limited to a certain cell population. Thus, conditional knockouts of LAG-3 would need to be created in order to narrow down the effects of LAG-3 deletion in different cell populations on CD8^{+} T cell function and tumor immunity. Alternatively, reconstitution experiments in immunodeficient or irradiated mice may also be useful in addressing this question. While there are clearly some benefits to deletion of LAG-3 in high avidity antigen-specific CD8^{+} T cells, it remains to be seen how expression of this molecule in other cell types interacts with T cells and therefore, how practical LAG-3 will be as a cancer therapeutic.
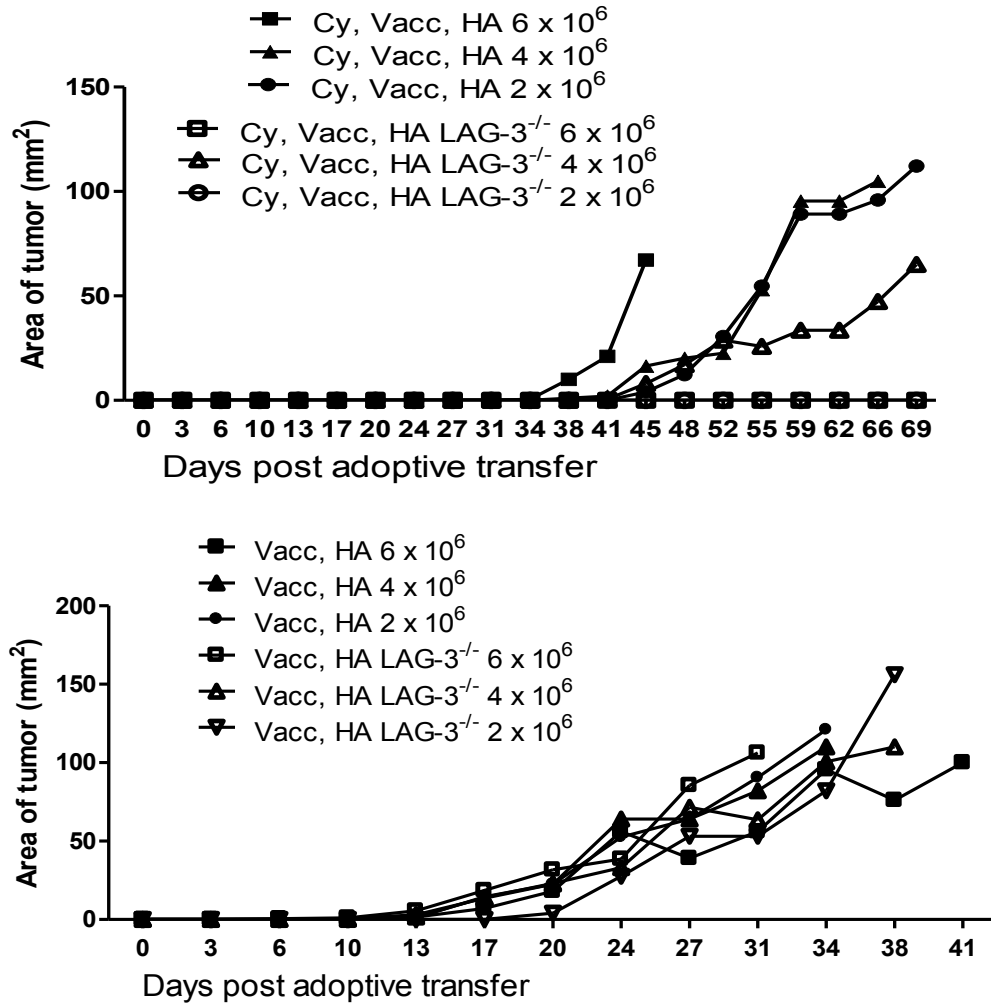
Figure 1. HA LAG-3$^{-/-}$ cells control NT2.5 tumors at lower doses than HA cells when given with Cy and 3T3neuGM vaccine. Tumor growth curves for *neu*-N mice given 5 x 10^4 NT2.5 cells subcutaneously in the mammary fat pad on day -5 and **(A)** treated with Cy (100 mg/kg) on day -2, 3T3neuGM at day -1, and an adoptive transfer of the indicated dose of high avidity or high avidity LAG-3$^{-/-}$ cells on day 0 or **(B)** treated with 3T3neuGM on day -1 and adoptive transfer on day 0 (*n* = 2 mice per treatment group and dose).

Figure 2. HA LAG-3$^{-/-}$ cells have enhanced tumor infiltration compared to HA cells in the presence of Cy and vaccine. (**A-B**) NT2.5 tumors (**A**) and tumor-draining lymph nodes (**B**) of mice treated with vaccine or with Cy and vaccine were harvested 5 days post-adoptive transfer of HA and HA LAG-3$^{-/-}$ T cells. The number of tumor-infiltrating lymphocytes was calculated based on total cells per mg of tumor or per lymph node and the percent of total cells that were CD8$^+$Thy1.2$^+$. (**C-F**) Tumor-draining nodes were removed from *neu*-N mice 3 or 5 days following adoptive transfer of T cells and cells were stained with antibodies to the following surface proteins: (**C**) α6 integrin, (**D**) β1 integrin, (**E**) α4 integrin, and (**F**) CXCR3. Mean fluorescence intensity was measured for the integrins and CXCR3 is shown by the percent of CD8$^+$Thy1.2$^+$ expressing the surface protein (*n* = 3 mice per treatment group, *p<0.05, **p<0.01, ***p<0.001).

A CD8⁺Thy1.2⁺/mg tumor

B CD8⁺Thy1.2⁺/Tumor-draining node

C Day 3: α6 Integrin   Day 5: α6 Integrin

D Day 3: β1 Integrin   Day 5: β1 Integrin

E Day 3: α4 Integrin   Day 5: α4 Integrin

F Day 3: %CXCR3⁺   Day 5: %CXCR3⁺
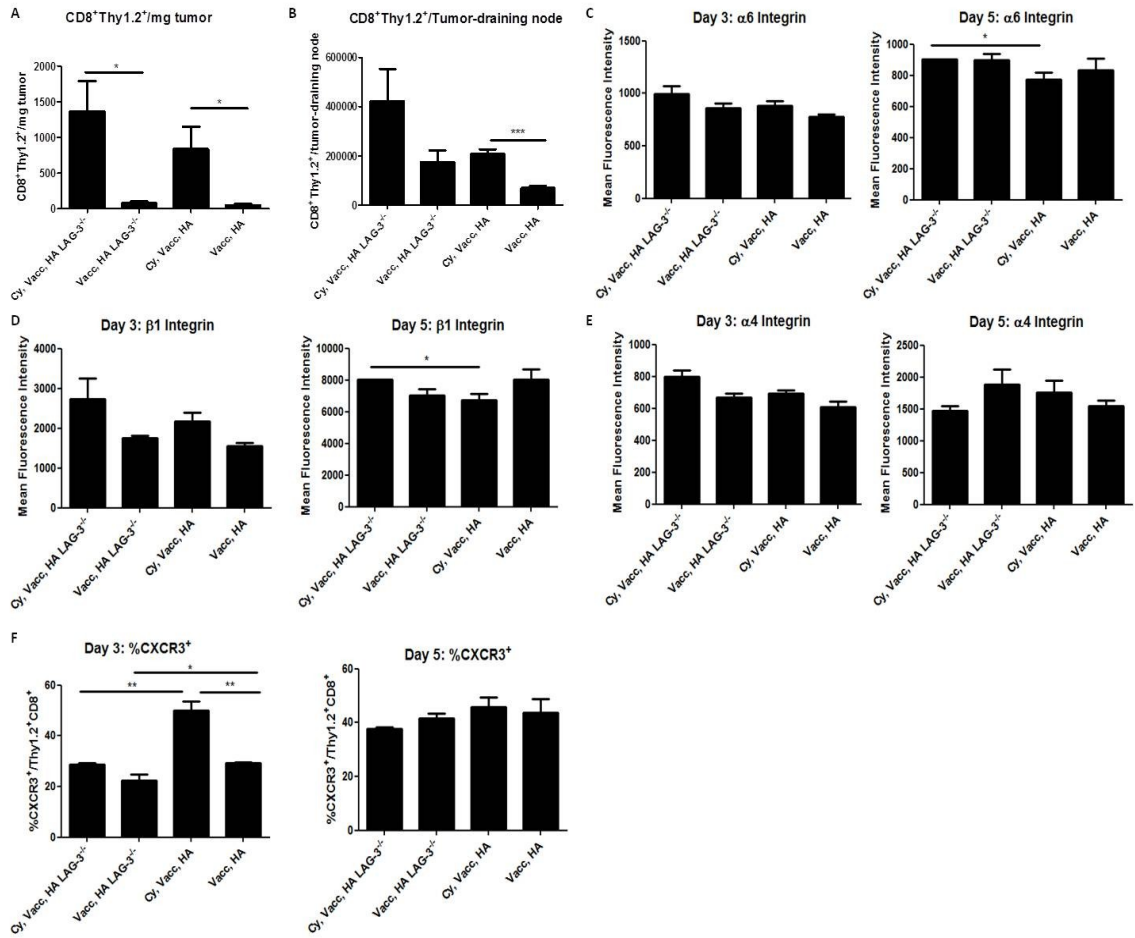
Figure 3. Cy, vaccine, and an adoptive transfer of HA LAG-3$^{-/-}$ cells result in polyfunctional T cells infiltrating tumors in *neu*-N mice. NT2.5 tumors from *neu*-N mice treated with vaccine with or without Cy were harvested 5 days post-adoptive transfer of HA or HA LAG-3$^{-/-}$ cells and adoptively transferred cells were identified by staining for the Thy1.2 marker after incubation with RNEU$^{420-429}$ and NP$^{118-126}$ peptides for 5 hours. The percentage of cells expressing each cytokine in response to RNEU$^{420-429}$ is normalized for each mouse's response to NP$^{118-126}$. (**A-E**) The total number of CD8$^+$Thy1.2$^+$ cells in each treatment group expressing the cytokine was calculated from the percentage of expressing cells and a total count of tumor-infiltrating lymphocytes. (**F**) Each pie chart shows the average percent of total cells expressing each possible combination of 0-5 cytokines and/or CD107a/b in response to RNEU$^{420-429}$ for the given treatment group. Red corresponds to expression of all 5 cytokines and purple corresponds to expression of 0 cytokines, with values in between representing particular combinations. Treatment group is denoted by: CVL: Cy, Vaccine, HA LAG-3$^{-/-}$ cells; VL: Vaccine, HA LAG-3$^{-/-}$ cells; CVH: Cy, Vaccine, HA cells; VH: Vaccine, HA cells. (**G**) Percent of CD8$^+$ Thy1.2$^+$ T cells expressing Tbet demonstrates that HA LAG-3$^{-/-}$ cells have a significantly higher percentage of Tbet expression than HA cells, with or without Cy ($n = 5$ mice per treatment group, *p<0.05, **p<0.01, ***p<0.001).

A IFNγ⁺CD8⁺Thy1.2⁺/mg tumor

B IL-2⁺CD8⁺Thy1.2⁺/mg tumor

C TNF⁺CD8⁺Thy1.2⁺/mg tumor

D GranzymeB⁺CD8⁺Thy1.2⁺/mg tumor

E CD107⁺CD8⁺Thy1.2⁺/mg tumor

F Cytokines and CD107 - number positive:

5 4 3 2 1 0

Treatment Group: CVL   Treatment Group: VL   Treatment Group: CVH   Treatment Group: VH

G %Tbet⁺/CD8⁺Thy1.2⁺
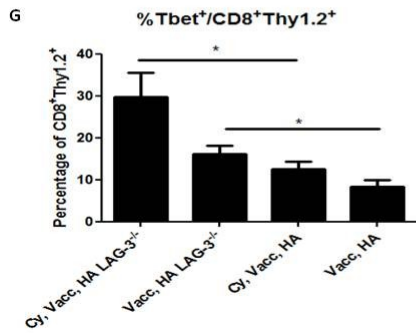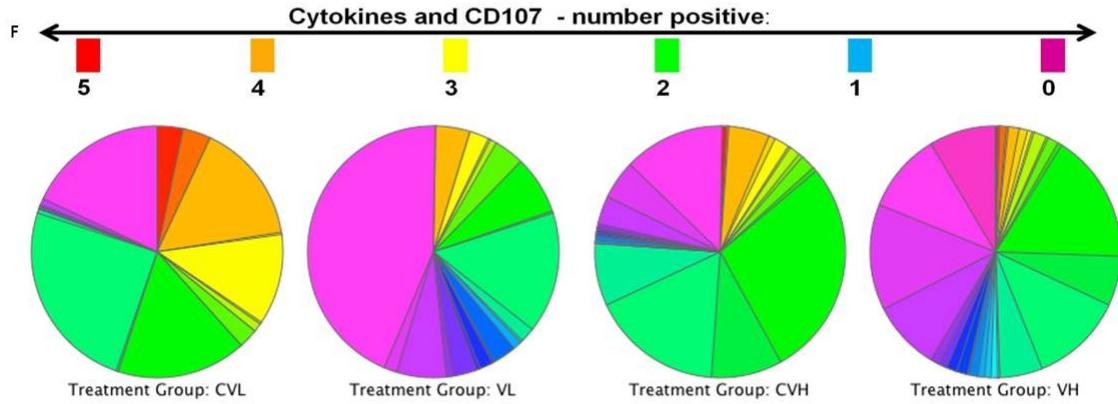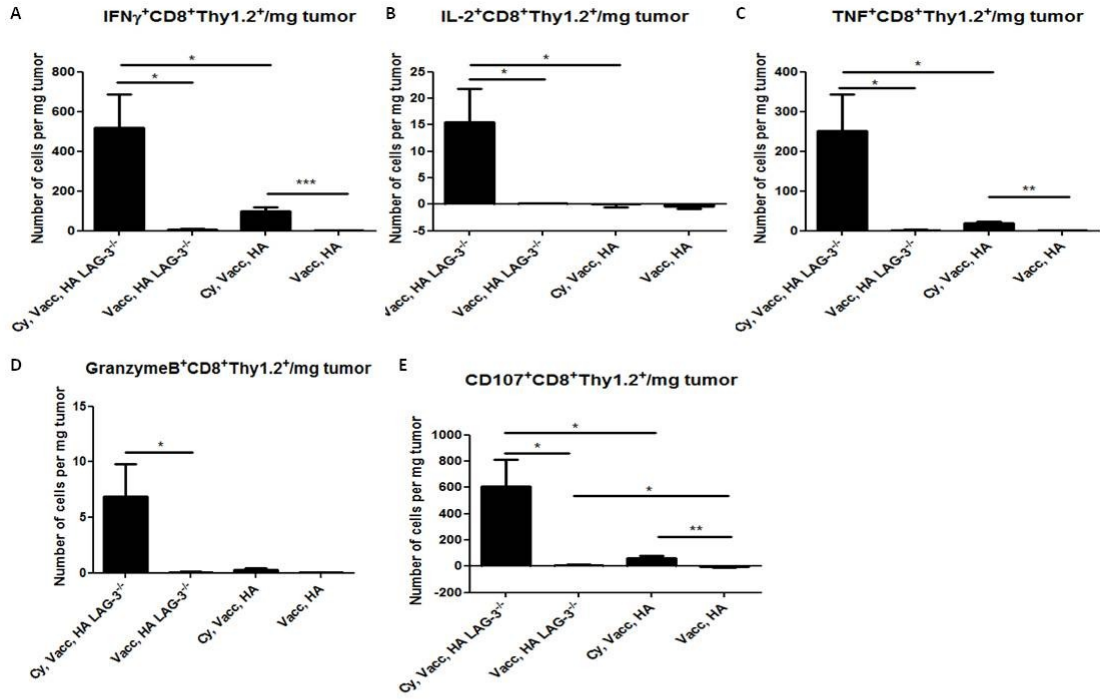
Figure 4. Endogenous deletion of LAG-3 signaling enhances tumor clearance but not activation of adoptively transferred HA cells. (**A**) *neu*-N LAG-3^{-/-} mice were challenged with NT2.5 cells and given either no treatment, vaccine alone, or vaccine and Cy with varying doses of HA or HA LAG-3^{-/-} T cells. Tumors failed to grow in mice given any dose of T cells with vaccine and with or without Cy. Treatment with vaccine resulted in statistically significant less tumor growth compared to untreated mice (p = 0.017, *n* = 2 mice per treatment group for each dose of T cells, 5-6 mice for all other treatment groups.) (**B-H**) T cell trafficking and cytokine responses to RNEU[420-429] (normalized to NP[118-126]) were compared in mice treated with vaccine, plus or minus Cy, and an adoptive transfer of HA or HA LAG-3^{-/-} T cells. In (B-G), the number of cells per mg tumor expressing each cytokine was calculated from the percentage of cells expressing each cytokine and the total of infiltrating lymphocytes per mg of tumor for each mouse. In (H), each pie chart shows the average percent of total cells expressing each possible combination of 0-5 cytokines and/or CD107a/b in response to the RNEU[420-429] for the given treatment group. Red corresponds to expression of all 5 cytokines and purple corresponds to expression of 0 cytokines, with values in between representing particular combinations. Treatment group is denoted first by host mouse and then by treatment type: CVL: Cy, Vaccine, HA LAG-3^{-/-} cells; VL: Vaccine, HA LAG-3^{-/-} cells; CVH : Cy, Vaccine, HA cells; VH: Vaccine, HA cells (*n* = 3 mice per treatment group, *p<0.05, **p<0.01).

A Tumor clearance in *neu*-N LAG-3$^{-/-}$

- Tumor
- Tumor + Vacc
- Tumor, Cy, Vacc, HA LAG-3$^{-/-}$ ‡
- Tumor, Cy, Vacc, HA ‡
- Tumor, Vacc, HA LAG-3$^{-/-}$ ‡
- Tumor, Vacc, HA ‡

‡Includes data for doses of 6×10^6, 4×10^6, 2×10^6 cells

B CD8$^+$Vβ4$^+$/mg tumor

C IFNγ$^+$CD8$^+$Vβ4$^+$/mg tumor

D TNF$^+$CD8$^+$Vβ4$^+$/mg tumor

E IL-2$^+$CD8$^+$Vβ4$^+$/mg tumor

F CD107$^+$CD8$^+$Vβ4$^+$/mg tumor

G GranzymeB$^+$CD8$^+$Vβ4$^+$/mg tumor

H Cytokines and CD107 - number positive:

5 4 3 2 1 0

Treatment Group: Neu−CVL
Treatment Group: Neu−VL
Treatment Group: Neu−CVH
Treatment Group: Neu−VH

Treatment Group: NeuLag−CVL
Treatment Group: NeuLag−VL
Treatment Group: NeuLag−CVH
Treatment Group: NeuLag−VH

42

Figure 5. *neu*-N LAG-3$^{-/-}$ do not harbor more activated anti-neu T cells, despite differences in APC activation. (A-C) *neu*-N and *neu*-N LAG-3$^{-/-}$ mice were assessed for the endogenous anti-neu CD8^{+} T cell response after vaccination. **(A)** *neu*-N LAG-3$^{-/-}$ mice have increased numbers of CD8^{+} T cells per spleen. **(B)** The average number of cells per spleen responding to RNEU$^{420\text{-}429}$ over background (irrelevant peptide, NP$^{118\text{-}126}$) for *neu*-N and *neu*-N LAG-3$^{-/-}$ mice does not significantly differ. **(C)** The individual IFNγ response to RNEU$^{420\text{-}429}$ (compared to negative control NP$^{118\text{-}126}$) is shown for all vaccinated *neu*-N and *neu*-N LAG-3$^{-/-}$ mice (*n* = 9 per group, *p<0.05). **(D-E)** CD11c^{+} cells from 9 vaccinated *neu*-N and *neu*-N LAG-3$^{-/-}$ mice each per group were incubated with CFSE-labeled CD8^{+} T cells from HA and HA LAG-3$^{-/-}$ mice. **(D)** CFSE dilution on day 7 is shown as a measure of proliferation. The percent of cells that are divided is calculated from the percentages of total cells found in CFSE peaks 3-6. **(E)** IFNγ expression was measured on day 5 from 2 wells of each combination of CD8^{+} T cells and APCs. APCs derived from vaccinated *neu*-N mice resulted in more IFNγ-producing T cells than APCs from *neu*-N x LAG-3$^{-/-}$ (*p<0.05. ****p<0.0001). **(F-G)** CD11c^{+}MHCII^{+} cells from tumor-draining lymph nodes **(F)** and vaccine-draining nodes **(G)** were stained for co-stimulatory surface markers and IL-12 one week after vaccination of *neu*-N and *neu*-N x LAG-3$^{-/-}$, that also received adoptive transfer of T cells and in some groups (as indicated), Cy (*n* = 2 per treatment group, *p<0.05, **p<0.01).
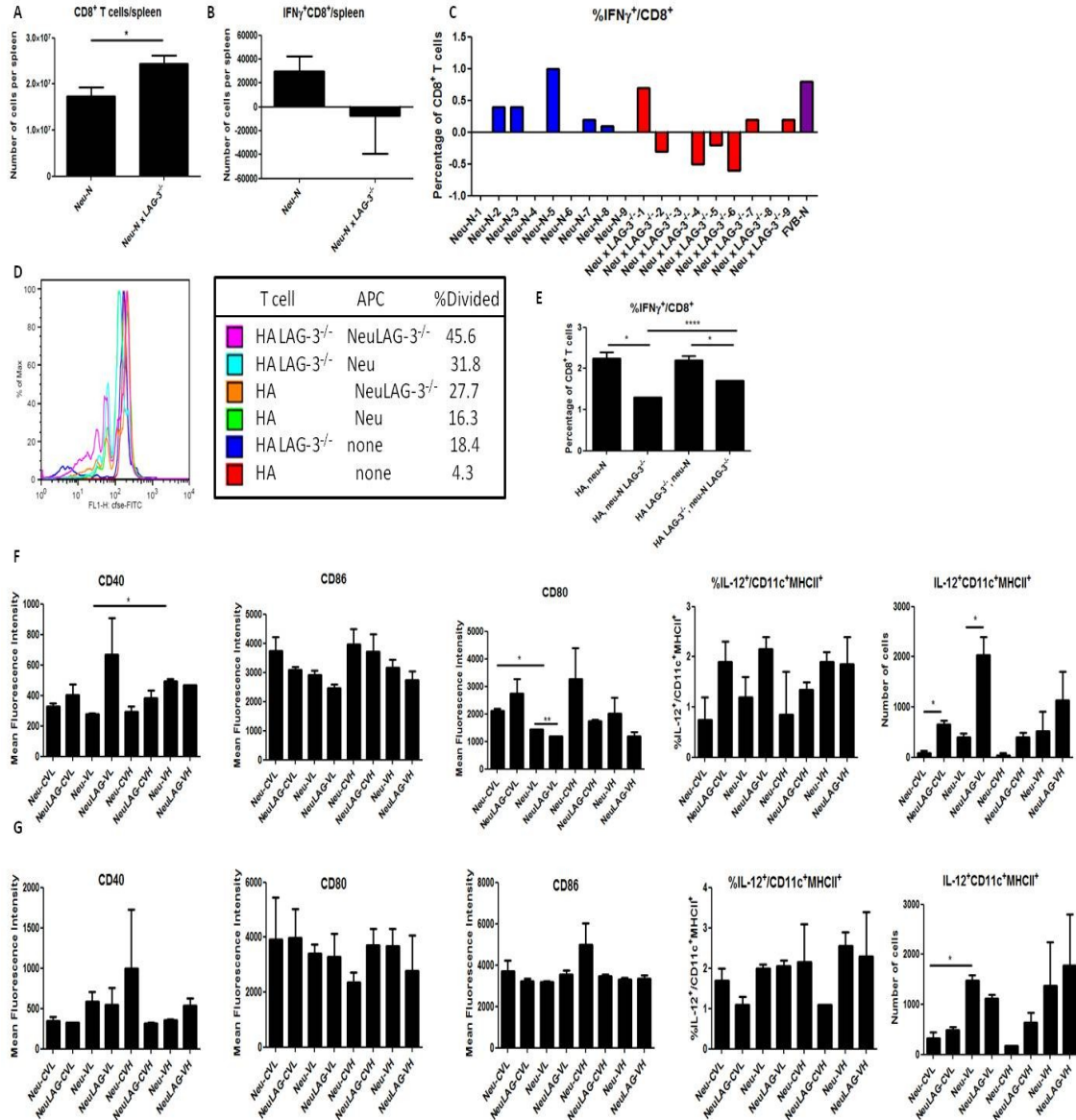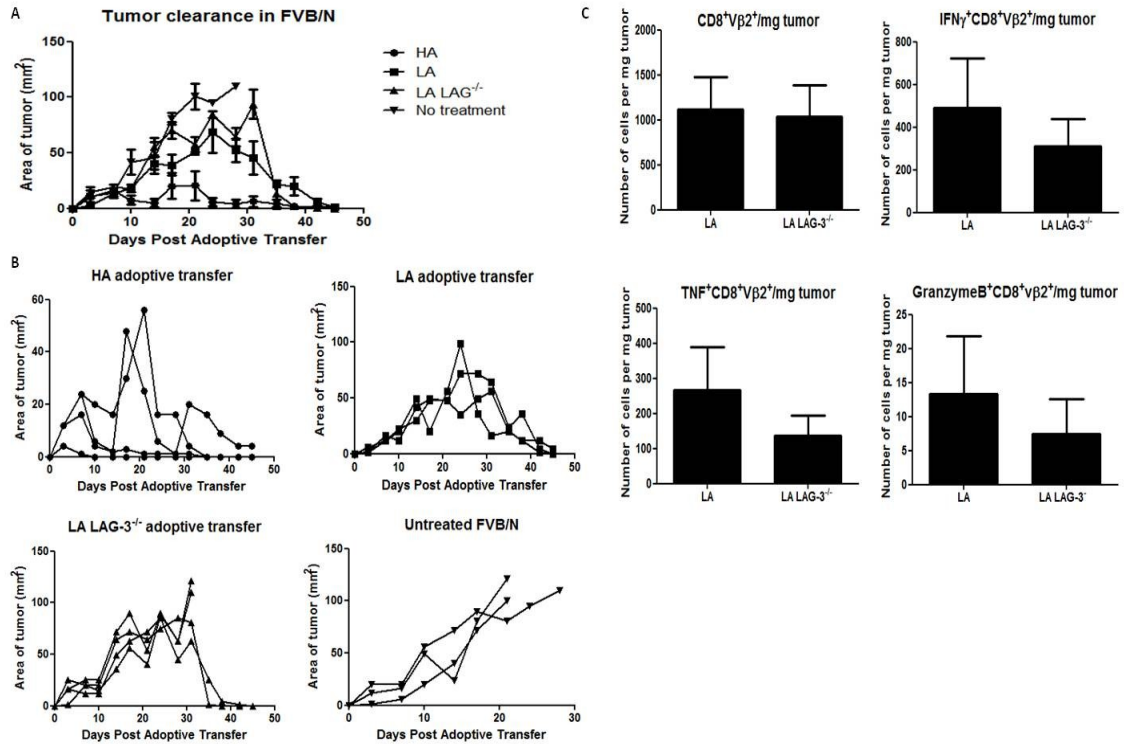
Figure 6. LAG-3 deletion in LA cells does not augment their function in FVB/N tumor-bearing mice. (A-B) Growth curves of mean tumor size (A) and individual mouse tumor growth curves (B) for FVB/N mice given 2 x 10^6 NT2.5 tumor cells and left untreated or treated with 6 x 10^6 HA, LA, or LA LAG-3$^{-/-}$ cells (n=3-4 per treatment group.) **(C)** Number of cells infiltrating NT2.5 tumors and producing each cytokine in FVB/N mice given 5x 10^6 NT2.5 cells and Cy, vaccine, and an adoptive transfer of 6 x 10^6 LA or LA LAG-3$^{-/-}$ cells. There was no significant difference between the two groups in any of the cell numbers (n=5 per group).

Chapter 3: A LISTERIA MONOCYTOGENES VACCINE TARGETING MUTATED KRAS, AN EARLY GENETIC EVENT IN PANCREAS CANCER DEVELOPMENT, PREVENTS PRE-MALIGNANT TUMOR PROGRESSION IN COMBINATION WITH TREG DEPLETION

Introduction

Pancreatic ductal adenocarcinoma (PDA) is clinically difficult to treat due to its late detection and resistance to conventional therapies. However, recent studies suggest that the process of PDA development from tumor initiation to metastasis formation requires years to decades for completion, providing a window of opportunity for prevention and treatment during the stage when pre-cancerous lesions, known as pancreatic intra-epithelial neoplasms (PanIN), are predominant [69]. One potential treatment approach involves the development of immunization strategies that target the driver genes, early genetic changes that initiate pre-malignant lesion formation.

Immune tolerance mechanisms to self-antigens are significant barriers to anti-tumor immunotherapy, especially once PDA has developed [70-72]. Treatments that break or bypass tolerance and induce a specific anti-tumor immune response in the periphery are still relatively ineffective due to the local immunosuppressive mechanisms at the site of the tumor. While LAG-3 is one checkpoint molecule upregulated on tumor antigen-specific T cells, the site of tumor development in pancreatic cancer harbors many additional immunosuppressive signals and cells populations which include Tregs, tolerogenic antigen presenting cells (APCs) and myeloid derived suppressor cells

(MDSC), and immunosuppressive cytokines (i.e. IL-4, IL-10, TGF-β) [10,73-75]. Of these barriers to effective cancer immunotherapy, Tregs and MDSC, have been shown to be increased in the peripheral blood and tumors of PDA in mice and patients [51,71,73,76]. Both Tregs and CD11b$^+$Gr-1$^+$ MDSC have been shown to inhibit protective CD8$^+$ T cell responses and to promote PDA growth [77-79]. Treatments that deplete or inhibit the activity of Tregs, such as low dose Cyclophosphamide (Cy) and anti-CD25 inhibitory monoclonal antibodies, have enhanced T cell activation by antigen-targeted vaccine approaches against many cancers including PDA in numerous pre-clinical and clinical studies [16,78]. Both Cy and the murine anti-CD25 antibody, PC61, appear to enhance T cell trafficking into tumors, allowing tumor eradication, by increasing the effector T cell to Treg ratio within the tumor and tumor draining lymph nodes, key sites of Treg accumulation and activation in mice [50,75,78].

Genetically engineered mice that mimic the genetic induction and progression of tumors at the natural organ site allow for the study of the immune response to cancer and its precursor lesions within the tissue specific microenvironment and in the context of natural regulatory mechanisms that result in tolerance to the initiating oncogene products [51]. The *Kras$^{G12D/+}$;Pdx-1-Cre* and *Kras$^{G12D/+}$;Trp53$^{R172H/+}$;Pdx-1-Cre* mice are genetically programmed to mimic the progression from normal tissue through all stages of pre-malignant PanIN lesions, and *Kras$^{G12D/+}$;Trp53$^{R172H/+}$;Pdx-1-Cre* mice progress onto fully developed PDA which recapitulates human PDA in both genetic and histological features [80,81]. This mouse model also possesses the advantage of mimicking the local immunosuppressive environment at the site of tumor development, including the

desmoplastic response which occurs in the stroma of pancreatic cancer as a response to tumor development. While transplantable tumor models such as the Panc02 mouse tumor model which has been used to study pancreatic cancer and the HER2/neu-expressing tumor line NT2.5 which has been used to study breast are useful for studying the effectiveness of various immunotherapy approaches, the *Kras$^{G12D/+}$;Trp53$^{R172H/+}$;Pdx-1-Cre* mouse model has the advantage of re-creating the microenvironment in the natural site of tumor development and therefore, gives the closest approximation of human tumor development [78].

The *Kras$^{G12D/+}$;Trp53$^{R172H/+}$;Pdx-1-Cre* mice have been reported to exhibit Treg infiltration of late stage PanINs and PDA [51]. Here we report for the first time the observation that Treg infiltration occurs as early as PanIN stage 1. In addition, we show that immunization with a *Listeria monocytogenes (*LM) vaccine genetically modified to express the driver *Kras^{G12D}* gene product (LM-Kras) induces a systemic CD8$^+$ T cell response directed against the oncogenic Kras protein at all stages of pre-malignant lesion formation. However, LM-Kras vaccination given together with Treg depletion at the time of PanIN 1 slows progression to PDA whereas the combination fails to slow progression when given at the time of PanIN stage 2-3 development. Importantly, the cytokine milieu is directed in favor of T cells secreting IFNγ and IL-17 that is associated with increased effector CD8$^+$ T cell infiltration and prevention of early PanIN progression. Combination immunotherapy is also associated with the influx of CD11b$^+$Gr-1$^+$ cells secreting immunostimulatory cytokines that have lost the ability to suppress CD8$^+$ T cells. These

findings have implications for the design of future immunotherapies for cancer and its pre-malignant precursors.

Materials and Methods

Mice

Lox-STOP-Lox (LSL)-*Trp53*$^{R172H/+}$*; LSL-Kras*$^{G12D/+}$*;* and *Pdx-1-Cre* strains on a mixed 129/SvJae/C57BL/6 background, were a gift from Dr. David Tuveson (Cold Spring Harbor Laboratory, Cold Spring, NY). These mice were backcrossed to the C57BL/6 genetic background and interbred to obtain *LSL-Kras*$^{G12D/+;}$*Pdx-1-Cre* and *LSL-Kras*$^{G12D/+;}$*LSL-Trp*$^{53R172H/+;}$*Pdx-1-Cre* mice, herein referred to as *Kras*$^{G12D/+}$*;Pdx-1-Cre* (KC) and *Kras*$^{G12D/+}$*;Trp53*$^{R172H/+}$*;Pdx-1-Cre* (KPC). Genotyping was performed according to gene assays as previously described and genotyping services were provided by Transnetyx, Inc. [80,81]. Animals were kept in pathogen-free conditions and treated in accordance with institutional and American Association of Laboratory Animal Committee approved policies. All animal studies were approved by the Institutional Animal Care and Use Committee of the Johns Hopkins University.

Patients and tumor samples.

Mesothelioma biopsies were collected from a subject on study #ADU-CL-02, a phase I study evaluating the safety and induction of immune response of CRS-207, a LM vaccine targeting mesothelin, in combination with chemotherapy in patients with malignant pleural mesothelioma [82]. Patients signed an informed consent after approval of the study by the institutional review board.

Listeria monocytogenes (LM) construct

LM strains were derived from the DP-L4056 strain that had been deleted for both the *actA* and *inlB* open reading frames as described [83]. The double 12 ras expression cassette was designed in silico to fuse the 25 amino acids of both V and D activating mutations (at position 12) in a synthetic gene codon optimized for expression in *LM* with Gene Designer software and synthesized (DNA2.0, Menlo Park, CA) [84]. The synthetic gene was cloned downstream of the *actA* promoter in a derivative of the vector pPL2 and stably integrated at the *tRNA*[Arg] locus of the bacterial chromosome as described previously [83]. All molecular constructs were confirmed by DNA sequencing. A schematic of the antigen construct is shown in **Figure 1A**.

LM Vaccine Preparation and Injection

Experimental stocks were prepared by growing bacteria to early stationary phase, washing in PBS, resuspending at approximately 1×10^{10} cfu/ml in PBS plus 10% glycerol, and freezing aliquots at -80 °C for later use. 5×10^5 cfu in 0.2 ml PBS were injected via the tail vein based on dose titrations for each batch of vaccine.

GM-CSF-secreting tumor cell vaccine

GM-CSF-secreting cell line B78H1-GM was grown and prepared as previously described [78]. The KPC tumor cell line was created from a spontaneously arising KPC

mouse tumor by digesting the diced tumor in RPMI 1640 plus 5% FBS, collagenase and hyaluronidase at 37°C for 1 hour, passing through a 100 μm strainer to obtain a single cell suspension, and culturing the cells in RPMI 1640 media containing 20% FBS, 1% L-glutamine, 1% MEM NEAA, 1% sodium pyruvate, 0.5% penicillin/streptomycin, and 0.2 units/mL insulin. Non-adherent cells were aspirated off the culture flask and epithelial cells were purified from fibroblasts by serial trypsinization. The vaccine was prepared by washing cells twice in PBS, mixing cells at a 1:1 ratio, and irradiating at 50 Gy. 4-6 week old KPC mice were injected with 3×10^6 cells of each line in three injections of 0.1 ml subcutaneously to one forelimb and both hindlimbs.

Survival Experiments

The anti-CD25 depleting monoclonal antibody, PC61 (ATCC), was produced from hybridoma supernatant as previously described [78]. Cyclophosphamide (Cytoxan, Cy, Bristol Myers Squibb) was reconstituted in sterile water at 20 mg/ml and then diluted in sterile PBS. KPC mice age 4-6 weeks or 8-14 weeks were treated with intraperitoneal (IP) PC61 (50 μg per mouse) and Cy (100 mg/kg), one day prior to vaccine injection as per experimental design. This regimen was repeated according to group assignment every 4 weeks and survival monitored weekly. Moribund animals were euthanized in accordance with institutional policies.

Splenocyte intracellular cytokine assays

Peptides were synthesized at >95% purity by the Peptide Synthesis Facility (Johns Hopkins, Baltimore, MD). 7 days after vaccination, mice were sacrificed and splenocytes were harvested. Splenocytes were briefly treated with ACK Lysis Buffer (Quality Biological Inc.) for red blood cell lysis. $CD8^+$ T cells were negatively selected using the Dynabeads Mouse Untouched CD8 Cells (Invitrogen), and then incubated for 5 hours with $T2K^b$ cells pulsed with the indicated peptides in the presence of GolgiStop (BD Biosciences) as per the manufacturer's instructions. Following incubation, cells were harvested, stained with CD3-APC (145-2C11), CD8-PerCP (53-6.7, BD Pharmingen) and then permeabilized with CytoFix Fixation Buffer, washed with Perm/Wash Buffer (BD Biosciences), and stained with interferon-gamma (IFNγ)-PE (XMG1.2, BD Pharmingen). To stain for intranuclear transcription factors, the PE anti-mouse/rat Foxp3 staining set (eBioscience) was used to fix, permeabilize, and stain cells with Foxp3-PE (FJK-16s, eBioscience) as per the manufacturer's instructions. Data was collected using a FACSCalibur and CellQuest Pro (BD Biosciences) and analyzed using Flowjo software (Treestar, Inc.).

Isolation of pancreatic infiltrating leukocytes and intracellular cytokine assays

Isolated pancreata were weighed, diced, and incubated with collagenase (1 mg/ml, Sigma) and hyaluronidase (25 mg/L, Sigma) for 30 minutes at 37^oC followed by passage through a 40 μm nylon cell strainer. Single cell suspensions were stained with CD3-APC-Cy7 (145-2C11, BioLegend), CD8-Pacific Blue (53-6.7, BD Pharmingen), CD4-Pacific

Orange (RM4-5, Invitrogen Molecular Probes) or CD4-PerCP (GK1.5, Biolegend), CD44-Alexa Fluor (AF) 700 (IM7, BD Pharmingen), and CD62L-AF647 (MEL-14, Biolegend). For cytokine assays, lymphocytes from pancreata were isolated as above and purified by Percoll gradient (GE Healthcare). Lymphocytes were stimulated with anti-CD3/CD28 beads (Invitrogen Dynal AS) overnight at 37°C followed by a 5 hour incubation with Golgistop, fixed and permeabilized, and stained with IFNγ-AF700 (XMG1.2, BD Pharmingen), TNF-AF488 (MP6-XT22, BD Pharmingen), IL-17-AF647 (eBio17B7, eBioscience), Foxp3-V450 (MF23, BD Horizon), Tbet-PE-Cy7 (4B10, eBioscience) and RORγt-PE (Q31-378, BD Pharmingen). For T cell cytokine analysis, lymphocytes from up to 3 mouse pancreata were pooled and stained as one flow cytometry sample due to small cell numbers. In assays for IL-17, IMDM (Gibco, Life Technologies Corporation) supplemented with 5% FCS, 1% L-glutamine, 1% penicillin/streptomycin, and 5×10^{-5} M β-mercaptoethanol was used for cell culture. For myeloid cell stains, the Percoll-purified cells were stained with CD45-APC-Cy7 (30-F11, BD Pharmingen), CD11b-PE-TexasRed (M1/70.15, Invitrogen), F4/80-PE-Cy7 (BM8, eBioscience), Gr-1-AF700 (RB6-8C5, BD Pharmingen) or Ly6G-V450 (1A8, BD Horizon) and Ly6C-PerCP-Cy5.5 (HK1.4, Ebioscience) and following fixation/permeabilization, IL-12-APC (C15.6, BD Pharmingen) and IL-10-V450 (JES5-16E3, BD Horizon). Prior to staining, all samples were incubated with Live/Dead Fixable Dead Cell Stain Kit (Invitrogen Molecular Probes) to assess cell viability and anti-CD16/CD32 antibody (Fc Block, BD Biosciences). Flow cytometry was performed using an LSR II and analyzed using FACSDiva software (BD Biosciences).

CD8, IL-17, and Ly6G Depletion Assays

The CD8-depleting antibody 2.43 (500 mg intraperitoneal injection) [48] or control rat IgG (Jackson ImmunoResearch Inc.) was given every other day for one week prior to vaccine treatment, followed by twice weekly injections throughout the 5 week course of two cycles of therapy with PC61, Cy, and LM-Kras. CD8 depletion was verified routinely throughout the study by flow cytometry. Anti-IL-17 antibody, a gift from Dr. Jerry Niederkorn [85], or rat IgG control was given in a 200 µg dose twice a week for the first week of treatment, followed by 100 µg twice weekly treatments for the duration of a five week cycle of treatment with LM-Kras and PC61/Cy four weeks apart, with harvest one week after the second vaccine. Anti-Ly6G antibody, 1A8, (Bio X Cell) was administered at a 0.5 mg dose 3 times in the first week of the experiment, followed by 0.25 mg twice a week for the following 4 weeks.

Immunohistochemistry (IHC)

Immunohistochemistry was carried out according to standard protocols [86]. Briefly, for CD4 and CD8 stains, pancreata were frozen in Tissue-Tek OCT (Sakura Finetek USA, Inc) with liquid nitrogen and cut in 5 µm sections using a cryostat, followed by -20°C acetone fixation. Sections were incubated with 5 µg/ml primary antibodies to CD4 (H129.19), CD8 (53-6.7), or isotype control (R35-95) (BD Pharmingen) for 1 hour and with biotin-conjugated secondary antibody (G28-5, BD Pharmingen) for thirty minutes. For Foxp3, F4/80 and Ly6G staining, pancreata were fixed in 10% neutral buffered

formalin (VWR International), embedded in paraffin and sectioned by the Johns Hopkins Medical Institutions Reference Histology Laboratory. Tissue sections were subjected to antigen retrieval by steam heating in Citra antigen retrieval solution (BioGenex) or for F4/80 antibody, proteinase K (Dako). The following antibodies were used: anti-F4/80 (Serotec, C1:A3-1, 1:100), anti-Ly6G (BD Bioscience, 1A8, 1:2000) and the corresponding biotinylated secondary antibodies (1:200, Vector Laboratories). For Foxp3, slides were stained by the Johns Hopkins IHC laboratory using the Envision FLEX, high pH system (Dako) for automated Dako platforms with a 1:100 dilution of anti-mouse Foxp3 antibody (Abbiotec, LLC.). For patient samples, sections were stained with anti-CD3 (2GV6, Ventana Medical Systems, Inc.) using ultraView Detection (Ventana Medical Systems, Inc.) according to standard Ventana protocols in the Johns Hopkins University Immunopathology Lab. For RORγt (6F3.1, EMD Millipore Corporation), antigen retrieval was performed with EDTA at 95°C for 20 min and slides were stained using Leica auto stainers and Bond Polymer Refine Detection (Leica Microsystems Inc., Buffalo Grove, IL). All slides were imaged using an Eos Rebel T2i camera (Canon U.S.A.) and Eclipse TS100 microscope (Nikon Inc.).

Histological analysis of pancreatic lesions

Pancreata were formalin fixed and paraffin embedded, cut at 4 μm thickness and stained using routine H&E staining protocols by the Johns Hopkins Reference Histology Lab and Tissue Microarray Lab. For analysis of vaccine and Treg depletion effect(s),

slides from each mouse pancreas were characterized based on number of each PanIN stage or PDA and graded based on highest stage PanIN (or PDA) present. For the CD8 depletion and IL-17 depletion studies, the Cavalieri estimator method was employed to estimate PanIN or PDA volumes present in the pancreata [87]. Two H&E-stained sections per pancreas spaced 400 microns apart were digitally scanned at 20x magnification (0.498 micrometers per pixel) using a ScanScope CS (Aperio, Inc., San Diego, CA). The whole slide images (WSIs) were then analyzed using the Cavalieri estimator implemented in custom Java software. Briefly, a point counting grid with a grid spacing of 75 micrometers was applied to each WSI. Intersection points that fell on each of all the following histologic features were counted: tissue, ADM, PanIN-1, PanIN-2, PanIN-3, and PDA and the percent tissue occupied by each type was calculated for each WSI. This software can be downloaded at https://bitbucket.org/tcornish/point-counting.

Suppression Assay, Cytokine Array, and Co-culture Conditions

Naïve $CD8^+$ T cells were isolated from spleens of C57Bl/6 mice and labeled with CFSE as previously described [50]. $CD11b^+Gr-1^+$ cells were isolated from the pancreas of KPC mice and stained as previously stated, followed by fluorescence-assisted cell sorting (FACS) of the $CD45^+CD11b^+Gr-1^+$ population using a FACSAria II (BD Biosciences). $Gr-1^+$ cells were incubated in a 1:1 ratio with $CD8^+$ T cells for 72 hours in the presence of Dynabeads Mouse T-Activator CD3/CD28 (Invitrogen) in HL-1 media (Lonza) for the suppression assay and in IMDM for the ICS. For the ICS of IL-17, those wells also

contained 0.02 μg/ml TGFβ and IL-6 (Shenandoah Biotechnology, Inc.) and 10 μg/ml anti-IL4 and anti-IFNγ (11B.11 and XMG1.2, Bio X Cell) for 72 hours. For the cytokine array, the pancreata of mice in a treatment group were pooled, Gr-1^{+} cells were sorted with FACS and lysed according to instructions, and lysate was blotted with the Mouse Cytokine Antibody Array, Panel A (R & D Systems). The resulting dot blot was scanned and analyzed using VisionWorks LS (UVP, LLC) to calculate density per pixel. The densities were used to calculate fold change of the treated groups over the untreated Gr-1^{+} cells.

Statistical analysis

Statistical significance was analyzed using GraphPad Prism (GraphPad Software, Inc.) and assessed using a two-tailed student T test. Welch correction was used when the variance was assumed to be unequal. For survival analysis, Log-rank (Mantel-Cox) test was used. For data included in the suppression assay, two experiments were normalized to a scale based on third experiment to account for variation of baseline proliferation between assays. Significance was defined as $p<0.05$. All experiments were repeated three times unless otherwise noted.

Results

LM-Kras induces systemic $CD8^+$ T cell responses in $Kras^{G12D/+}$-expressing mice

The $Kras^{G12D/+}$;*Pdx-1-Cre* (KC) and $Kras^{G12D/+}$;$Trp53^{R172H/+}$;*Pdx-1-Cre* (KPC) transgenic mouse models in which the pancreas is genetically programmed to develop pre-malignant PanINs prior to malignant PDA provides the opportunity to develop vaccine strategies that can be employed at an early stage of cancer development when fewer mechanisms of immune tolerance would be expected to be at play. Mutant Kras was chosen as a target for immunotherapy because it is the most prevalent and earliest oncogene known to be involved in human PDA development [88]. The bacterial vector, LM, was selected to target Kras since LM vaccines have been shown to be efficacious in multiple preclinical models of infectious disease and cancer [89-91]. In addition, a safe and bioactive dose was recently reported for the treatment of patients with PDA [82]. LM vaccines directly infect APCs (dendritic cells and macrophages) and LM-expressed antigens are presented on both MHC class I and class II molecules due to the natural lifecycle of LM, which after initial entry into APCs via the phagosome, replicates in the cytosol [89]. In addition, inflammatory cytokines produced by infected APCs foster a Th1 immune response favorable to anti-tumor immunity [91]. I therefore employed this model to test the hypothesis that an LM vaccine expressing mutated $Kras^{G12D}$ (LM-Kras) would induce $Kras^{G12D}$-specific $CD8^+$ T cell responses capable of slowing PanIN progression. I used an attenuated LM strain deficient in the virulence factors ActA and InlB that is being developed clinically for treating patients with PDA and that was further modified

59

with a vector designed to express and secrete a portion of the Kras protein encompassing the G12D mutation (**Figure 7A**) [82,92].

The LM-Kras vaccine was first tested for the ability to induce CD8$^+$ T cell reactivity against the Kras^{G12D} target. To accomplish this, the specific 9 amino acid (9-mer) peptides presented by the MHC I allele, H-2K^b, expressed by transgenic mice, were identified using a previously described strategy that screens overlapping peptides for recognition by activated immunized lymphocytes using an intracellular cytokine secretion assay (ICS) (**Figure 7B**) [61]. It was confirmed that vaccinated non-tolerant, MHC-matched mice harbor significant numbers of CD8$^+$ T cells that secrete IFNγ in response to multiple mutant Kras epitopes (Kras B-G) in contrast to the control tyrosinase-related protein 2 (Trp2) epitope which also binds the MHC I K^b allele (**Figure 7C**). I next evaluated whether the LM-Kras vaccine can induce similar Kras-specific T cells in KC mice that do express the Kras protein mutated at position 12. KC mice vaccinated with the same LM-Kras vaccine showed a similar level of vaccine induced Kras-specific IFNγ CD8$^+$ T cell responses as vaccinated parental mice (**Figure 7D**). Similar responses were also seen in KPC mice (**Figure 7E**). These responses peaked at day 7 post-vaccination and declined by day 14 post-vaccination, the kinetics of which are similar to what is observed for LM-induced CD8$^+$ T cell responses specific for other antigens (**Figure 7D**) [90]. Kras-specific CD8$^+$ T cell responses were not detected in unvaccinated mice suggesting that the mutation itself is not naturally immunogenic (**Figure 7D**). Surprisingly, these studies failed to identify differences in the magnitude of Kras-specific CD8$^+$ T cell responses in the non-tolerant parental versus the transgenic

mice expressing the Kras[G12D] mutation (**Figure 7F**). Thus, these data demonstrate that the LM-Kras vaccine can induce a sizable systemic CD8$^+$ T cell response against mutant Kras in both parental and potentially tolerant KC and KPC mice.

Inhibition of PanIN progression requires both Treg depletion and LM-Kras

The next question was whether these Kras-specific T cell responses in Kras-mutated mice correlated with a delay in PanIN development and with prolonged survival. A previous study reported that Tregs are present in PanINs and PDA of KPC mice [51]. On further evaluation of the kinetics of Treg infiltration, it was found that Foxp3$^+$ cells are an early inflammatory change, present even at the time of the earliest stage of PanIN development, PanIN 1, and continue to increase with progression to malignancy (**Figure 8A**). While both an anti-IL2Rα (CD25) monoclonal antibody and low dose cyclophosphamide (Cy) have been shown to deplete Tregs and improve survival in mice and patients, a combination of the murine anti-CD25 antibody, PC61, and Cy, resulted in the most complete depletion of Tregs in one PDA mouse model [16,55,78]. As shown in other models, the combination of Treg-depleting agents given with vaccine resulted in a significant depletion of splenic CD4$^+$Foxp3$^+$ T cells when compared to vaccine alone-treated mice (**Figure 8B-C**).

Therefore, a combination of PC61 (50 μg) and Cy (100 mg/kg) given 1 day prior to vaccination was used to test the ability of LM-Kras given alone or with Treg depletion to inhibit tumors and prolong survival. The KPC rather than KC mice were used for this

experiment because the *Trp53*^{R172H/+} mutation is required for development of cancers at a predictable rate, which facilitates survival analysis. Two age groups were evaluated for survival, mice less than 2 months of age (low grade PanINs predominate), and mice older than 2 months of age (high grade PanINs predominate), to determine the effects of the vaccine relative to the degree of PanIN development at the time of initial vaccination. Neither the LM-Kras vaccine alone nor the Treg-depleting agents (PC61 plus Cy) given alone affected survival when treatment was given to either age group. However, combination therapy with the LM-Kras vaccine and Treg depletion with PC61 and Cy conferred a significant survival advantage to animals given treatment early, at the time of PanIN 1 development, but not to mice beginning treatment at the time of later stage PanIN 2 and 3's (**Figure 8D-E**). These data provide evidence that Treg depletion enhances a vaccine's ability to improve survival of mice treated at early stages of PanIN development, but not when treatment is initiated at later stages of PanIN development. Furthermore, the failure of LM-Kras and Treg depletion to delay PanIN progression in mice with later stage PanINs was not due to poor antigen-specific CD8$^+$ T cell generation as systemic CD8$^+$ T cell responses to LM-Kras did not significantly differ between 4-6 week and 8-12 week old KPC mice (**Figure 8F**).

To confirm that the combination of vaccine and Treg depletion was slowing PanIN progression, similarly designed experiments were conducted to perform histological analyses of the pancreas of mice beginning treatment at less than 2 months old using the same treatment groups as in Figure 8D and harvested after two cycles of treatment. Mice given LM-Kras in combination with PC61 and Cy showed fewer late

stage PanINs and fewer occurrences of PDA (**Figure 8G**). Thus, at 5 weeks following initiation of immunotherapy, the overall lower stage of PDA development in mice treated with combination therapy is consistent with improved survival seen in Figure 8D.

Combination immunotherapy alters local Treg to effector T cell ratio

I hypothesized the vaccine enhancing effects of PC61 and Cy were mediated through the enhanced induction of Kras-specific CD8$^+$ T cell responses. KPC mice with early stage PanINs were vaccinated at 4-6 weeks old and again one month later, with or without PC61/Cy pretreatment. Splenocytes were isolated and analyzed for IFNγ production in response to one of the mutated Kras peptides, KrasF, by ICS one week after the second vaccination. The response to the ovalbumin H-2K^b-binding peptide, SIINFEKL (Ova), was also assessed since the LM-Kras construct contains this immunogenic positive control peptide to confirm vaccine potency. Interestingly, administration of PC61/Cy one day prior to LM-Kras vaccination decreased the systemic response to KrasF peptide when compared to LM-Kras vaccination alone as measured by percent of splenic CD8$^+$ T cells producing IFNγ (**Figure 9A**). In contrast, there was no significant difference between splenocyte CD8$^+$ T cell responses measured against Ova between LM-Kras and PC61/Cy versus LM-Kras alone (**Figure 9A**). While the total numbers of CD8$^+$ T cells responding to either Ova or KrasF decreased with combination therapy compared to LM-Kras alone, this was not statistically significant and was not as profound for Ova as it was for KrasF, indicating that this was not solely due to the non-

antigen-specific deletion of T cells by PC61 and Cy (**Figure 9A**). Furthermore, the percentage and total number of splenic CD4$^+$ T cells from the same mice that produced IFNγ in response to non-antigen specific activation was not altered by PC61 and Cy (Kras peptides were not available for CD4$^+$ T cells) (**Figure 9B**).

Both PC61 and Cy deplete Tregs, which can inhibit the activation and trafficking of vaccine-induced effector T cells, systemically and within tumors and tumor draining lymph nodes [93-95]. Analysis of the CD4$^+$ T cell populations by flow cytometry demonstrated a statistically significant decrease in CD4$^+$Foxp3$^+$ T cells relative to CD4$^+$Foxp3$^-$ T cells in the pancreas-draining lymph nodes of mice with early stage PanINs receiving PC61 and Cy plus the LM-Kras vaccine when compared to vaccine alone for 2 months (**Figure 9C**). While the depletion of CD4$^+$Foxp3$^+$ T cells within the pancreas at this time point by flow cytometric staining did not achieve statistical significance (**Figure 9C**), decreased Tregs were evident by IHC staining for Foxp3 in pancreata from mice treated with PC61 and Cy plus LM-Kras (**Figure 9D**).

Increasing evidence demonstrates that the ability of effector T cells to traffic to the tumor microenvironment correlates best with tumor regression rather than a specific quantity of systemically measured T cell responses [50,96]. In untreated KPC mice, effector CD8$^+$ T cells fail to infiltrate PanINs and PDA [51]. I therefore evaluated whether PC61 and Cy given with the LM-Kras vaccine sequestered the effector T cell populations from the periphery, recruiting them into the pre-malignant pancreas. In support of this hypothesis, I observed a significant increase in the number of CD3$^+$ T cells within the pancreata of mice treated with PC61 and Cy with LM-Kras relative to the LM-Kras alone-treated mice

(**Figure 9E**). This increase in CD3$^+$ T cells included both significantly more CD8$^+$ and CD4$^+$Foxp3$^-$ T cells (**Figure 9E**). The presence of increased numbers of CD4$^+$ and CD8$^+$ T cells in mice treated with PC61, Cy, and the LM-Kras vaccine was confirmed by immunohistochemistry (IHC) (**Figure 9F**).

Combination immunotherapy alters the cytokine milieu in PanINs

Along with an influx of CD4$^+$ and CD8$^+$ T cells into the pancreas, a higher percentage of the CD4$^+$Foxp3$^-$ and CD8$^+$ T cells found within PanINs of mice treated with Cy/PC61 and LM-Kras were CD62L^{low}CD44^{high}, indicating an antigen-experienced phenotype when compared with the vaccine alone group (**Figure 10A**). Although attempted, the small number of cells in the pancreas limited the use of an ICS assay to assess the T cell response to Kras with peptides directly *ex vivo*. However, anti-CD3/CD28 beads were used to stimulate lymphocytes isolated from the pancreata of LM-Kras treated and LM-Kras plus PC61/Cy-treated mice that began immunotherapy treatment at 4-6 weeks of age, allowing for evaluation of the cytokine profile of all PanIN-infiltrating T cells. In the mice receiving combination therapy, there were significantly more IFNγ and TNFα-producing CD4$^+$ T cells and increased numbers of IL-17-producing CD4$^+$ T cells (**Figure 10B**). Increased numbers of Tbet$^+$CD4$^+$ T cells were observed in mice receiving the combination of PC61 and Cy with the LM-Kras vaccine and there was a trend towards increased RORγt$^+$CD4$^+$ T cells, the transcription factors regulating Th1 and Th17 responses, respectively (**Figure 10D**). Despite smaller numbers

of CD8$^+$ T cells within the pancreas, there was also a trend toward increased IL-17, IFNγ, and TNFα-producing CD8$^+$ T cells with the combination of LM-Kras and PC61/Cy treatment, as well as greater numbers of Tbet$^+$ and RORγt$^+$CD8$^+$ T cells (**Figures 10C and E**).

I further investigated the ability of LM-Kras to produce IL-17 responses in the tumor microenvironment and the periphery. First, I used a GM-CSF-secreting irradiated tumor cell vaccine derived from KPC tumors (GVAX), similar to vaccines which are currently in clinical trials for human PDA, to test the ability of other vaccine platforms to induce IL-17-secreting cells in mouse PDA. IL-17 production was not unique to LM-Kras and PC61/Cy as GVAX in combination with PC61/Cy also appeared to induce IL-17-secreting CD4$^+$ and CD8$^+$ T cells in PanINs of treated mice, although not to the extent of LM-Kras (**Figures 11A-B**). Secondly, as the production of IFNγ by T cells in the spleen following LM-Kras had been demonstrated and decreased peripheral numbers of these cells in the spleen correlated with enhanced numbers in the tumor microenvironment, I similarly assayed CD4$^+$ and CD8$^+$ splenocytes for the production of IL-17 to determine the relationship to IL-17-producing cells in the pancreatic microenvironment. In contrast, CD4$^+$ and CD8$^+$ T cells from the spleens of both LM-Kras alone and LM-Kras plus PC61/Cy-treated mice failed to produce IL-17 above background levels present in the untreated mice (**Figures 11C-D**). Therefore, the peripheral response to LM-Kras does not seem to explain IL-17 production in the tumor microenvironment and this response is likely shaped from additional factors relating to local populations of cells, potentially including the depletion of Tregs.

CD8$^+$ T cells and IL-17 are required for delaying PanIN progression

To confirm that the delay in PanIN progression to PDA observed in KPC mice treated with PC61/Cy and LM-Kras during early PanIN development is CD8$^+$ T cell dependent, 4-6 week old mice were treated with LM-Kras plus Cy and PC61 and with either the CD8-depleting antibody, 2.43 [19], or a control antibody. Mice were sacrificed 5 weeks after completing two LM-Kras and Cy/PC61 treatment cycles (age 9-11 weeks). Since these younger treated mice are expected to have lower stage PanINs at this early time point and this time point was too early to observe major differences in survival or tumor development, we quantified the percent of the total tissue area per slide occupied by acinar-ductal metaplasia (ADM), PanIN 1, 2, 3, and PDA using a stereology method [87] rather than giving each pancreas a single grade representing the predominant lesion stage. KPC mice receiving PC61/Cy and LM-Kras immunotherapy with the control (rat IgG) had a lower percentage of tissue occupied by late stage PanINs (PanIN 2 and 3) when compared to mice receiving the same treatment and CD8$^+$ T cell depletion, while levels of ADM and low grade PanINs (PanIN 1) were similar in both groups (**Figures 12A-B**). CD8-depletion did not have an effect on PanIN stage in unvaccinated mice, consistent with the lack of CD8$^+$ T cells in the pancreas of untreated mice (**Figures 12C-D**). While it cannot be determined if CD8$^+$ T cell-depleted mice would have developed PDA at a faster rate given this early time point, the data suggest that effector CD8$^+$ T cells induced by the combination therapy are at least partially responsible for protection against the progression of early to late stage PanINs. As shown in Figures 9 and 10, CD4$^+$ T cell

infiltration is also enhanced in the pancreas of KPC mice treated with PC61/Cy and LM-Kras, with increased Th1 and Th17 subsets and a decreased Treg subset, suggesting that Th1 and Th17 effectors likely contribute to inhibition of PanIN progression as well. As total CD4$^+$ T cell depletion may have a mixed effect due to the various CD4$^+$ T cell subtypes found in pancreata of treated KPC mice and Th1 cells already have a recognized role in protecting against cancer, I tested the effect of IL-17 depletion in KPC mice treated similarly to mice in the CD8$^+$ depletion experiments [97]. As before, pancreata were harvested in the fifth week of treatment and the percent of tissue occupied by each PanIN stage was assessed by the stereology method. KPC mice treated with LM-Kras and PC61/Cy with ongoing IL-17 depletion had similar amounts of tissue occupied by ADM and PanIN 1, but a significantly increased percent of tissue with late stage PanINs (2 and 3) and PDA when compared to mice treated with PC61/Cy and LM-Kras and a control antibody (**Figures 12E-G**). There were no significant differences in IL-17-depleted or control-treated KPC mice that did not receive the LM-Kras vaccine and Treg depletion (**Figures 12H-I**). Thus, these studies confirm that both CD8$^+$ T cells and IL-17 secreting effector T cells are each contributing to the slowing of PanIN progression following Treg depletion given with the LM-Kras vaccination.

LM-Kras and PC61/Cy enhances the recruitment of pancreatic Gr-1$^+$ cells

MDSC have been shown to infiltrate PanINs and PDA in KPC mice, promoting tumorigenesis and inhibiting effector T cells [51,77]. I also observed an intense infiltration of

mixed morphology leukocytes by H&E stain in late stage PanINs and PDA, regardless of treatment group. This was an interesting observation given the presence of IL-17-producing T cells in the pancreata of LM-Kras and PC61/Cy-treated mice, which can recruit monocytes, macrophages, and neutrophils [98]. I evaluated the effect of immunotherapy on myeloid cell recruitment more systematically with flow cytometry and IHC. First, I investigated the effect of LM-Kras and PC61/Cy individually on the systemic myeloid populations. The effect of PC61 and Cy, with or without LM-Kras, was a significant increase in the percentage of Ly6G$^-$Ly6C^{high} cells, with a trend towards a higher percent of Ly6G$^+$Ly6C^{low} cells, in the spleen (**Figure 13A**). With PC61 and Cy alone, there was also a statistically significant expansion of F4/80$^+$ macrophages compared to LM-Kras alone or the combination of LM-Kras and PC61/Cy (**Figure 13A**). In the pancreatic microenvironment, total Gr-1$^+$ cells, including both Ly6G$^-$Ly6C^{high} and Ly6G$^+$Ly6C^{low} populations, were of similar or increased total number as well as by percentage of total CD11b$^+$ cells in LM-Kras plus PC61/Cy-treated mice when compared to LM-Kras alone or untreated mice of the same age (**Figures 13B-D**). There was no statistically significant difference in the number or percent of F4/80$^+$ macrophages in LM-Kras plus PC61/Cy-treated mice compared to vaccine alone or untreated mice (**Figure 13E**). Ly6G$^+$Ly6C^{low} cells were the predominant Gr-1$^+$ population identified with flow cytometry so the Ly6G marker was chosen for IHC. Ly6G$^+$ cells began infiltrating in mid-stage PanINs and increased with progression to PDA in untreated KPC mice (**Figures 13F-H**). In comparison to similarly staged untreated mice, both LM-Kras alone and LM-Kras plus PC61/Cy-treated mice also had abundant infiltration of Ly6G$^+$ cells (**Figures 13I-K**). F4/80$^+$ macrophages were less numerous, but nevertheless also

showed a similar increased infiltration with progression from early stage PanIN to PDA in untreated KPC mice (**Figures 13L-N**) and were similar in abundance between treated and untreated mice (**Figures 13O-Q**).

LM-Kras and Treg depletion repolarize PanIN-infiltrating Gr-1$^+$ cells

As the number of Gr-1$^+$ myeloid cells and F4/80$^+$ macrophages was either increased or unchanged with LM-Kras and PC61/Cy treatment compared to untreated KPC mice, I hypothesized rather than inhibiting innate immune cells from infiltrating the pancreas, that the phenotype of these cells was altered by immunotherapy. Although CD11b$^+$Gr-1$^+$ cells have previously been shown to be suppressive in the KPC mouse model of PDA, Ly6C and Ly6G are expressed by both the immature and mature counterparts of cells in the myeloid and granulocytic lineages and potentially represent less suppressive cell populations in our treatment model [99]. As with T cells, innate immune cells can be either pro-tumorigenic (M2/N2-polarized macrophages and neutrophils) or anti-cancer (M1/N1-polarized macrophages and neutrophils) depending on the microenvironment cytokine milieu [4]. I investigated IL-12 and IL-10 production by CD11b$^+$Gr-1$^+$ and F4/80$^+$ cells from the pancreata of mice treated with two cycles of LM-Kras, LM-Kras with Cy/PC61, or left untreated, and found that LM-Kras with or without Treg depletion was able to induce IL-12 secretion in Gr-1$^+$ cells, which resulted in an increased total number of IL-12-secreting Gr-1$^+$ cells in LM-Kras and PC61/Cy-treated pancreata (**Figure 14A**). While PanIN-infiltrating macrophages also produced IL-12,

there were no statistically significant differences between groups, except for in the percentage of IL-12-producing cells between LM-Kras alone and untreated mice (**Figure 14B**), demonstrating that while macrophages may also be repolarized by LM-Kras, the predominant shifts between treatment groups occur in Gr-1$^+$ population. There was no significant difference in IL-10 production by F4/80$^+$ macrophages or Gr-1$^+$ cells by percentages or total numbers (**Figure 14B**). CD11b$^+$Gr-1$^+$ cells from the pancreata of treated mice also secreted higher levels of many other immunostimulatory cytokines than untreated mice (**Figure 14C**). PC61/Cy and LM-Kras-treated Gr-1$^+$ cells were capable of producing more cytokines than LM-Kras alone-treated Gr-1$^+$ cells although either treatment resulted in upregulation of these pro-inflammatory cytokines compared to untreated Gr-1$^+$ cells. These included chemokines responsible for recruiting myeloid and lymphoid cells such as CCL-1, CCL-2 (MCP-1), CCL-3 (MIP-1α), CCL-4 (MIP-1β), CCL-5 (RANTES), CCL-11 (Eotaxin), CCL-12 (MCP-5), CXCL-2 (MIP-2), CXCL-9 (MIG), CXCL-10 (IP-10), CXCL-12 (SDF-1), M-CSF, and IL-16, and the N1-associated cytokines TNFα, IL-12, IFNγ, IL-6 , and IL-7. There was an upregulation of cytokines responsible for promoting Th(c)1 and Th(c)17 responses (IL-23, IL-12, IFNγ, and IL-27), and a downregulation of IL-4, responsible for promoting Th2 responses. Due to limited number of cells from each mouse and the large amount of cell lysate needed for this type of analysis, I used pooled cell lysate from all of the CD11b$^+$Gr-1$^+$ sorted cells in one treatment group and thus, the resulting data is more qualitative, rather than quantitative, in nature but serves to demonstrate that Gr-1$^+$ cells from treated pancreata secrete more pro-inflammatory cytokines.

Using CD11b$^+$Gr-1$^+$ cells sorted from the pancreata of KPC mice treated with LM-Kras with or without Treg depletion or left untreated, I analyzed suppressive capability on naïve isogenetic CD8$^+$ T cells stimulated with anti-CD3/CD28 beads for 3 days. Due to the small numbers of cells available for the suppression assay which limited the number of replicates for any given experiment, this experiment was repeated several times and the results of 3 individual experiments are shown. CD11b$^+$Gr-1$^+$ cells isolated from untreated KPC pancreata suppressed T cell proliferation while LM-Kras and Cy/PC61-treated Gr-1$^+$ cells caused levels of cell division in naïve CD8$^+$ T cells which were closest to CD8$^+$ T cells stimulated in the absence of Gr-1$^+$ cells, as shown in one representative experiment (**Figure 14D**). LM-Kras and PC61/Cy treatment induced Gr-1$^+$ cells which allowed for significantly higher T cell proliferation than Gr-1$^+$ cells from untreated pancreata in two of the three experiments and showed the same trend in a third (**Figure 14E**). LM-Kras alone-treated Gr-1$^+$ cells cultured with CD8$^+$ T cells resulted in an intermediate amount of cell division compared to the effects of LM-Kras and Cy/PC61-treated and untreated Gr-1$^+$ cells, in one representative experiment (**Figure 14D**). Repeated experiments revealed significantly enhanced proliferation of T cells when cultured with LM-Kras-treated Gr-1$^+$ cells compared to untreated Gr-1$^+$ cells (**Figure 14E**).

CD11b$^+$Gr-1$^+$ cells fail to drive cytokine production of T cells

72

Based on my findings that CD11b$^+$Gr-1$^+$ cells from LM-Kras and PC61/Cy-treated KPC pancreata were less suppressive to CD8$^+$ T cell proliferation and secreted many cytokines which could be responsible for recruiting and shaping the T cell response, I evaluated the ability of Gr-1$^+$ cells to drive cytokine production in both naïve T cells and in the tumor microenvironment. First, to determine the role of CD11b$^+$Gr-1$^+$ cells in T cell production of IFNγ and IL-17 in mice treated with LM-Kras and PC61/Cy, Ly6G$^+$ cells were depleted with an anti-Ly6G monoclonal antibody throughout the course of treatment, as Ly6G$^+$Ly6C^{low} are the main Gr-1$^+$ cell population in the pancreata of KPC mice. In verifying that Ly6G$^+$ cells were depleted, one caveat of this study was uncovered in that Ly6G$^-$Ly6C^{high} cells expanded in the spleen and pancreata of mice treated with the antibody to Ly6G (**Figures 15A-B**). There was no effect on F4/80$^+$ cells in the spleen or pancreas (**Figures 15A-B**). Without Ly6G$^+$ cells in the pancreas microenvironment, there was no significance change in the amount of cytokines produced by CD4$^+$ and CD8$^+$ T cells by the percentage of cells expressing IL-17 or IFNγ nor by the total number of cytokine-producing cells per mg of pancreas compared to isotype control-treated mice (**Figures 15C-D**). While this suggests that CD11b$^+$Ly6G$^+$ cells are not responsible for driving IFNγ or IL-17 production in pancreatic lymphocytes, it is also possible that there is redundancy and that another cell population such as Ly6G$^-$Ly6C^{high} cells can contribute to T cell phenotype in the absence of Ly6G$^+$ cells.

Thus, to more directly evaluate the effect of the pancreatic Gr-1$^+$ cells on shaping the T cell cytokine profile, I isolated CD11b$^+$Gr-1$^+$ cells from the pancreata of KPC mice left untreated or treated with LM-Kras alone or in combination with Treg depletion and

cultured them with naïve syngeneic $CD4^+$ and $CD8^+$ T cells in the presence of anti-CD3/CD28 beads or for the IL-17 ICS assay, anti-CD3/CD28 beads, IL-6, TGFβ, anti-IFNγ and anti-IL-4 as naïve T cells are unlikely to develop to a IL-17-producing phenotype without additional signals. $Gr-1^+$ cells from PC61/Cy and LM-Kras-treated and LM-Kras-treated mice had no effect on IL-17 or IFNγ in both $CD4^+$ and $CD8^+$ T cells compared to $Gr-1^+$ cells derived from untreated KPC pancreata (**Figure 15E**). The only observed change in cytokine production was that co-culture with $Gr-1^+$ cells from any treatment group decreased the percentage of T cells that could produce cytokines in comparison to the stimulated T cells alone, although this could have been a non-specific effect and the percentage of cells producing cytokine did not reach the low level observed for non-stimulated T cells. Overall, this demonstrates little evidence for the capability of $CD11b^+Gr-1^+$ cells to drive either Th(c)1 and Th(c)17 phenotypes although it is possible that they contribute to the maintenance of these in the tumor microenvironment along with other cell populations and signals present in mice treated with immunotherapy. It is also possible that their recruitment and phenotype is induced by activated T cells versus inducing or maintaining activated T cells themselves.

Increased RORγt-expressing human lymphocytes following Listeria administration

Listeria vaccines are being actively evaluated in several clinical trials in settings of advanced cancer using the same attenuated vector utilized here to target mutated Kras. We therefore evaluated lymphocyte subsets from patient tumors following *Listeria*

administration to determine whether IL-17 is a mediator of LM vaccine response in patients [82]. We obtained tissue from a patient with malignant pleural mesothelioma who received CRS-207, a recombinant *Listeria* vaccine expressing mesothelin [82], prior to vaccination and following 2 prime vaccination doses given 2 weeks apart. Staining for RORγt revealed enhanced staining at the post-LM time point (**Figure 16A**). Staining of serial sections from each time point with anti-CD3 revealed that the intranuclear RORγt staining correlated with CD3$^+$ cells in the post-LM biopsy (**Figure 16B**). CD3$^+$ cells in the pre-LM biopsy were negative for RORγt (**Figure 16A-B**).

<u>Discussion</u>

In this chapter, I report several new findings relevant to the treatment of pancreatic cancer and premalignant lesions with immunotherapy. First, a *Listeria monocytogenes* vector targeting the earliest driver gene in pancreatic cancer initiation, mutated Kras, can prolong PanIN progression to PDA and increase survival in young mice with the earliest stages of PanINs only when Tregs are simultaneously reduced within the pancreata. Second, vaccination with LM-Kras is able to induce Kras-specific T cell responses that are necessary but not sufficient to delay PanIN progression in Kras-expressing mice that are genetically programmed to develop the multiple stages of pre-malignant PanINs prior to developing PDA. Third, prolonged survival as a result of vaccination with the LM-Kras vaccine given in sequence with Treg depleting therapy is associated with enhanced T cell trafficking into the pancreas and an alteration in cytokine profiles toward increased IFNγ, TNFα, and IL-17. Fourth, Treg depletion together with an LM-Kras vaccine shifts the immunosuppressive phenotype of innate immune cells present in PanINs towards a more immunostimulatory anti-tumor population.

This is the first example of a vaccine targeting the initiating driver gene for a non-virus induced cancer that can prevent pre-malignant lesion progression. Specifically, a LM vaccine targeting the earliest mutated gene, Kras, that is involved in PDA development, is effective in prolonging survival in KPC mice. This vaccine is only effective when given early at the time of the earliest genetic alteration and even at this earliest stage requires Treg depletion within the pancreata. This result is consistent with our finding that Tregs are present in early PanIN lesions and increase in abundance with

PanIN progression and invasive tumor development. These data support the testing of vaccine based therapy in patients who are at high risk for developing cancer and also highlights the importance of initiating cancer immunotherapy at an early stage of disease development. The fact that the LM-Kras vaccine worked best at preventing progression of the earliest PanIN lesions and did not have an effect on mice harboring more advanced pre-malignant PanINs was not surprising since pre-clinical models demonstrate that vaccines can work well in cancer bearing mice, but only when paired with modulation of the pre-existing systemic and local tolerance to tumor antigens [49,71,78]. Our findings are consistent with data from studies testing two human vaccines that are approved for preventing virus-associated cancers, HPV-associated cervical cancer and HBV-associated hepatomas. Even though these vaccines target virally associated proteins that should be perceived as foreign by the immune system, both vaccines work best when given to young individuals who have not yet been exposed to the virus and its proteins [100,101]. Taken together, these observations would suggest that mechanisms of immune suppression within the target organ of cancer development occur very early, at the time of the earliest genetic alteration and the development of the earliest pre-malignant lesion. Thus, future studies should evaluate immune-suppressing mechanisms within target organs in which pre-malignant lesions develop to identify the multiple mechanisms involved in early immune suppression.

Cancer progressed when KPC mice were treated with the LM-Kras vaccine alone even though the vaccine induced a significant peripheral CD8$^+$ T cell response directed against an epitope within the Kras protein containing the oncogenic mutation,

demonstrating that the induction of T cells by a LM vaccine targeting a mutation does not constitute effective anti-tumor immunity or true breaching of "self-tolerance." This data is consistent with previous findings that elevated levels of systemic T cell responses to a viral HPV antigen encoded by LM vaccines do not correlate with efficacy in an orthotopic model of cervical cancer [102] despite a well documented requirement for CD8$^+$ T cells for efficacy of the vaccine [89]. Furthermore, systemic CD8$^+$ T cell responses to tumor antigens are insufficient for preventing disease progression in patients with PDA and malignant melanoma [74,103]. These data also have implications for developing vaccine approaches that target multiple mutations within a sequenced tumor, an approach that is being developed as part of individualized vaccine therapy for cancer treatment [104,105]. Specifically, targeting mutated proteins, even recently developed mutations, may not be enough on its own to overcome immune tolerance mechanisms at the tumor site.

Both PC61 [93,106] and Cy [94,95] have been shown to reduce Treg numbers and function within developing tumors and their draining lymph nodes, improving effector T cell number and function within the nodes and facilitating trafficking into tumors [50,106]. However, this has been shown mainly in transplantable tumors derived from cancer cell lines and grown subcutaneously in mouse models. The KPC mouse model mimics naturally developing human PDA, a tumor characterized by hypovascularity and surrounded by a dense fibrotic stromal response [53,107]. Unlike transplantable PDA, spontaneously developing pancreatic tumors in mice are resistant to gemcitibine unless the stromal desmoplastic reaction is inhibited [54,108]. PanINs and PDA in this mouse model may also differ in susceptibility to penetration by other chemotherapeutic agents,

including Cy, explaining the statistically significant depletion of Tregs in the draining lymph nodes but not the tumor. Regardless, Cy and PC61 had an effect on the number of Tregs found in the tumor draining lymph node, an important site for orchestrating tumor antigen tolerance [14,75] and correlated with an increase in both CD8$^+$ and CD4$^+$ effector T cell numbers in the pancreas.

Cy has also been shown to have additional effects on the cytokine milieu in the tumor microenvironment, promoting the development of both IL-17 and IFNγ-secreting T cells [109,110]. In our study, there was a shift towards increased numbers of Th1 and Th17 cells in mice treated with the LM-Kras vaccine given with PC61 and Cy as compared to mice treated with the LM-Kras alone, and depletion of IL-17 throughout treatment with combination immunotherapy abrogated the combination treatment's effect on slowing of PanIN progression to PDA. Recent evidence has shown that in addition to traditional Th1 effector cells, Th17 cells also have potent anti-tumor effects. In a transplantable melanoma model, adoptively transferred Th17 CD4$^+$ T cells were superior to Th1 CD4$^+$ T cells as measured by dendritic cell and CD8$^+$ T cell recruitment and tumor eradication, which may be due in part to the ability of Th17 cells to persist and develop into other Th subsets *in vivo* [111,112]. Increasing evidence supports the concept of plasticity among the different CD4$^+$ T cell subsets and the existence of pathogenic and non-pathogenic populations even with the same defined Th subset [4,113]. Tc1 and Tc17 cells have both been shown to be effective in mouse tumor models through different mechanisms; Tc1 directly through the expression of tumor-cytotoxic IFNγ, and Tc17 through the capability to secrete IFNγ and IL-17 as well as maintain a central memory phenotype in vivo [114-116].

Additionally, the production of IFNγ and cytotoxic effects of Tc17 cells can be potentiated by IL-12, a cytokine produced in response to natural *Listeria* infection and the LM vaccine used in our study, and a cytokine I also observed produced in response to LM by innate cells in the pancreas [91,116]. Although IL-17 has also been implicated in the recruitment of neutrophils and MDSC which can promote cancer progression, IL-17 can also recruit tumor-associated neutrophils which promote anti-cancer responses, depending on the context and tumor type [117,118]. It is possible that our observation of Th1/Th17 and Tc1/Tc17 phenotypes represents a period during which T cell subsets are undergoing reprogramming in response to the change in the microenvironment, in this case due to treatment with the LM-Kras vaccine and removal of Tregs. If true, this would provide a window of opportunity for re-directing a potentially pro-oncogenic or inhibitory inflammatory response in the cancer susceptible organ microenvironment, to an effective anti-tumor immune response.

Cells of both neutrophil and macrophage lineages accumulate with increasing frequency with PanIN progression, underscoring the concept that inflammation caused by acute and chronic pancreatitis is associated with pancreatic cancer development [119,120]. Cytokines such as IL-8 and GM-CSF, which can recruit innate inflammatory cells, are induced by Kras signaling pathways that are activated in PDA precursors [77,79,121]. Additional inflammatory mediators play a role in PDA progression, including NF-κB, STAT3 and matrix metalloproteinases [122-124]. Constitutive activation of these pathways leads not only to inhibition of apoptosis in pre-neoplastic and PDA cells, but also, to innate inflammatory cell recruitment and signaling [122-124]. Subsequent fibrotic remodeling

of the stroma and release of pro-inflammatory cytokines and proliferative factors promotes further genetic alterations and suppresses protective immune responses [107,125]. Surprisingly, I found that LM-Kras given with PC61 and Cy in early stage PanINs, actually enhanced the prevalence of CD11b$^+$Gr-1$^+$ cells, including both granulocytic Ly6G$^+$Ly6C^{low} and monocytic Ly6G$^-$Ly6C^{high} cells. However, I also found that the addition of LM-Kras, with or without Treg depletion, resulted in a higher percentage of IL-12-producing Gr-1$^+$ cells in the tumor microenvironment and numbers of these IL-12-producing cells were the greatest with LM-Kras and Cy/PC61. One potential explanation for this change in phenotype is pro-inflammatory cytokines secreted after infection of APCs by LM, including IL-12 [91]. IL-12 with Cy co-administration has been shown to alter the phenotype of cells infiltrating tumors from MDSC to less suppressive immature myeloid cells [126]. Additional cytokines and chemokines secreted by the less suppressive Gr-1$^+$ population in LM-Kras and PC61/Cy-treated mice may actually enhance the protective T cell response, which is further supported by the ability of Gr-1$^+$ cells from treated mice to stimulate, rather than suppress, T cell proliferation. To this end, I tested the direct effect of Gr-1$^+$ cells from the pancreata of treated or untreated mice on naïve T cells to drive cytokine production and found that the effects of Gr-1$^+$ cells from LM-Kras-treated and Treg depleted KPC mice were minimal. Despite differences in suppressive capability and production of immunostimulatory cytokines, Gr-1$^+$ cells did not seem to directly shape the phenotype of CD4$^+$ or CD8$^+$ T cells; however, it is possible that they play a role in maintenance of T cell activation and phenotype in the tumor microenvironment. At the very least, the lack of suppression from MDSC (which has previously been shown in this model of pancreatic cancer) likely contributes to a more

productive and protective T cell response [77]. Further studies are required to investigate additional alterations in inflammatory signals and cell populations in the developing pancreatic tumors and the role of vaccination and Treg depletion in these tumor microenvironment changes. Polarization of these cells towards an anti-tumor phenotype should serve as a therapeutic goal in the treatment of PDA, both in the early and late stages.

Listeria vaccines represent an effective strategy for inducing immune responses to tumor antigens. In our study, the altered LM vector was transformed with a construct encoding a segment of the Kras gene containing the G12D mutation, a common mutation in human PDA and the same mutation found in the KPC transgenic mouse model [80,88]. However, this vector is easily modified to express other cancer-associated proteins, can express multiple antigens within the same vector, and has shown safety and the induction of immune responses in patients with PDA [82]. Furthermore, LM vaccination was associated with enhanced RORγt expression in a *Listeria*-treated patient with malignant mesothelioma. While these studies will need to be expanded as clinical trials utilizing LM vaccines in cancer patients progress, this suggests LM vaccines may be particularly efficacious in inducing potent anti-cancer phenotypes in tumor-infiltrating lymphocytes.

Despite effective induction of immune responses with LM-Kras vaccination, this was not sufficient to protect against PDA and delay progression of PanINs unless intervention included Treg-depleting therapies and was initiated at an age representative of the earliest PanIN stages. Early intervention with the combination of LM-Kras vaccination and Treg suppression resulted in activated $CD8^+$ and $CD4^+$ T cells at the site

82

of tumor development and decreased the suppressive phenotype in myeloid cells found infiltrating PanINs. Future vaccine strategies require incorporating agents designed to alter the inflammatory milieu within the developing tumor's microenvironment, even when designed for prophylactic treatment of patients with premalignant lesions or with a genetic predisposition for cancer development.

Figure 7. Immunogenicity of the LM-Kras vaccine. (**A**) Synthetic 12ras construct. Activated ras 25mers cloned downstream of the actA promoter are connected with a linker and tagged with immunologic positive control T cell epitopes for Balb/c mice ("A", SYIPSAEKI) and C57BL/6 mice ("B", SIINFEKL) as well as a C-terminal antibody epitope ("C", Myc). (**B**) Sequence of epitopes used to test immunogenicity of the LM-Kras vaccine, with mutant residue 12 in bold. (**C**) 129/SvJae/C57Bl/6 mice ($n = 5$) were injected with LM-Kras via tail vein and 7 days later splenic $CD8^+$ T cell responses were assessed after incubation with the indicated peptide and $T2K^b$ cells by intracellular staining for IFNγ. Significantly increased levels of IFNγ-producing $CD8^+$ T cells were noted for Kras B, Kras C, Kras D, Kras E, Kras F, and Kras G. (**D**) 6-9 week old KC mice were vaccinated with the LM-Kras vaccine or left untreated. At 7 or 14 days post-vaccine animals, IFNγ secretion by $CD8^+$ T cells isolated from the spleen was assessed as in (C). (**E**) 4-6 week old *Kras*$^{G12D/+}$*; Pdx-1-Cre* ($n = 5$) and *Kras*$^{G12D/+}$*; Trp53*^{R172H}*;Pdx-1-Cre* ($n = 7$) mice were treated with LM-Kras twice four weeks apart, sacrificed one week post-vaccine, splenocytes were harvested, and intracellular cytokine staining was used to assess response to KrasF and Trp2 peptides as in (C-D). No significant difference in IFNγ production was found in the response to KrasF. (**F**) Cumulative results of 5 experiments showing no significant difference in the magnitude of $CD8^+$ T cell responses to Kras F in mice expressing the Kras^{G12D} mutation compared with littermates not expressing the mutation (KrasG12D$^-$) (*$p<0.05$, **$p<0.01$, ***$p<0.001$).

B

| Epitope	Sequence
Trp2	SVYDFFVWL
Kras A	KLVVVGA**D**G
Kras B	LVVVGA**D**GV
Kras C	VVVGA**D**GVG
Kras D	VVGA**D**GVGK
Kras E	VGA**D**GVGKS
Kras F	GA**D**GVGKSA
Kras G	A**D**GVGKSAL
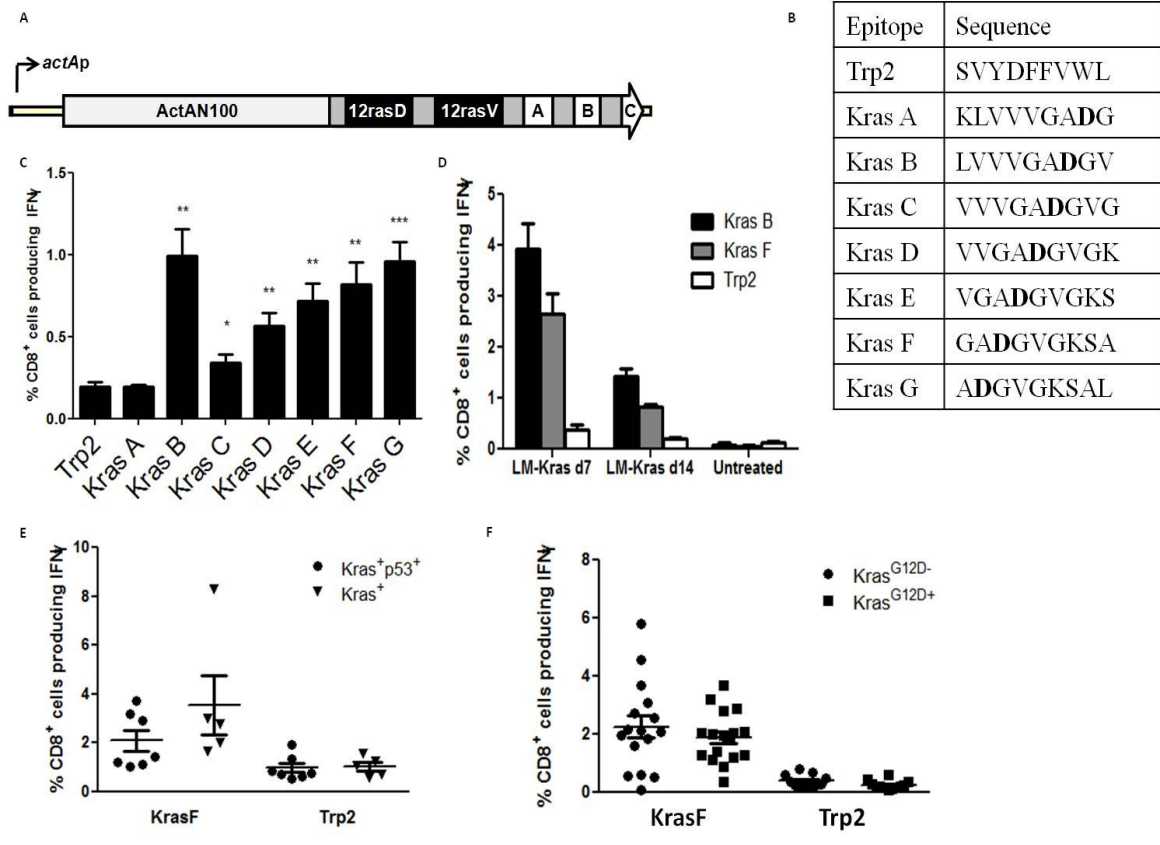
Figure 8. Effect of vaccination and Treg depletion on KPC mice. (**A**) Several Foxp3$^+$ cells can be seen per 40x field in the pancreas of KPC mice containing an early stage PanIN (left, PanIN 1), mid-stage PanIN (middle, PanIN 2) and PDA (right). (**B-C**) Splenocytes were harvested from 4-6 week old KPC mice one week after vaccination with LM-Kras. PC61 and Cy was given one day prior to vaccine, according to treatment group. (B) Flow cytometry shows reduction in percentage of Foxp3$^+$CD4$^+$ in representative LM-Kras-treated KPC mouse versus LM-Kras and PC61/Cy-treated KPC mouse. (**C**) The percentage of Foxp3$^+$ cells in CD4$^+$-gated splenocytes from LM-Kras and PC61/Cy-treated KPC mice is significantly decreased in comparison to LM-Kras-treated KPC mice (n = 4 per group, ***P<0.001). (**D**) KPC mice (n = 11-30 per group) less than 2 months old were injected with LM-Kras with or without pretreatment 24 hours prior with PC61 and Cy or with Treg depletion alone. Booster vaccinations were administered monthly with or without pretreatment according to group assignment and animals were monitored for survival. Log rank (Mantel-Cox) analysis showed a significant improvement in survival in the combination group relative to no treatment (p = 0.002) and to Treg depletion or LM-Kras vaccine alone (p = 0.048 and p = 0.050, respectively). There was no statistically significant difference in survival between the untreated group and animals receiving PC61/Cy without LM-Kras or between untreated and LM-Kras. (**E**) Mice older than 2 months were treated and monitored as in (D). No statistically significant difference was noted in survival between groups using Mantel-Cox analysis. (**F**) Young (4-6 week old) and older (8-12 week old) KPC mice were vaccinated with LM-Kras and splenocytes were harvested one week later, stimulated with KrasF and Trp2 peptides, and ICS used to assess response. The CD8$^+$ T cell response to

KrasF is normalized for control peptide (Trp2) response. Total numbers of CD8$^+$ T cells responding to KrasF were calculated based on percent responders and total number of CD8$^+$ T cells per spleen (n = 5-6 per group). **(G)** 4-6 week old KPC mice (n = 4-6 per group) were treated with either LM-Kras, PC61/Cy, the combination, or left untreated. Treatment was repeated at 4 weeks based on group assignment and at week 5, animals were sacrificed and pancreatic histology was assessed.
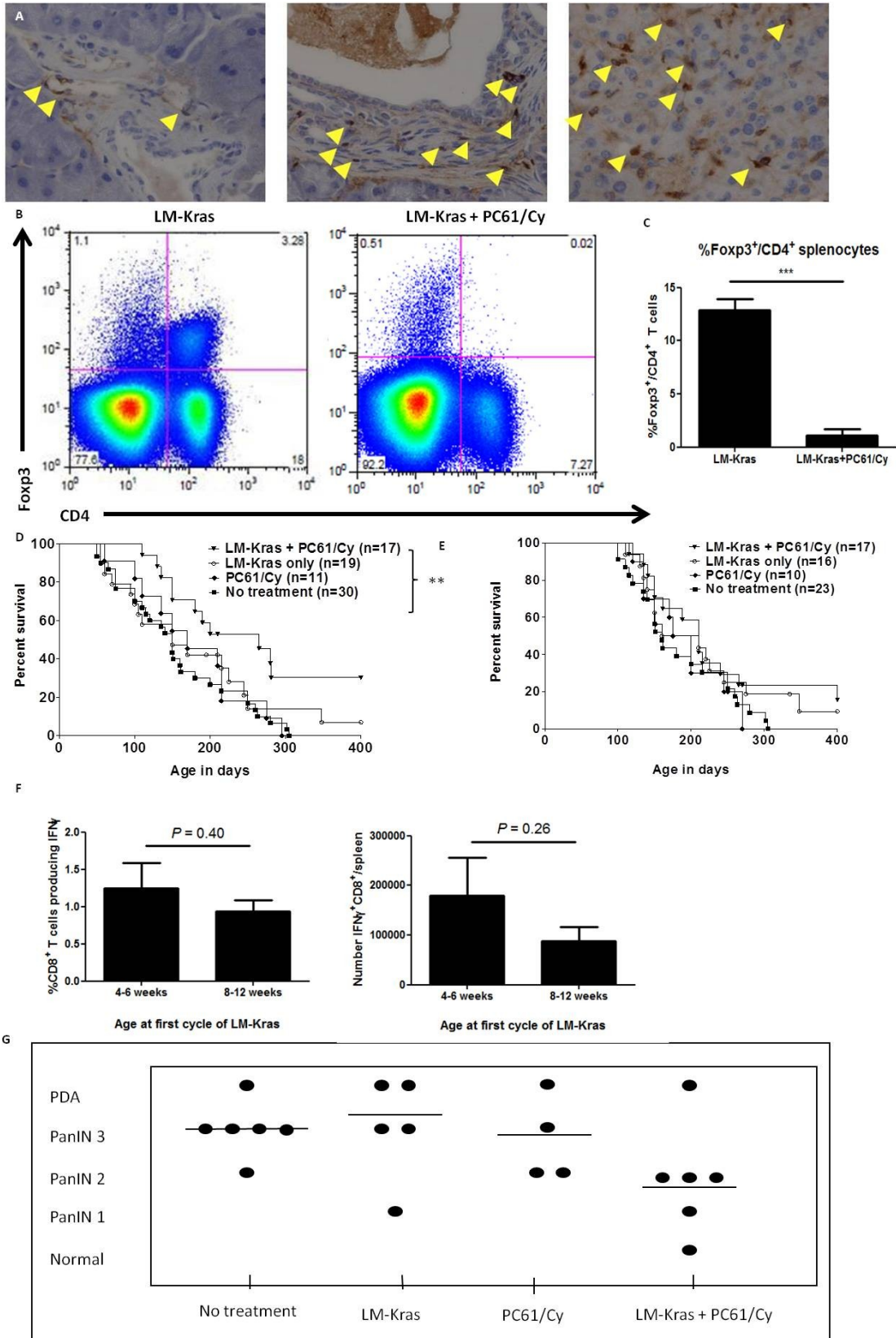
Figure 9. Systemic and local T cell responses with Treg depletion and LM-Kras. 4-6 week old KPC mice were harvested after 2 cycles of treatment with LM-Kras with or without Treg depletion, 1 week after the second vaccine. (**A**) The percentage of splenic CD8$^+$ cells producing IFNγ in response to KrasF and Ova peptides were normalized for response to negative control peptide (Trp2) and total numbers were calculated from the normalized percentages and the total number of CD8$^+$ T cells per spleen. (N.S. = not significant, *n* = 6-9 per treatment group). (**B**) Splenocytes were stimulated with anti-CD3/CD28 beads overnight, followed by 5 hour incubation with Golgi-Stop and intracellular cytokine staining. IFNγ was gated on non-stimulated controls (N.S. = not significant, *n* = 2-3 per group). (**C**) The ratio of CD4$^+$Foxp3$^+$ cells is shown relative to CD4$^+$Foxp3$^-$ cells in the pancreatic lymph node. There was also a decrease in the ratio of CD4$^+$Foxp3$^+$ cells to CD4$^+$Foxp3$^-$ cells in the pancreas, but this was not significant (*n* = 5-10 per treatment group). (**D**) Mice treated with the LM-Kras vaccine without Treg depletion have many Foxp3$^+$ T cells per 40X field (left panel), whereas mice treated with PC61/Cy and the LM-Kras vaccine have few Foxp3$^+$ T cells within the pancreas (right panel). (**E**) The total number of CD3$^+$, CD8$^+$, and CD4$^+$Foxp3$^-$ cells per mg of pancreas is shown for mice treated with PC61/Cy and LM-Kras or vaccine alone (*n* = 7-8 per group). (**F**) Immunohistochemistry of mice left untreated (right), treated with LM-Kras (middle) or LM-Kras and PC61/Cy (left) for CD4 (top) and CD8 (bottom) at 20X magnification. All data are representative of two or more independent experiments. Populations of cells positive for cell surface markers and cytokines were gated using isotype controls and non-stimulated controls for each sample (*p<0.05, ***p<0.001).
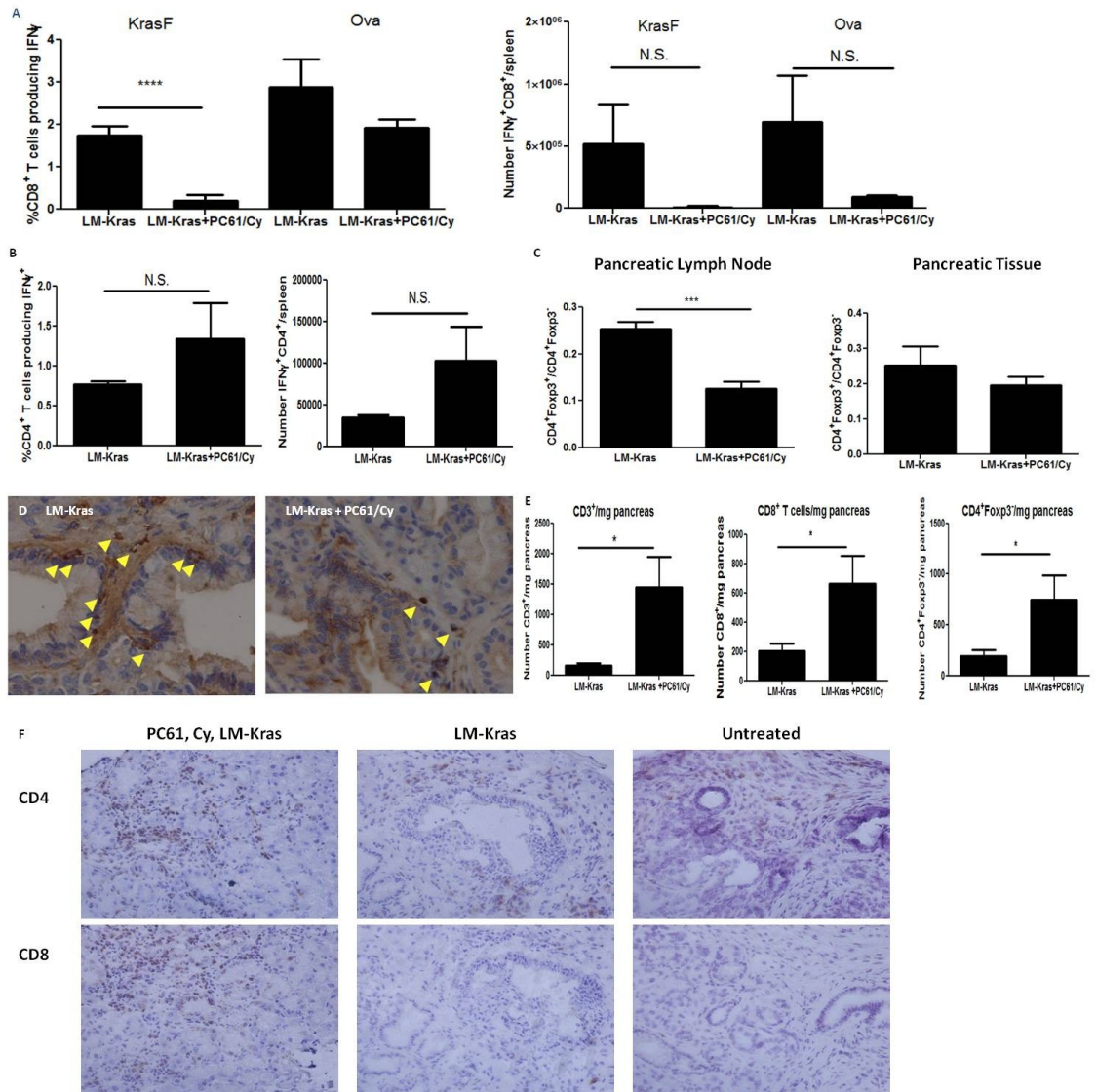
Figure 10. Phenotypic shifts in pancreatic lymphocytes with LM-Kras and Treg depletion. LM-Kras with or without PC61/Cy pre-treatment was given to mice aged 4-6 weeks old mice at week 0 and week 4, and pancreata were harvested at week 5. (**A**) Pancreas-infiltrating lymphocytes (n = 7-15 mice per treatment group) were gated on CD3$^+$ and CD4$^+$ or CD8$^+$ and analyzed for CD62L and CD44 expression. PC61/Cy treatment in addition to vaccine correlated with a significant increase in percentage of CD44^{high}CD62L^{low} CD4$^+$ (top panel) or CD8$^+$ cells (bottom panel). (**B-E**) Pancreatic lymphocytes were re-stimulated with CD3/CD28 activation beads overnight and gated on CD3$^+$ and CD4$^+$ or CD8$^+$ (n = 4 samples of 3 pooled pancreata per group). LM-Kras and PC61/Cy increased the total number of IFNγ$^+$, TNFα$^+$, and IL-17$^+$ CD4$^+$ T cells (B) and showed a trend towards more IFNγ$^+$, TNFα$^+$, and IL-17$^+$ CD8$^+$ T cells (C). Numbers of total Tbet$^+$ and RORγt$^+$ CD4$^+$ (D) and CD8$^+$ (E) cells are shown for PC61/Cy and LM-Kras and LM-Kras alone-treated mice. Data are representative of two or more independent experiments. Populations of cells positive for cell surface markers and cytokines were gated using isotype controls and non-stimulated controls for each sample (*P<0.05, **P<0.01).
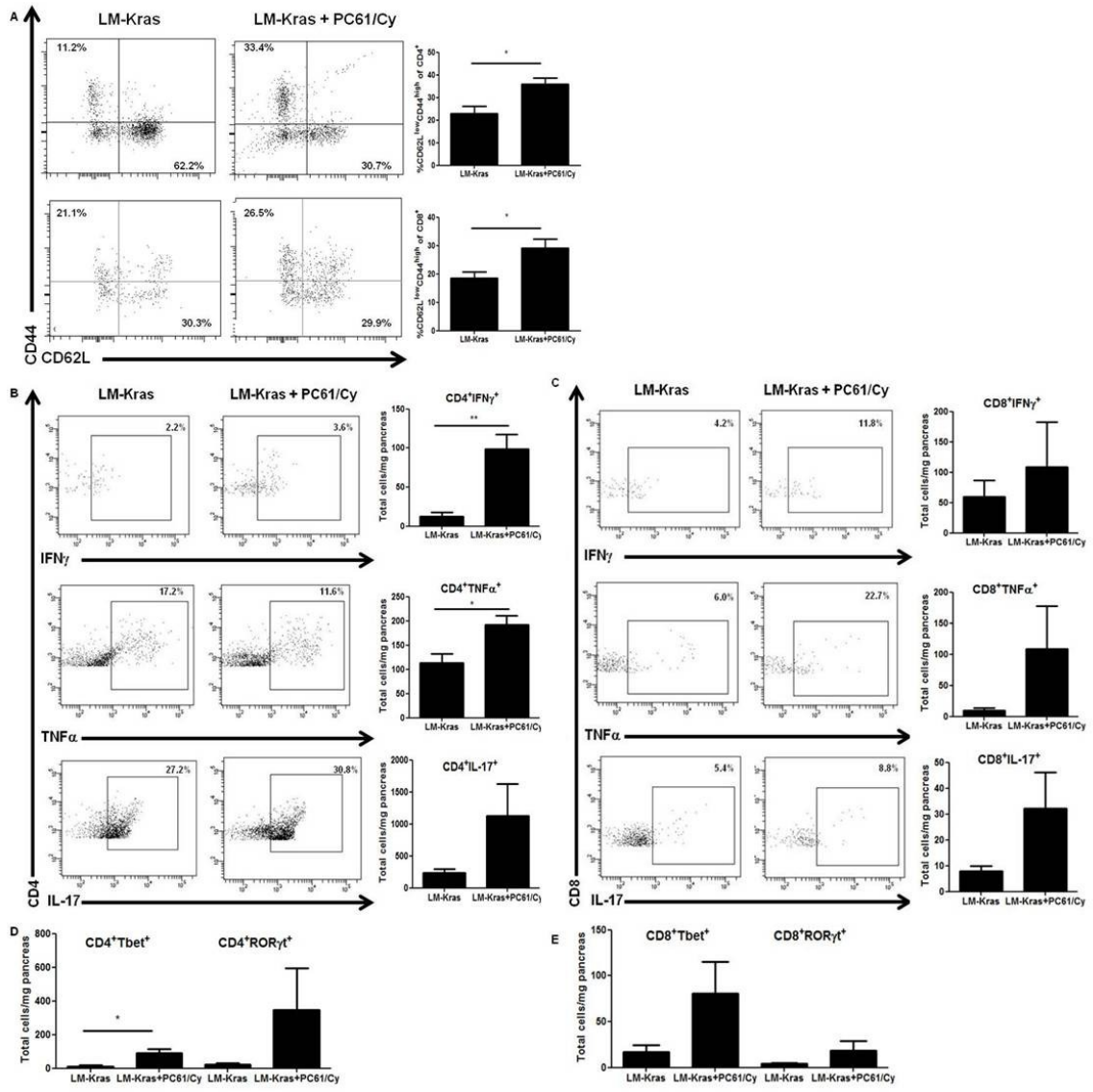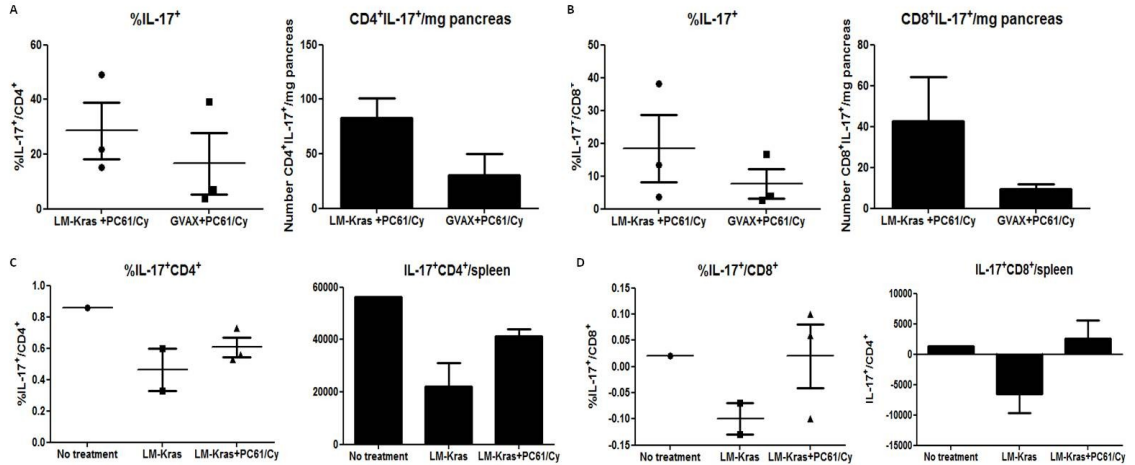
**Figure 11. IL-17 production by PanIN-infiltrating T cells induced by LM-Kras or GM-CSF-secreting vaccines and the peripheral IL-17 T cell response. (A-B)** 4-6 week old KPC mice were treated with LM-Kras and PC61/Cy as in previous experiments or PC61/Cy followed one day later by GM-CSF-secreting irradiated KPC tumor cell vaccine (GVAX). Treatment was repeated 4 weeks later and pancreata harvested one week post vaccination. Lymphocytes were stimulated overnight with anti-CD3/CD28 beads. The percentage of CD4$^+$ cells secreting IL-17 and the total number of IL-17$^+$CD4$^+$ T cells per mg of pancreas for LM-Kras and GVAX-treated mice is shown in (A) and the percentage of CD8$^+$ cells secreting IL-17 and number of IL-17$^+$CD8$^+$ T cells per mg of pancreas in (B) (n = 3 samples, 2-3 pancreata pooled per sample). **(C-D)** 4-6 week old KPC mice were treated with LM-Kras, LM-Kras and PC61/Cy, or left untreated for two cycles of treatment. Spleens were harvested 1 week post vaccine and splenocytes were stimulated overnight with anti-CD3/CD28 beads as in previous experiments. Percentage of T cells producing IL-17 and the total number of cells per spleen is shown for CD4$^+$ T cells in (C) and for CD8$^+$ T cells in (D) (n = 1-3 mice per group).

Figure 12. PanIN progression with the depletion of CD8$^+$ cells or IL-17. (A-I) Mice

were treated with LM-Kras and PC61/Cy or left untreated for two cycles of therapy

together with depleting antibodies for CD8 (A-D) or IL-17 (E-I) or with isotype control

prior to and throughout the course of treatment. Following harvest, two slides per

pancreas were assessed for percent of tissue occupied by each PanIN stage, acinar-ductal

metaplasia (ADM), and PDA. Percentage of tissue occupied by each lesion (A) or by

PanIN 2 and 3 together (B) in KPC mice treated with LM-Kras and PC61/Cy and anti-

CD8 or isotype control (n = 12 per group). Percentage of tissue occupied by each lesion

(C) or by PanIN 2 and 3 together (D) in KPC mice left untreated and CD8-depleted or

given isotype control (n = 6-8 per group). Percentage of tissue occupied by each lesion

(E), by PanIN 2 and 3 together (F), or by PDA (G) in KPC mice treated with LM-Kras

and PC61/Cy while given IL-17 neutralizing antibody or isotype control (n = 15-16 per

group). In (H) and (I), the percent tissue occupied by each lesion and by high grade

PanINs (PanIN 2 and 3) is shown for IL-17-depleted and isotype control-treated KPC

mice that were not given the vaccine or Treg depletion (n = 5-6 per group) (*P<0.05,

**P<0.01).
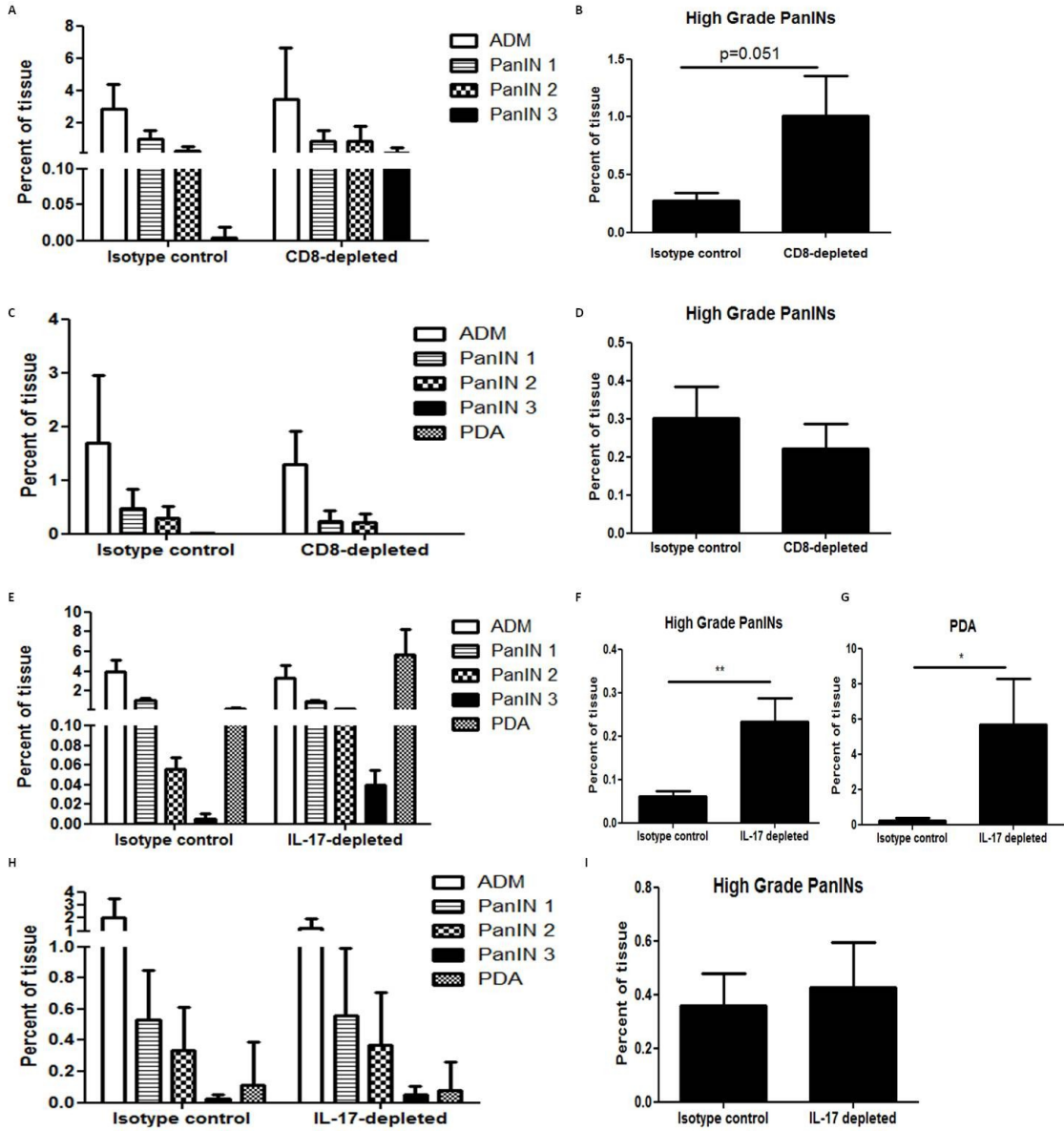
Figure 13. Myeloid cell recruitment into untreated and treated spleens, PanIN, and PDA. (**A**) Spleens of KPC mice treated with PC61/Cy, LM-Kras, or the combination were harvested one week post-vaccination after 2 cycles of therapy beginning at 4-6 weeks old and analyzed for the percents of the various cell populations ($n = 2$-3 per group). (**B-E**) Pancreata from KPC mice treated with two cycles of LM-Kras with or without PC61/Cy starting at 4-6 weeks old or left untreated for the same timeframe were analyzed by flow cytometry ($n = 4$-6 mice per group). The percentage of Gr-1$^+$ cells of CD11b$^+$ cells (B), percentage of Ly6G$^+$Ly6C^{low} cells of CD11b$^+$ (C), the percent of Ly6G$^-$Ly6C^{high} cells of CD11b$^+$ (D), and percentage of F4/80$^+$ of CD45$^+$ cells (E) and the total numbers of each per mg of pancreas (B-E) is shown for all 3 treatment groups. Representative of two experiments. (**F-Q**) Pancreata were harvested from KPC mice of various ages, representing early and late PanIN stages and PDA, or from 4-6 week old KPC mice treated with two cycles of LM-Kras with or without Treg depletion, and slides were stained with Ly6G or F4/80 antibodies. Representative images of Ly6G staining are shown for the following: untreated PanIN 1 (F), untreated PanIN 2/3 (G), untreated PDA (H), LM-Kras-treated PanIN 1 (I), PC61/Cy and LM-Kras-treated PanIN 1 (J) and PC61/Cy and LM-Kras-treated PanIN 1/2 (K). Representative F4/80 staining in: untreated PanIN 1 (L), untreated PanIN 2 (M), untreated PDA (N), LM-Kras-treated PanIN 1 (O), PC61/Cy and LM-Kras-treated PanIN 1 (P), and PC61/Cy and LM-Kras-treated PanIN 2 (Q) (*p<0.05, **p<0.01).
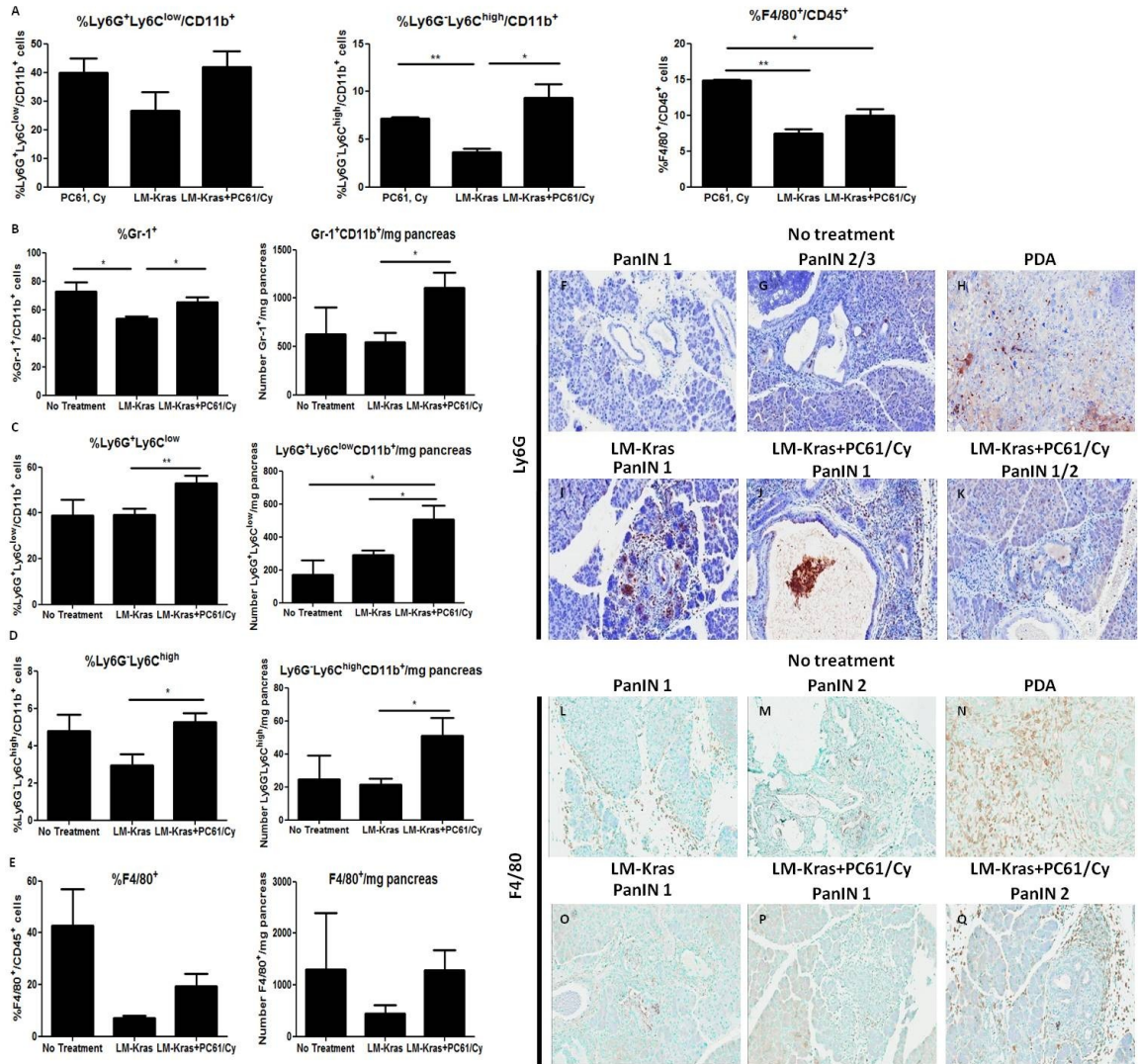
Figure 14. Phenotype of innate populations in the pre-malignant pancreas of KPC mice. (A-B) IL-12 and IL-10 were assessed by intracellular cytokine staining of pancreatic-infiltrating CD11b$^+$Gr-1$^+$ and F4/80$^+$ cells from mice treated at age 4-6 weeks old with LM-Kras with or without Treg depletion or left untreated for five weeks. Flow cytometry plots for a representative sample of each treatment group are shown with percentages of the cells found in each quadrant for Gr-1$^+$ (top panel) and F4/80$^+$ (bottom panel) cells (A). The mean percentage of Gr-1$^+$ or F4/80$^+$ cells expressing IL-12 or IL-10 and total number of cytokine-expressing Gr-1$^+$ or F4/80$^+$ cells per mg of pancreas is shown in (B) (n = 4-6 mice per group). Representative of two experiments. **(C)** Qualitative cytokine antibody array using cell lysate from pooled CD11b$^+$ Gr-1$^+$ cells from pancreata of untreated, LM-Kras-treated or PC61/Cy and LM-Kras-treated KPC mice $(n$ = 10 mice per treatment group, 2 technical replicates each). The fold change in expression for Gr-1$^+$ cells from the pancreata of treated mice compared to untreated mice is shown for each cytokine. **(D)** Representative flow cytometry plots showing CFSE dilution demonstrate enhanced CD8$^+$ T cell division with Gr-1$^+$ cells pooled from the pancreata of LM-Kras and PC61/Cy-treated mice (right) compared to Gr-1$^+$ cells from LM-Kras-treated (middle) or untreated KPC mice (left). Black solid line: Gr-1$^+$ cells cultured with CD8$^+$ T cells and anti-CD3/CD28 beads, black dashed line: unstimulated CD8$^+$ T cells, grey shaded line: CD8$^+$ T cells cultured with anti-CD3/CD28 beads. **(E)** Average percent of cells that have divided as determined by CFSE fluorescence are shown from three representative experiments from the following treatment groups: T cells cultured with Gr-1$^+$ cells from untreated mice (No treatment), LM-Kras-treated mice (LM-Kras-treated), or PC61/Cy and LM-Kras-treated mice (PC61/Cy, LM-Kras-treated)

(n = 1-3 wells per treatment group per experiment). In addition, mean fluorescence

intensity for CFSE is shown from one representative experiment for the same treatment

groups (*p<0.05, **p<0.01).
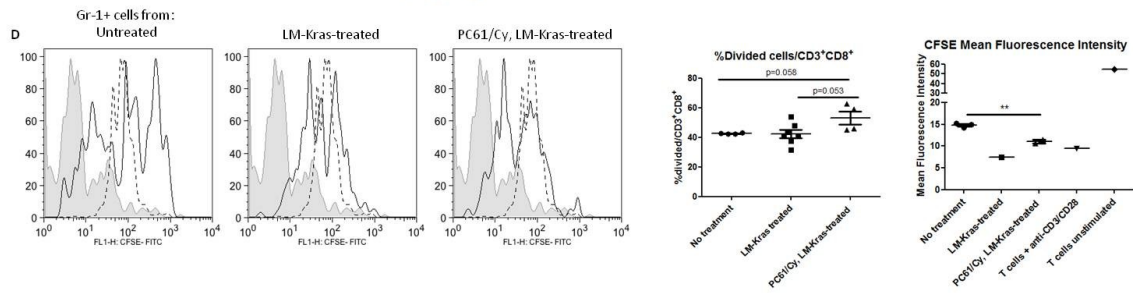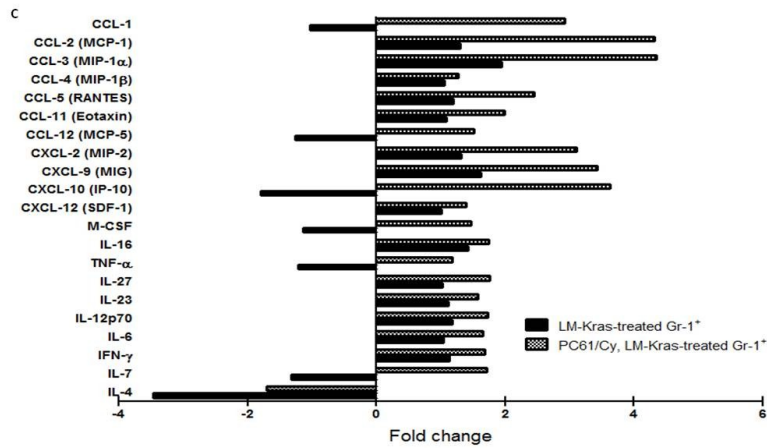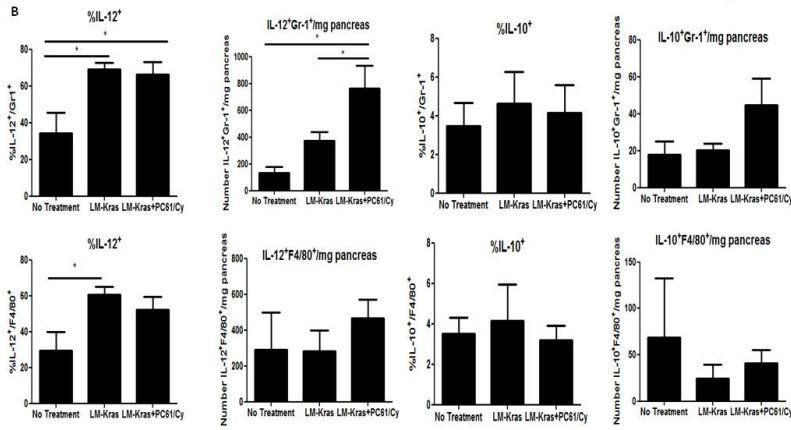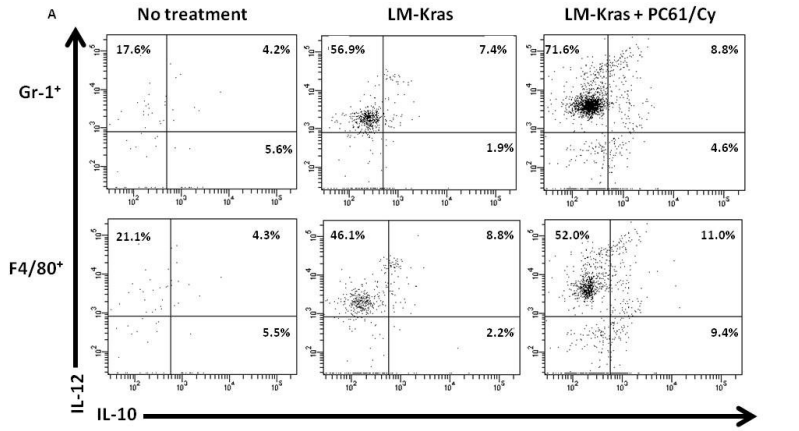
Figure 15. Effects of CD11b$^+$Gr-1$^+$ cells on the cytokine profile of T cells. (A-D)
Ly6G-depleting antibody or isotype control was given throughout treatment with LM-Kras and PC61/Cy to 4-6 week old KPC mice for 2 cycles of treatment. In (A), spleens were harvested 1 week after the second vaccine and assayed for the total number of each cell population (n = 14 per group). In (B), pancreata were harvested 1 week after the second vaccine and assayed for the total number of each cell population per mg of pancreas (n = 1-2 mice per group). In (C-D), pancreata were harvested and T cells were stimulated overnight with anti-CD3/CD28 beads, followed by intracellular cytokine staining. The percentage of CD4$^+$ (C) and CD8$^+$ (D) T cells expressing each cytokine as well as the total number of cells is shown (n = 5 samples per group of 2-3 pooled pancreata). None of the comparisons shown were significant. (**E**) CD11b$^+$Gr-1$^+$ cells were sorted from the pancreata of 4-6 week old KPC mice treated with 2 cycles of LM-Kras with or without PC61/Cy or left untreated and cultured with naïve CD4$^+$ and CD8$^+$ T cells in the presence of anti-CD3/CD28 beads. The percentage of T cells expressing each cytokine is shown (n = 1-2 wells/treatment group representing Gr-1$^+$ cells pooled from 8-10 pancreata). Data is representative of 2 experiments.
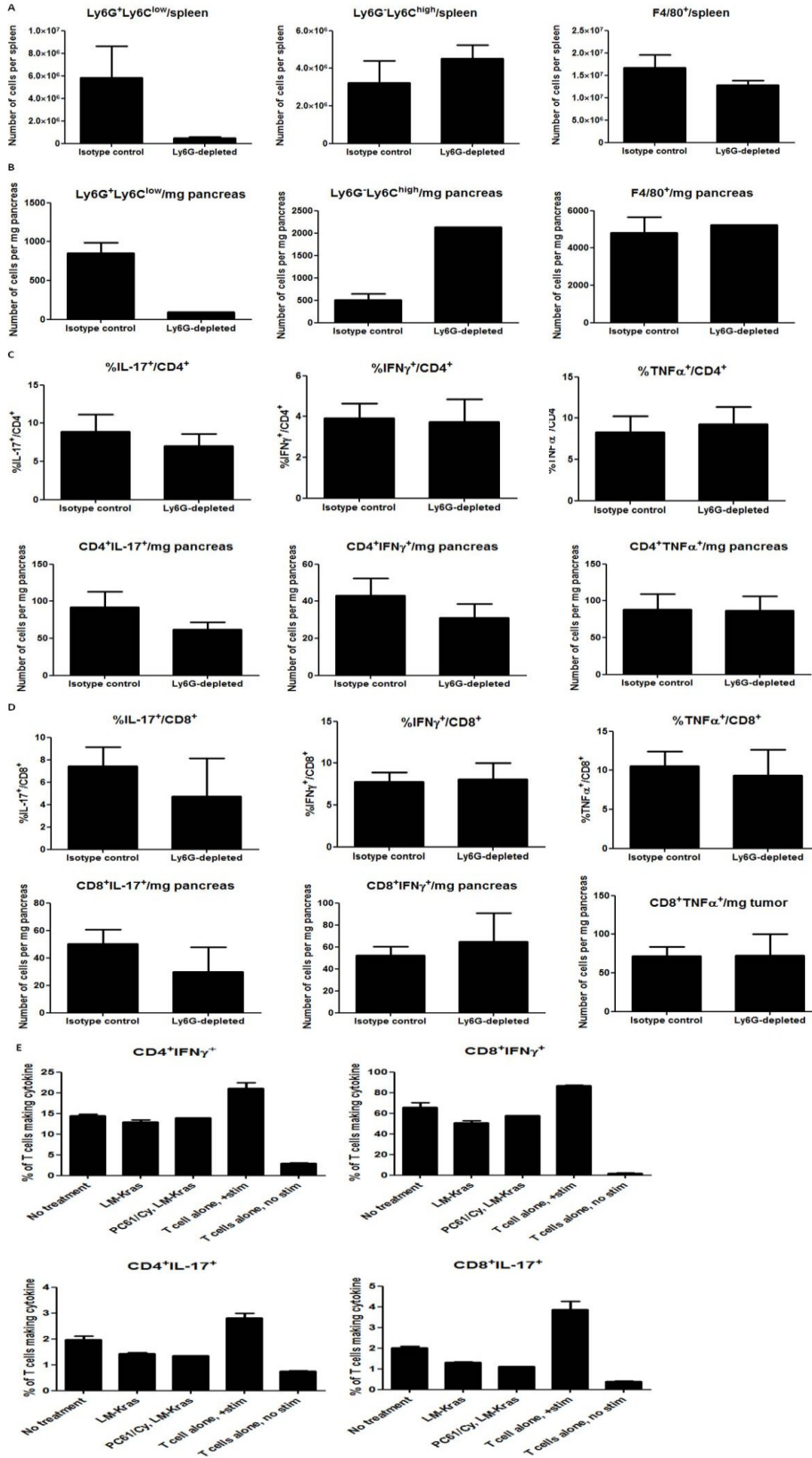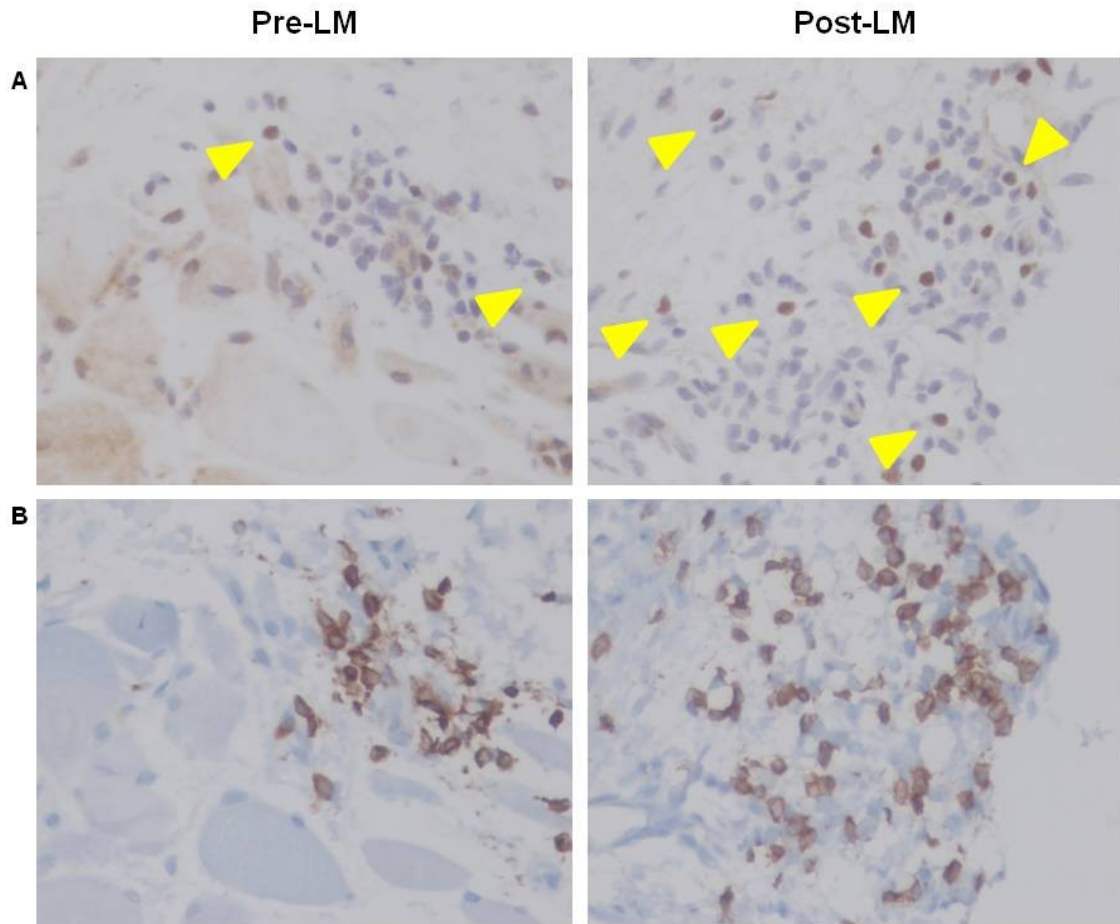
Figure 16. Immune infiltrates in pre- and post-vaccination mesothelioma biopsies with a *Listeria* vaccine targeting mesothelin. Serial sections from biopsies of malignant pleural mesothelioma in a patient receiving a *Listeria* vaccine targeting mesothelin (CRS-207) prior to administration (left panels) and 2 weeks after the second dose (given 2 weeks following the first dose) of CRS-207 (right panels) were stained with antibodies to RORγt **(A)** or CD3 **(B)**. Arrowheads designate cells or areas with cells containing intranuclear staining for RORγt. Representative images are shown at 40X magnification.

Chapter 4: SUMMARY

The widespread use of vaccines to protect against infectious disease has been one of the most important developments in human health in the past century and has eradicated many pathogens which were once a leading cause of death and illness in the United States and worldwide. In recent years, partly due to vaccine-induced protection among many other public health interventions, cancer has bypassed infectious disease as a cause of mortality in developed countries. Cancer vaccines have the potential to make an impact on human health just as traditional vaccines have for infectious disease, albeit through different strategies. As discussed in Chapter 3, vaccines targeting viruses that cause cancer such as hepatitis B and human papillomavirus have already seen success in decreasing virally-associated cancers in young individuals who have not yet been exposed to the pathogens. However, these types of vaccines often rely on neutralizing antibody responses which are ineffective after the virus has infected host cells. Vaccines given after there is already established infection have been less effective due to mechanisms that pathogens have evolved to evade the immune system.

For the majority of cancer types that are not associated with infectious causes, immune evasion and tolerance are also barriers to the effective use of cancer vaccines. As has been described in this dissertation and outlined in chapter 1, even in early stage disease, many immune-suppressing populations have already entered the site of tumor development and inhibit protective responses induced by vaccines. To study the mechanisms of immune tolerance, I have used two mouse models to mimic human disease: one of pancreatic ductal adenocarcinoma (PDA) and one of mammary

adenocarcinoma as well as novel CD8$^+$ TCR transgenic and LAG-3$^{-/-}$ mice to better understand tumor antigen–specific T cell activation and regulation. In Chapter 2, the inhibition of an immune checkpoint, LAG-3, on high and low avidity T cells was tested in combination with a whole cell, GM-CSF-secreting, tumor vaccine and Treg depletion in the form of low dose Cy. Inhibition of LAG-3 in high avidity CD8$^+$ T cells boosted the effects of low dose Cy and vaccine to enhance T cell trafficking, activation, and control of tumors, but failed to enhance the function of low avidity T cells which already have very low levels of cytokine production and ability to traffic to and lyse tumors. Thus, it was shown that immune checkpoint blockade is one solution to overcoming suppressive tumor microenvironments, but only is useful when a high avidity T cell population exists in large numbers and is supplemented with a vaccine and Treg depletion.

In Chapter 3, I used a mouse model of PDA which is more relevant to human disease as it starts with early PDA precursors (PanINs) that progress in a step-wise process to metastatic pancreatic cancer, and occurs in the natural organ and site of tumor development, acquiring similar features of the tumor microenvironment that have been observed in human PDA. Tregs and MDSC are two immunosuppressive populations shown to infiltrate early stage PanINs. An anti-CD25 antibody and low dose Cy were used to deplete Tregs and the combination of these Treg-depleting agents with a highly immunogenic *Listeria* vaccine targeting Kras was able to switch tumor-infiltrating MDSCs to a phenotype more consistent with N1 neutrophils. However, the two Treg-depleting agents were not enough to completely eliminate Tregs in the pancreas, providing evidence of how the dense stroma induced by tumor cells in pancreatic cancer is an additional barrier to effective immunotherapy.

The role of different immune cell types, both innate and adaptive, in cancer immunotherapy was explored in this work. T cells have long been thought of the main effector cell type in both cancer and infectious disease. Therefore, in Chapter 2, I studied the effect of further enabling potent, high avidity $CD8^+$ T cells by inhibiting an immune checkpoint. The $CD8^+$ intrinsic effects were obviously beneficial in a mouse model of breast cancer; however, the effect of deletion of LAG-3 globally and in the tumor microenvironment was not as concrete and likely was due to LAG-3 inhibition in antigen-presenting cells and other innate immune cell types. These mixed results on $CD8^+$ T cells when LAG-3 signaling was abrogated in all cells have ramifications for the use of LAG-3 blocking antibodies in the treatment of cancer patients. In Chapter 3, the interaction of T cells with other cells in the tumor microenvironment was again studied. A *Listeria* vaccine was able to induce Kras-specific $CD8^+$ T cells and when given with Treg depletion, allowed for trafficking into the pre-malignant pancreas. Increases in T cell number and activation within the pancreas correlated with the induction of an immunogenic phenotype in innate $CD11b^+Gr-1^+$ and $F4/80^+$ cells. An exhaustive study of additional innate cells in both models remains to be done, but remains an important question, as the alteration of these cells likely has effects on the microenvironment cytokine milieu and thus, may polarize additional cell types from a pro- to anti-cancer phenotype.

It is clear from the work described within this thesis, as well as in published work from many other groups, that mechanisms of immune tolerance begin early and thus, we will need to intervene with immunotherapy as early as possible. One future strategy must be to identify people who are at risk for developing cancer and this will become easier

with improved diagnostics and recent efforts to sequence an individual's cancer genome. However, even when it is possible to identify cancer at its earliest stages, more than one form of immunotherapy and/or traditional therapy will be necessary for successful cancer treatment. Combination therapy for cancer has been a long established principle; combinations of chemotherapy drugs or chemotherapy with radiation have been shown to be more efficacious in preventing recurrence than one modality alone. The same principle holds true for immunotherapy; additional therapies directed at overcoming suppressive signals or re-directing suppressive into protective immune cell populations will be necessary in addition to cancer vaccines, if we intend to fulfill the promise of immunotherapy for cancer.

References

1.   American Cancer Society I. 2013 7/31/13. Cancer Facts and Figures 2013.

      American Cancer Society, Inc.

      <http://www.cancer.org/acs/groups/content/@epidemiologysurveilance/document

      s/document/acspc-036845.pdf>. Accessed 2013 7/31/13.

2.   American Cancer Society I. 2013 3/24. Survival rates for pancreatic cancer.

      American Cancer Society, Inc.

      <http://www.cancer.org/cancer/pancreaticcancer/overviewguide/pancreatic-

      cancer-overview-survival-rates>. Accessed 2013 3/24.

3.   Hidalgo M. Pancreatic cancer. N Engl J Med 2010;362(17):1605-17.

4.   Lanca T, Silva-Santos B. The split nature of tumor-infiltrating leukocytes:

      Implications for cancer surveillance and immunotherapy. Oncoimmunology

      2012;1(5):717-725.

5.   Keenan B, Jaffee EM. Immunotherapy in preneoplastic disease: targeting early

      procarcinogenic inflammatory changes that lead to immune suppression and

      tumor tolerance. Ann N Y Acad Sci 2013;1284:12-6.

6.   Pardoll DM. The blockade of immune checkpoints in cancer immunotherapy. Nat

      Rev Cancer 2012;12(4):252-64.

7.   Gardner TA, Elzey BD, Hahn NM. Sipuleucel-T (Provenge) autologous vaccine

      approved for treatment of men with asymptomatic or minimally symptomatic

      castrate-resistant metastatic prostate cancer. Hum Vaccin Immunother

      2012;8(4):534-9.

8.   Domschke C, Schuetz F, Ge Y, Seibel T, Falk C, Brors B, Vlodavsky I, Sommerfeldt N, Sinn HP, Kuhnle MC and others. Intratumoral cytokines and tumor cell biology determine spontaneous breast cancer-specific immune responses and their correlation to prognosis. Cancer Res 2009;69(21):8420-8.

9.   Lutz E, Yeo CJ, Lillemoe KD, Biedrzycki B, Kobrin B, Herman J, Sugar E, Piantadosi S, Cameron JL, Solt S and others. A lethally irradiated allogeneic granulocyte-macrophage colony stimulating factor-secreting tumor vaccine for pancreatic adenocarcinoma. A Phase II trial of safety, efficacy, and immune activation. Ann Surg 2011;253(2):328-35.

10.   Drake CG, Jaffee E, Pardoll DM. Mechanisms of immune evasion by tumors. Adv Immunol 2006;90:51-81.

11.   Sato E, Olson SH, Ahn J, Bundy B, Nishikawa H, Qian F, Jungbluth AA, Frosina D, Gnjatic S, Ambrosone C and others. Intraepithelial CD8+ tumor-infiltrating lymphocytes and a high CD8+/regulatory T cell ratio are associated with favorable prognosis in ovarian cancer. Proc Natl Acad Sci U S A 2005;102(51):18538-43.

12.   Barnett JC, Bean SM, Whitaker RS, Kondoh E, Baba T, Fujii S, Marks JR, Dressman HK, Murphy SK, Berchuck A. Ovarian cancer tumor infiltrating T-regulatory (T(reg)) cells are associated with a metastatic phenotype. Gynecol Oncol 2010;116(3):556-62.

13.   DeNardo DG, Barreto JB, Andreu P, Vasquez L, Tawfik D, Kolhatkar N, Coussens LM. CD4(+) T cells regulate pulmonary metastasis of mammary

carcinomas by enhancing protumor properties of macrophages. Cancer Cell 2009;16(2):91-102.

14.   Deng L, Zhang H, Luan Y, Zhang J, Xing Q, Dong S, Wu X, Liu M, Wang S. Accumulation of foxp3+ T regulatory cells in draining lymph nodes correlates with disease progression and immune suppression in colorectal cancer patients. Clin Cancer Res 2010;16(16):4105-12.

15.   Zhao E, Wang L, Dai J, Kryczek I, Wei S, Vatan L, Altuwaijri S, Sparwasser T, Wang G, Keller ET and others. Regulatory T cells in the bone marrow microenvironment in patients with prostate cancer. Oncoimmunology 2012;1(2):152-161.

16.   Laheru D, Lutz E, Burke J, Biedrzycki B, Solt S, Onners B, Tartakovsky I, Nemunaitis J, Le D, Sugar E and others. Allogeneic granulocyte macrophage colony-stimulating factor-secreting tumor immunotherapy alone or in sequence with cyclophosphamide for metastatic pancreatic cancer: a pilot study of safety, feasibility, and immune activation. Clin Cancer Res 2008;14(5):1455-63.

17.   Cesana GC, DeRaffele G, Cohen S, Moroziewicz D, Mitcham J, Stoutenburg J, Cheung K, Hesdorffer C, Kim-Schulze S, Kaufman HL. Characterization of CD4+CD25+ regulatory T cells in patients treated with high-dose interleukin-2 for metastatic melanoma or renal cell carcinoma. J Clin Oncol 2006;24(7):1169-77.

18.   Zou W. Regulatory T cells, tumour immunity and immunotherapy. Nat Rev Immunol 2006;6(4):295-307.

19. Ranges GE, Figari IS, Espevik T, Palladino MA, Jr. Inhibition of cytotoxic T cell development by transforming growth factor beta and reversal by recombinant tumor necrosis factor alpha. J Exp Med 1987;166(4):991-8.

20. Liu Y, Zhang P, Li J, Kulkarni AB, Perruche S, Chen W. A critical function for TGF-beta signaling in the development of natural CD4+CD25+Foxp3+ regulatory T cells. Nat Immunol 2008;9(6):632-40.

21. van Vlasselaer P, Punnonen J, de Vries JE. Transforming growth factor-beta directs IgA switching in human B cells. J Immunol 1992;148(7):2062-7.

22. Kehrl JH, Roberts AB, Wakefield LM, Jakowlew S, Sporn MB, Fauci AS. Transforming growth factor beta is an important immunomodulatory protein for human B lymphocytes. J Immunol 1986;137(12):3855-60.

23. Fridlender ZG, Sun J, Kim S, Kapoor V, Cheng G, Ling L, Worthen GS, Albelda SM. Polarization of tumor-associated neutrophil phenotype by TGF-beta: "N1" versus "N2" TAN. Cancer Cell 2009;16(3):183-94.

24. Sanchez-Elsner T, Botella LM, Velasco B, Corbi A, Attisano L, Bernabeu C. Synergistic cooperation between hypoxia and transforming growth factor-beta pathways on human vascular endothelial growth factor gene expression. J Biol Chem 2001;276(42):38527-35.

25. Duivenvoorden WC, Hirte HW, Singh G. Transforming growth factor beta1 acts as an inducer of matrix metalloproteinase expression and activity in human bone-metastasizing cancer cells. Clin Exp Metastasis 1999;17(1):27-34.

26. Bellone G, Carbone A, Smirne C, Scirelli T, Buffolino A, Novarino A, Stacchini A, Bertetto O, Palestro G, Sorio C and others. Cooperative induction of a

tolerogenic dendritic cell phenotype by cytokines secreted by pancreatic carcinoma cells. J Immunol 2006;177(5):3448-60.

27.   Beckebaum S, Zhang X, Chen X, Yu Z, Frilling A, Dworacki G, Grosse-Wilde H, Broelsch CE, Gerken G, Cicinnati VR. Increased levels of interleukin-10 in serum from patients with hepatocellular carcinoma correlate with profound numerical deficiencies and immature phenotype of circulating dendritic cell subsets. Clin Cancer Res 2004;10(21):7260-9.

28.   Phan GQ, Yang JC, Sherry RM, Hwu P, Topalian SL, Schwartzentruber DJ, Restifo NP, Haworth LR, Seipp CA, Freezer LJ and others. Cancer regression and autoimmunity induced by cytotoxic T lymphocyte-associated antigen 4 blockade in patients with metastatic melanoma. Proc Natl Acad Sci U S A 2003;100(14):8372-7.

29.   Peggs KS, Quezada SA, Chambers CA, Korman AJ, Allison JP. Blockade of CTLA-4 on both effector and regulatory T cell compartments contributes to the antitumor activity of anti-CTLA-4 antibodies. J Exp Med 2009;206(8):1717-25.

30.   Grosso JF, Kelleher CC, Harris TJ, Maris CH, Hipkiss EL, De Marzo A, Anders R, Netto G, Getnet D, Bruno TC and others. LAG-3 regulates CD8+ T cell accumulation and effector function in murine self- and tumor-tolerance systems. J Clin Invest 2007;117(11):3383-92.

31.   Fourcade J, Sun Z, Benallaoua M, Guillaume P, Luescher IF, Sander C, Kirkwood JM, Kuchroo V, Zarour HM. Upregulation of Tim-3 and PD-1 expression is associated with tumor antigen-specific CD8+ T cell dysfunction in melanoma patients. J Exp Med 2010;207(10):2175-86.

32.   Ohta A, Gorelik E, Prasad SJ, Ronchese F, Lukashev D, Wong MK, Huang X, Caldwell S, Liu K, Smith P and others. A2A adenosine receptor protects tumors from antitumor T cells. Proc Natl Acad Sci U S A 2006;103(35):13132-7.

33.   Brahmer JR, Drake CG, Wollner I, Powderly JD, Picus J, Sharfman WH, Stankevich E, Pons A, Salay TM, McMiller TL and others. Phase I study of single-agent anti-programmed death-1 (MDX-1106) in refractory solid tumors: safety, clinical activity, pharmacodynamics, and immunologic correlates. J Clin Oncol 2010;28(19):3167-75.

34.   Woo SR, Turnis ME, Goldberg MV, Bankoti J, Selby M, Nirschl CJ, Bettini ML, Gravano DM, Vogel P, Liu CL and others. Immune inhibitory molecules LAG-3 and PD-1 synergistically regulate T-cell function to promote tumoral immune escape. Cancer Res 2012;72(4):917-27.

35.   Matsuzaki J, Gnjatic S, Mhawech-Fauceglia P, Beck A, Miller A, Tsuji T, Eppolito C, Qian F, Lele S, Shrikant P and others. Tumor-infiltrating NY-ESO-1-specific CD8+ T cells are negatively regulated by LAG-3 and PD-1 in human ovarian cancer. Proc Natl Acad Sci U S A 2010;107(17):7875-80.

36.   Huang CT, Workman CJ, Flies D, Pan X, Marson AL, Zhou G, Hipkiss EL, Ravi S, Kowalski J, Levitsky HI and others. Role of LAG-3 in regulatory T cells. Immunity 2004;21(4):503-13.

37.   Workman CJ, Wang Y, El Kasmi KC, Pardoll DM, Murray PJ, Drake CG, Vignali DA. LAG-3 regulates plasmacytoid dendritic cell homeostasis. J Immunol 2009;182(4):1885-91.

38. Mantovani A, Schioppa T, Porta C, Allavena P, Sica A. Role of tumor-associated macrophages in tumor progression and invasion. Cancer Metastasis Rev 2006;25(3):315-22.

39. Allavena P, Sica A, Garlanda C, Mantovani A. The Yin-Yang of tumor-associated macrophages in neoplastic progression and immune surveillance. Immunol Rev 2008;222:155-61.

40. Ma J, Liu L, Che G, Yu N, Dai F, You Z. The M1 form of tumor-associated macrophages in non-small cell lung cancer is positively associated with survival time. BMC Cancer 2010;10:112.

41. Ohri CM, Shikotra A, Green RH, Waller DA, Bradding P. Macrophages within NSCLC tumour islets are predominantly of a cytotoxic M1 phenotype associated with extended survival. Eur Respir J 2009;33(1):118-26.

42. Fridlender ZG, Albelda SM. Tumor-associated neutrophils: friend or foe? Carcinogenesis 2012;33(5):949-55.

43. Zea AH, Rodriguez PC, Culotta KS, Hernandez CP, DeSalvo J, Ochoa JB, Park HJ, Zabaleta J, Ochoa AC. L-Arginine modulates CD3zeta expression and T cell function in activated human T lymphocytes. Cell Immunol 2004;232(1-2):21-31.

44. Yu J, Du W, Yan F, Wang Y, Li H, Cao S, Yu W, Shen C, Liu J, Ren X. Myeloid-derived suppressor cells suppress antitumor immune responses through IDO expression and correlate with lymph node metastasis in patients with breast cancer. J Immunol 2013;190(7):3783-97.

45. Srivastava MK, Sinha P, Clements VK, Rodriguez P, Ostrand-Rosenberg S. Myeloid-derived suppressor cells inhibit T-cell activation by depleting cystine and cysteine. Cancer Res 2010;70(1):68-77.

46. Jia W, Jackson-Cook C, Graf MR. Tumor-infiltrating, myeloid-derived suppressor cells inhibit T cell activity by nitric oxide production in an intracranial rat glioma + vaccination model. J Neuroimmunol 2010;223(1-2):20-30.

47. Nagaraj S, Schrum AG, Cho HI, Celis E, Gabrilovich DI. Mechanism of T cell tolerance induced by myeloid-derived suppressor cells. J Immunol 2010;184(6):3106-16.

48. Reilly RT, Gottlieb MB, Ercolini AM, Machiels JP, Kane CE, Okoye FI, Muller WJ, Dixon KH, Jaffee EM. HER-2/neu is a tumor rejection target in tolerized HER-2/neu transgenic mice. Cancer Res 2000;60(13):3569-76.

49. Ercolini AM, Ladle BH, Manning EA, Pfannenstiel LW, Armstrong TD, Machiels JP, Bieler JG, Emens LA, Reilly RT, Jaffee EM. Recruitment of latent pools of high-avidity CD8(+) T cells to the antitumor immune response. J Exp Med 2005;201(10):1591-602.

50. Weiss VL, Lee TH, Song H, Kouo TS, Black CM, Sgouros G, Jaffee EM, Armstrong TD. Trafficking of high avidity HER-2/neu-specific T cells into HER-2/neu-expressing tumors after depletion of effector/memory-like regulatory T cells. PLoS One 2012;7(2):e31962.

51. Clark CE, Hingorani SR, Mick R, Combs C, Tuveson DA, Vonderheide RH. Dynamics of the immune reaction to pancreatic cancer from inception to invasion. Cancer Res 2007;67(19):9518-27.

52. Provenzano PP, Hingorani SR. Hyaluronan, fluid pressure, and stromal resistance in pancreas cancer. Br J Cancer 2013;108(1):1-8.

53. Sofuni A, Iijima H, Moriyasu F, Nakayama D, Shimizu M, Nakamura K, Itokawa F, Itoi T. Differential diagnosis of pancreatic tumors using ultrasound contrast imaging. J Gastroenterol 2005;40(5):518-25.

54. Olive KP, Jacobetz MA, Davidson CJ, Gopinathan A, McIntyre D, Honess D, Madhu B, Goldgraben MA, Caldwell ME, Allard D and others. Inhibition of Hedgehog signaling enhances delivery of chemotherapy in a mouse model of pancreatic cancer. Science 2009;324(5933):1457-61.

55. Machiels JP, Reilly RT, Emens LA, Ercolini AM, Lei RY, Weintraub D, Okoye FI, Jaffee EM. Cyclophosphamide, doxorubicin, and paclitaxel enhance the antitumor immune response of granulocyte/macrophage-colony stimulating factor-secreting whole-cell vaccines in HER-2/neu tolerized mice. Cancer Res 2001;61(9):3689-97.

56. Ercolini AM, Machiels JP, Chen YC, Slansky JE, Giedlen M, Reilly RT, Jaffee EM. Identification and characterization of the immunodominant rat HER-2/neu MHC class I epitope presented by spontaneous mammary tumors from HER-2/neu-transgenic mice. J Immunol 2003;170(8):4273-80.

57. Workman CJ, Rice DS, Dugger KJ, Kurschner C, Vignali DA. Phenotypic analysis of the murine CD4-related glycoprotein, CD223 (LAG-3). Eur J Immunol 2002;32(8):2255-63.

58. Sierro S, Romero P, Speiser DE. The CD4-like molecule LAG-3, biology and therapeutic applications. Expert Opin Ther Targets 2011;15(1):91-101.

59. Kisielow M, Kisielow J, Capoferri-Sollami G, Karjalainen K. Expression of lymphocyte activation gene 3 (LAG-3) on B cells is induced by T cells. Eur J Immunol 2005;35(7):2081-8.

60. Miyazaki T, Dierich A, Benoist C, Mathis D. Independent modes of natural killing distinguished in mice lacking Lag3. Science 1996;272(5260):405-8.

61. Uram JN, Black CM, Flynn E, Huang L, Armstrong TD, Jaffee EM. Nondominant CD8 T cells are active players in the vaccine-induced antitumor immune response. J Immunol 2011;186(7):3847-57.

62. Roederer M, Nozzi JL, Nason MX. SPICE: Exploration and analysis of post-cytometric complex multivariate datasets. Cytometry A 2011.

63. Yuan J, Gnjatic S, Li H, Powel S, Gallardo HF, Ritter E, Ku GY, Jungbluth AA, Segal NH, Rasalan TS and others. CTLA-4 blockade enhances polyfunctional NY-ESO-1 specific T cell responses in metastatic melanoma patients with clinical benefit. Proc Natl Acad Sci U S A 2008;105(51):20410-5.

64. Bos R, Marquardt KL, Cheung J, Sherman LA. Functional differences between low- and high-affinity CD8(+) T cells in the tumor environment. Oncoimmunology 2012;1(8):1239-1247.

65. Pfannenstiel LW, Lam SS, Emens LA, Jaffee EM, Armstrong TD. Paclitaxel enhances early dendritic cell maturation and function through TLR4 signaling in mice. Cell Immunol 2010;263(1):79-87.

66. Liang B, Workman C, Lee J, Chew C, Dale BM, Colonna L, Flores M, Li N, Schweighoffer E, Greenberg S and others. Regulatory T cells inhibit dendritic

cells by lymphocyte activation gene-3 engagement of MHC class II. J Immunol 2008;180(9):5916-26.

67. Casati C, Camisaschi C, Novellino L, Mazzocchi A, Triebel F, Rivoltini L, Parmiani G, Castelli C. Human lymphocyte activation gene-3 molecules expressed by activated T cells deliver costimulation signal for dendritic cell activation. J Immunol 2008;180(6):3782-8.

68. El Mir S, Triebel F. A soluble lymphocyte activation gene-3 molecule used as a vaccine adjuvant elicits greater humoral and cellular immune responses to both particulate and soluble antigens. J Immunol 2000;164(11):5583-9.

69. Yachida S, Jones S, Bozic I, Antal T, Leary R, Fu B, Kamiyama M, Hruban RH, Eshleman JR, Nowak MA and others. Distant metastasis occurs late during the genetic evolution of pancreatic cancer. Nature 2010;467(7319):1114-7.

70. Laheru D, Jaffee EM. Immunotherapy for pancreatic cancer - science driving clinical progress. Nat Rev Cancer 2005;5(6):459-67.

71. Morse MA, Hall JR, Plate JM. Countering tumor-induced immunosuppression during immunotherapy for pancreatic cancer. Expert Opin Biol Ther 2009;9(3):331-9.

72. Houghton AN, Guevara-Patino JA. Immune recognition of self in immunity against cancer. J Clin Invest 2004;114(4):468-71.

73. Kleeff J, Beckhove P, Esposito I, Herzig S, Huber PE, Lohr JM, Friess H. Pancreatic cancer microenvironment. Int J Cancer 2007;121(4):699-705.

74. Schmitz-Winnenthal FH, Volk C, Z'Graggen K, Galindo L, Nummer D, Ziouta Y, Bucur M, Weitz J, Schirrmacher V, Buchler MW and others. High frequencies of

functional tumor-reactive T cells in bone marrow and blood of pancreatic cancer patients. Cancer Res 2005;65(21):10079-87.

75.   Munn DH, Mellor AL. The tumor-draining lymph node as an immune-privileged site. Immunol Rev 2006;213:146-58.

76.   Liyanage UK, Moore TT, Joo HG, Tanaka Y, Herrmann V, Doherty G, Drebin JA, Strasberg SM, Eberlein TJ, Goedegebuure PS and others. Prevalence of regulatory T cells is increased in peripheral blood and tumor microenvironment of patients with pancreas or breast adenocarcinoma. J Immunol 2002;169(5):2756-61.

77.   Bayne LJ, Beatty GL, Jhala N, Clark CE, Rhim AD, Stanger BZ, Vonderheide RH. Tumor-derived granulocyte-macrophage colony-stimulating factor regulates myeloid inflammation and T cell immunity in pancreatic cancer. Cancer Cell 2012;21(6):822-35.

78.   Leao IC, Ganesan P, Armstrong TD, Jaffee EM. Effective depletion of regulatory T cells allows the recruitment of mesothelin-specific CD8 T cells to the antitumor immune response against a mesothelin-expressing mouse pancreatic adenocarcinoma. Clin Transl Sci 2008;1(3):228-39.

79.   Pylayeva-Gupta Y, Lee KE, Hajdu CH, Miller G, Bar-Sagi D. Oncogenic Kras-induced GM-CSF production promotes the development of pancreatic neoplasia. Cancer Cell 2012;21(6):836-47.

80.   Hingorani SR, Petricoin EF, Maitra A, Rajapakse V, King C, Jacobetz MA, Ross S, Conrads TP, Veenstra TD, Hitt BA and others. Preinvasive and invasive ductal

pancreatic cancer and its early detection in the mouse. Cancer Cell 2003;4(6):437-50.

81. Hingorani SR, Wang L, Multani AS, Combs C, Deramaudt TB, Hruban RH, Rustgi AK, Chang S, Tuveson DA. Trp53R172H and KrasG12D cooperate to promote chromosomal instability and widely metastatic pancreatic ductal adenocarcinoma in mice. Cancer Cell 2005;7(5):469-83.

82. Le DT, Brockstedt DG, Nir-Paz R, Hampl J, Mathur S, Nemunaitis J, Sterman DH, Hassan R, Lutz E, Moyer B and others. A live-attenuated Listeria vaccine (ANZ-100) and a live-attenuated Listeria vaccine expressing mesothelin (CRS-207) for advanced cancers: phase I studies of safety and immune induction. Clin Cancer Res 2012;18(3):858-68.

83. Lauer P, Chow MY, Loessner MJ, Portnoy DA, Calendar R. Construction, characterization, and use of two Listeria monocytogenes site-specific phage integration vectors. J Bacteriol 2002;184(15):4177-86.

84. Villalobos A, Ness JE, Gustafsson C, Minshull J, Govindarajan S. Gene Designer: a synthetic biology tool for constructing artificial DNA segments. BMC Bioinformatics 2006;7:285.

85. De Paiva CS, Chotikavanich S, Pangelinan SB, Pitcher JD, 3rd, Fang B, Zheng X, Ma P, Farley WJ, Siemasko KF, Niederkorn JY and others. IL-17 disrupts corneal barrier following desiccating stress. Mucosal Immunol 2009;2(3):243-53.

86. DeNardo DG, Brennan DJ, Rexhepaj E, Ruffell B, Shiao SL, Madden SF, Gallagher WM, Wadhwani N, Keil SD, Junaid SA and others. Leukocyte

complexity predicts breast cancer survival and functionally regulates response to chemotherapy. Cancer Discov 2011;1(1):54-67.

87.   Mouton PR. Principles and Practices of Unbiased Stereology. Baltimore: Johns Hopkins University Press; 2002. 88-112 p.

88.   Jones S, Zhang X, Parsons DW, Lin JC, Leary RJ, Angenendt P, Mankoo P, Carter H, Kamiyama H, Jimeno A and others. Core signaling pathways in human pancreatic cancers revealed by global genomic analyses. Science 2008;321(5897):1801-6.

89.   Singh R, Paterson Y. Listeria monocytogenes as a vector for tumor-associated antigens for cancer immunotherapy. Expert Rev Vaccines 2006;5(4):541-52.

90.   Olino K, Wada S, Edil BH, Pan X, Meckel K, Weber W, Slansky J, Tamada K, Lauer P, Brockstedt D and others. Tumor-associated antigen expressing Listeria monocytogenes induces effective primary and memory T-cell responses against hepatic colorectal cancer metastases. Ann Surg Oncol 2012;19 Suppl 3:S597-607.

91.   Brockstedt DG, Dubensky TW. Promises and challenges for the development of Listeria monocytogenes-based immunotherapies. Expert Rev Vaccines 2008;7(7):1069-84.

92.   Brockstedt DG, Giedlin MA, Leong ML, Bahjat KS, Gao Y, Luckett W, Liu W, Cook DN, Portnoy DA, Dubensky TW, Jr. Listeria-based cancer vaccines that segregate immunogenicity from toxicity. Proc Natl Acad Sci U S A 2004;101(38):13832-7.

93.   Onizuka S, Tawara I, Shimizu J, Sakaguchi S, Fujita T, Nakayama E. Tumor rejection by in vivo administration of anti-CD25 (interleukin-2 receptor alpha) monoclonal antibody. Cancer Res 1999;59(13):3128-33.

94.   North RJ. Cyclophosphamide-facilitated adoptive immunotherapy of an established tumor depends on elimination of tumor-induced suppressor T cells. J Exp Med 1982;155(4):1063-74.

95.   Hirschhorn-Cymerman D, Rizzuto GA, Merghoub T, Cohen AD, Avogadri F, Lesokhin AM, Weinberg AD, Wolchok JD, Houghton AN. OX40 engagement and chemotherapy combination provides potent antitumor immunity with concomitant regulatory T cell apoptosis. J Exp Med 2009;206(5):1103-16.

96.   Trimble CL, Clark RA, Thoburn C, Hanson NC, Tassello J, Frosina D, Kos F, Teague J, Jiang Y, Barat NC and others. Human papillomavirus 16-associated cervical intraepithelial neoplasia in humans excludes CD8 T cells from dysplastic epithelium. J Immunol 2010;185(11):7107-14.

97.   Gerloni M, Zanetti M. CD4 T cells in tumor immunity. Springer Semin Immunopathol 2005;27(1):37-48.

98.   Silva MT. When two is better than one: macrophages and neutrophils work in concert in innate immunity as complementary and cooperative partners of a myeloid phagocyte system. J Leukoc Biol 2010;87(1):93-106.

99.   Youn JI, Nagaraj S, Collazo M, Gabrilovich DI. Subsets of myeloid-derived suppressor cells in tumor-bearing mice. J Immunol 2008;181(8):5791-802.

100.   Trimble CL, Frazer IH. Development of therapeutic HPV vaccines. Lancet Oncol 2009;10(10):975-80.

101. Michel ML, Deng Q, Mancini-Bourgine M. Therapeutic vaccines and immune-based therapies for the treatment of chronic hepatitis B: perspectives and challenges. J Hepatol 2011;54(6):1286-96.

102. Gunn GR, Zubair A, Peters C, Pan ZK, Wu TC, Paterson Y. Two Listeria monocytogenes vaccine vectors that express different molecular forms of human papilloma virus-16 (HPV-16) E7 induce qualitatively different T cell immunity that correlates with their ability to induce regression of established tumors immortalized by HPV-16. J Immunol 2001;167(11):6471-9.

103. Rosenberg SA, Sherry RM, Morton KE, Scharfman WJ, Yang JC, Topalian SL, Royal RE, Kammula U, Restifo NP, Hughes MS and others. Tumor progression can occur despite the induction of very high levels of self/tumor antigen-specific CD8+ T cells in patients with melanoma. J Immunol 2005;175(9):6169-76.

104. Segal NH, Parsons DW, Peggs KS, Velculescu V, Kinzler KW, Vogelstein B, Allison JP. Epitope landscape in breast and colorectal cancer. Cancer Res 2008;68(3):889-92.

105. Castle JC, Kreiter S, Diekmann J, Lower M, van de Roemer N, de Graaf J, Selmi A, Diken M, Boegel S, Paret C and others. Exploiting the mutanome for tumor vaccination. Cancer Res 2012;72(5):1081-91.

106. Viehl CT, Moore TT, Liyanage UK, Frey DM, Ehlers JP, Eberlein TJ, Goedegebuure PS, Linehan DC. Depletion of CD4+CD25+ regulatory T cells promotes a tumor-specific immune response in pancreas cancer-bearing mice. Ann Surg Oncol 2006;13(9):1252-8.

107. Pandol S, Edderkaoui M, Gukovsky I, Lugea A, Gukovskaya A. Desmoplasia of pancreatic ductal adenocarcinoma. Clin Gastroenterol Hepatol 2009;7(11 Suppl):S44-7.

108. Provenzano PP, Cuevas C, Chang AE, Goel VK, Von Hoff DD, Hingorani SR. Enzymatic targeting of the stroma ablates physical barriers to treatment of pancreatic ductal adenocarcinoma. Cancer Cell 2012;21(3):418-29.

109. Viaud S, Flament C, Zoubir M, Pautier P, LeCesne A, Ribrag V, Soria JC, Marty V, Vielh P, Robert C and others. Cyclophosphamide induces differentiation of Th17 cells in cancer patients. Cancer Res 2011;71(3):661-5.

110. Sharabi A, Ghera NH. Breaking tolerance in a mouse model of multiple myeloma by chemoimmunotherapy. Adv Cancer Res 2010;107:1-37.

111. Martin-Orozco N, Muranski P, Chung Y, Yang XO, Yamazaki T, Lu S, Hwu P, Restifo NP, Overwijk WW, Dong C. T helper 17 cells promote cytotoxic T cell activation in tumor immunity. Immunity 2009;31(5):787-98.

112. Wei S, Zhao E, Kryczek I, Zou W. Th17 cells have stem cell-like features and promote long-term immunity. Oncoimmunology 2012;1(4):516-519.

113. Lee Y, Awasthi A, Yosef N, Quintana FJ, Xiao S, Peters A, Wu C, Kleinewietfeld M, Kunder S, Hafler DA and others. Induction and molecular signature of pathogenic TH17 cells. Nat Immunol 2012;13(10):991-9.

114. Yu Y, Cho HI, Wang D, Kaosaard K, Anasetti C, Celis E, Yu XZ. Adoptive Transfer of Tc1 or Tc17 Cells Elicits Antitumor Immunity against Established Melanoma through Distinct Mechanisms. J Immunol 2013.

115. Saxena A, Desbois S, Carrie N, Lawand M, Mars LT, Liblau RS. Tc17 CD8+ T cells potentiate Th1-mediated autoimmune diabetes in a mouse model. J Immunol 2012;189(6):3140-9.

116. Tajima M, Wakita D, Satoh T, Kitamura H, Nishimura T. IL-17/IFN-gamma double producing CD8+ T (Tc17/IFN-gamma) cells: a novel cytotoxic T-cell subset converted from Tc17 cells by IL-12. Int Immunol 2011;23(12):751-9.

117. Zhuang Y, Peng LS, Zhao YL, Shi Y, Mao XH, Chen W, Pang KC, Liu XF, Liu T, Zhang JY and others. CD8(+) T cells that produce interleukin-17 regulate myeloid-derived suppressor cells and are associated with survival time of patients with gastric cancer. Gastroenterology 2012;143(4):951-62 e8.

118. Garcia-Hernandez Mde L, Hamada H, Reome JB, Misra SK, Tighe MP, Dutton RW. Adoptive transfer of tumor-specific Tc17 effector T cells controls the growth of B16 melanoma in mice. J Immunol 2010;184(8):4215-27.

119. Carriere C, Young AL, Gunn JR, Longnecker DS, Korc M. Acute pancreatitis markedly accelerates pancreatic cancer progression in mice expressing oncogenic Kras. Biochem Biophys Res Commun 2009;382(3):561-5.

120. Whitcomb DC, Pogue-Geile K. Pancreatitis as a risk for pancreatic cancer. Gastroenterol Clin North Am 2002;31(2):663-78.

121. Sparmann A, Bar-Sagi D. Ras-induced interleukin-8 expression plays a critical role in tumor growth and angiogenesis. Cancer Cell 2004;6(5):447-58.

122. Zhang Z, Rigas B. NF-kappaB, inflammation and pancreatic carcinogenesis: NF-kappaB as a chemoprevention target (review). Int J Oncol 2006;29(1):185-92.

123. Chiao PJ, Ling J. Kras, Pten, NF-kappaB, and inflammation: dangerous liaisons. Cancer Discov 2011;1(2):103-5.

124. Fukuda A, Wang SC, Morris JPt, Folias AE, Liou A, Kim GE, Akira S, Boucher KM, Firpo MA, Mulvihill SJ and others. Stat3 and MMP7 contribute to pancreatic ductal adenocarcinoma initiation and progression. Cancer Cell 2011;19(4):441-55.

125. Coussens LM, Zitvogel L, Palucka AK. Neutralizing tumor-promoting chronic inflammation: a magic bullet? Science 2013;339(6117):286-91.

126. Medina-Echeverz J, Fioravanti J, Zabala M, Ardaiz N, Prieto J, Berraondo P. Successful colon cancer eradication after chemoimmunotherapy is associated with profound phenotypic change of intratumoral myeloid cells. J Immunol 2011;186(2):807-15.

Curriculum Vitae

BRIDGET P. KEENAN

Email: Bkeenan3@jhmi.edu

School Address:
Johns Hopkins University
CRB 4M86
1650 Orleans St.
Baltimore, MD 21287

Birthplace: Richboro, PA
Date of Birth: June 23, 1984

EDUCATION

2007-present Johns Hopkins University School of Medicine   Baltimore, MD

M.D. - Ph.D. Candidate, Expected Graduation Date: May 2015

PhD in Immunology

2002-2006   Loyola University Maryland   Baltimore, MD

B.S., Biology Major, Chemistry Minor, Pre-medicine

Summa Cum Laude, Cumulative GPA: 3.94, Major GPA: 4.00

Study Abroad 2004-2005 at the University of Newcastle, England

ADDITIONAL TRAINING

2013   **Emerging Women's Leadership Program, Johns Hopkins University**

  School of Medicine   Baltimore, MD

2006   **Foundation for Advanced Education in the Sciences, National**

  Institutes of Health   Bethesda, MD

  Graduate Level Course in Developmental Biology

AWARDS

2012   Scholar-in-Training Award, AACR Special Conference on Tumor

  Immunology

2011-2013   Student Training and Research in Tumor Immunology (StaRT) Pre-

  doctoral Grant, Cancer Research Institute

2006-2007   Post-baccalaureate Intramural Research Training Award, National

  Institutes of Health

2006   Phi Beta Kappa

2006   Tri-Beta (National Biology Honor Society)

2006   Alpha Sigma Nu (Jesuit Schools' Honor Society)

2002-2006   Loyola Presidential Scholarship, Full Tuition

2002-2006   Maryland Hope Science and Technology Scholarship

2002-2006   Maryland Distinguished Scholar Scholarship

RESEARCH EXPERIENCE

2009-2013   **Laboratory of Dr. Elizabeth Jaffee**   Baltimore, MD

Doctoral Candidate in Immunology, Johns Hopkins University School of Medicine

Thesis Work Focused on Characterizing Immunesuppressive Mechanisms in the Tumor Microenvironment and Using Targeted Immunotherapy to Overcome Immunesuppression in Mouse Models of Breast and Pancreatic Cancer

2006-2007   **Laboratory of Dr. Peter Aplan**   Bethesda, MD

IRTA (Intramural Research Training Award) Program Student, Genetics Branch, Center for Cancer Research, National Cancer Institute, National Institutes of Health

Studied Mechanisms of DNA Damage and Repair Leading to Translocation Events in Leukemia Using *In Vitro* Models

2005-2006   **Laboratory of Dr. David Rivers**   Baltimore, MD

Independent Research Elective, Biology Department, Loyola University Maryland

Utilized Cell Imaging Techniques to Investigate the Mechanism of Action

of Venom from the Parasitic Wasp *Pimpla Turionella* in Insect Cell Lines

2003-2005   Laboratory of Dr. Gerald Wilson   Baltimore, MD

Summer Research Assistant, University of Maryland, School of Medicine,

Department of Biochemistry and Molecular Biology

Responsibilities Included the Purification of Recombinant Proteins and

Production of Plasmids for Studying for mRNA/Protein Interactions and

Gene Expression Regulation

PUBLICATIONS

Keenan BP, Saenger Y, Kafrouni MI, Leubner A, Lauer P, Maitra A, Rucki AA,

Gunderson AJ, Coussens LM, Brockstedt DG, Dubensky TW, Hassan R, Armstrong TD,

Jaffee EM. A Listeria Vaccine and Depletion of T-regulatory Cells Activate Immunity

Against Early-stage Pancreatic Intra-epithelial Neoplasms and Prolong Survival of Mice.

Gastroenterology. 2014 Mar 6. doi: 10.1053/j.gastro.2014.02.055.

Keenan BP, Jaffee EM, Armstrong TA. Tumor Immunology: Multidisciplinary Science

Driving Basic and Clinical Advances. *Cancer Immunol Res.* 2013 Jul;1:16-23.

Keenan B, Jaffee EM. Immunotherapy in preneoplastic disease: targeting early

procarcinogenic inflammatory changes that lead to immune suppression and tumor

tolerance. *Ann N Y Acad Sci.* 2013 May;1284(1):12-6.

Keenan BP, Jaffee EM. Whole cell vaccines-past progress and future strategies. *Semin Oncol.* 2012 Jun;39(3):276-86.

Keenan BP, Abuav R. Acneiform eruption in a patient receiving bevacizumab for glioblastoma multiforme. *Arch Dermatol.* 2010 May;146(5):577.

Cheng Y, Zhang Z, **Keenan B**, Roschke AV, Nakahara K, Aplan PD. Efficient repair of DNA double-strand breaks in malignant cells with structural instability. *Mutat Res.* 2010 Jan 5;683(1-2):115-22.

Fialcowitz EJ, Brewer BY, **Keenan BP**, Wilson GM. A hairpin-like structure within an AU-rich mRNA-destabilizing element regulates trans-factor binding selectivity and mRNA decay kinetics. *J Biol Chem.* 2005 Jun 10;280(23):22406-17.

ABSTRACTS

Yang WR, Heikamp EB*, **Keenan BP***, Montaño C*, Mukherjee-Clavin B*, Shamir ER*, Buntin M, Welling SA, Siliciano JD, Siliciano RF. Gender differences in the career outcomes of Johns Hopkins MD-PhD program graduates. Johns Hopkins University School of Medicine, Baltimore, MD. at: American Physician Scientists Association Annual Meeting, April 26-28, 2013.

*These authors contributed equally to this work.

Keenan B, Saenger Y, Kafrouni M, Leubner A, Lauer P, Maitra A, Gunderson A, Coussens L, Armstrong T, Jaffee E. Prevention of pancreatic intra-epithelial neoplasm

progression by a *Listeria monocytogenes* vaccine targeting mutated Kras, an early genetic event in pancreatic tumor development. Johns Hopkins University School of Medicine, Baltimore, MD. at: American Association of Cancer Research Annual Meeting, April 6-10, 2013.

Keenan B, Saenger Y, Kafrouni M, Leubner A, Lauer P, Maitra A, Gunderson A, Coussens L, Armstrong T, Jaffee E. Prevention of pancreatic intra-epithelial neoplasm progression by a *Listeria monocytogenes* vaccine targeting mutated Kras, an early genetic event in pancreatic tumor development. Johns Hopkins University School of Medicine, Baltimore, MD. at: American Association of Cancer Research Special Conference on Tumor Immunology: Multidisciplinary Science Driving Basic and Clinical Advances, December 2-5, 2012.**

****Chosen for a short talk in symposium on "The Tumor Microenvironment: Translational Updates"**

Keenan B, Saenger Y, Armstrong T, Jaffee E. Prevention of pancreatic intra-epithelial neoplasm (PanIN) progression by a *Listeria monocytogenes* vaccine targeting mutated Kras, an early genetic event in pancreatic tumor development. Johns Hopkins University School of Medicine, Baltimore, MD. at: Cancer Research Institute Annual International Cancer Immunotherapy Symposia Series, October 1-3, 2012.

PROFESSIONAL AND VOLUNTEER EXPERIENCES

2012-present Founding Member and Co-Leader, Association of Women Student MD-PhDs (AWSM), Johns Hopkins University School of Medicine

2011-present Founding Member and Co-Chair, MSTP Student Advisory Board, and member of Professional Development & Ethics sub-committee, Johns Hopkins University School of Medicine

2011-2012 Teaching Assistant, Cell Physiology, Johns Hopkins University School of Medicine

2010 Contributed to Development of Graduate Elective in Tumor Immunology, Offered Fall 2010 Semester, Johns Hopkins University School of Medicine

2008-2012 Co-president, Medical Student Oncology Interest Group, Johns Hopkins University School of Medicine

2008-2011 Peer Advisor, Johns Hopkins University School of Medicine

2007-present Lead Mentor and Team Leader of a "Family" of Mentors, Incentive Mentoring Program, Baltimore, MD

2007-2009 Volunteer, Programa Salud (Clinic Offering Free TB Testing and Serving the Latino Population), Baltimore, MD

PROFESSIONAL SOCIETY MEMBERSHIPS

2012-present Women in Cancer Research, American Association of Cancer Research

2008-present American Medical Women's Association

2007-present American Medical Student Association